Atlastin Mediated Endoplasmic Reticulum Network Formation In Hereditary Spastic Paraplegia

by

Idil Ulengin

A thesis submitted in partial fulfillment of the requirements for the degree of Doctor of Philosophy in the field of Biological Sciences

Department of Biological Sciences
Carnegie Mellon University
Pittsburgh, Pennsylvania

June 11th, 2015

Thesis Advisor: Dr. Tina H. Lee, Ph.D.

For my Grandmother Servet Yilmaz

ACKNOWLEDGEMENTS

Doing my PhD was one of the most challenging tasks I have ever tackled in my life. Being oceans away from my home, my family and my friends made it even more challenging. Looking back now, I can see that I have grown both professionally and personally. For this reason, I would like to acknowledge people that helped me not only to complete this process but also had a great influence on my personal and professional development through out this process.

First, I would like to thank my advisor Dr. Tina H. Lee for setting the bar of excellence so high and guiding me to achieve my goals. Her steady support, generous attention and belief in me, made me more self-confident and able to cope with the challenges (failures) through out my graduate career. She taught me to never give up, to trust myself, learn from my mistakes and recover from the failure. I feel ready for the next challenges in my life and it is all because she made me a more stubborn and a more ambitious scientist. Thank you Tina for never giving up on me even, when I have given up on myself, and devoting your time to making sure I do the best I can.

I would also like to thank my committee members, Dr. Adam D. Linstedt, Dr. John Woolford and Dr. Jeffrey Brodsky. It was a privilege to have them as my committee members. They were always very helpful and supportive with their valuable feedback. I truly appreciate the time each of you spared for me. With your help and your recommendation letters reflecting your belief in me, I have great opportunies for the next phase of my career.

I could not have finished my PhD without the support of my friends from all over the world. Irem and Idil, they have not only been my best friends but my sisters. Their endless encouragements help me fulfill my dreams. Also, I am very happy to add more friends to my life throughout the years I have been here. I would like to thank all my classmates especially Ritika Tewari and Simran Saini; the current and former members of Lee Lab (Dr. Jeanne Morin-Leisk, Dr. Kaitlyn Dykstra, James Winsor); and the members of Puthenveedu and Linstedt labs for being a part of my journey. I would also like to thank Esra and Vefa Kucukboyaci. They have been a family for me and made me feel at home, I could not have finished this journey without you.

More of all, I am thankful for my family: my parents Fusun and Burc Ulengin, my grandmother Necla Ulengin and my aunt Berna Ulengin. They have always been there for me, encouraged me to make my own decisions and supported me endlessly to pursue my dreams even if it required me to be so far away from them. They shared my struggles, my failures and my accomplishments through out my graduate studies and made sure that I never felt alone. My parents, both professors, have always been my role models. I have always admired their hard-working, discipline, dedication and constant search for improvement in their studies. I hope one day, I can be as successful as they are.

I would like to thank Jason Talkish. Coming here for my graduate studies, I would not have taught that I would find a soul mate who would become a partner to me. I am grateful for him for putting up with me all these years and always supporting me. Being a dedicated scientist, you have been a role model and have given me the strength that I needed to complete this part of my journey. I am looking forward to the next episodes of our lives together.

Lastly, I would like to thank my grandmother Servet Yilmaz, for encouraging me to dream big and to be brave to pursue these dreams. She always reminded me that I should work hard but also spare time to have fun and enjoy life. I continue to feel your support and your looking out for me everyday since you passed away. You will always be my best friend.

ABSTRACT

The endoplasmic reticulum is an extensive multifunctional membrane bound organelle present in all eukaryotic cells. It houses a wide array of essential processes including protein and lipid synthesis, drug detoxification and regulation of intracellular Ca^{+2}. This very large organelle is organized into morphologically distinct subdomains, presumably to maximize the efficiency of each of its many functions. Yet the ER is interconnected at hundreds of branchpoints. maintaining both luminal and membrane continuity. Despite its complex structure, the ER undergoes continuous membrane remodeling, which may enable it to adopt to environmental changes.

Due to their extreme polarity and the long distances that need to be traversed by cellular constituents, neurons may rely more heavily than other cell types on the proper structure, function and dynamics of organelles such as the ER. In support of this idea, a number of neurological disorders are linked to mutations in genes whose products are proposed to structure the ER. In particular, mutations in the neuronal isoform of atlastin (ATL), a conserved dynamin-related GTPase implicated in homotypic ER membrane fusion and ER network formation, cause a motor neurological disorder called Hereditary Spastic Paraplegia (HSP).

Determining the role of ATLs in ER morphology has obvious implications in the context of the neurodegeneration seen in Hereditary Spastic Paraplegia patients. To this end, in my thesis I worked on three projects. One focused on testing the hypothesis that disease mutations cause HSP because they disrupt neuronal ATL-1's fusion-dependent ER structuring function. Using a cell-based assay for ATL-mediated ER network formation, I showed that neuronal ATL-1 can fully restore a branched ER network in HeLa cells depleted of endogenous ATL, and yet surprisingly, not all the disease mutations disrupt ER morphology. Furthermore, at least two disease variants, including that most commonly identified in patients, displayed wild type levels of activity in all assays, including a biochemical assay for membrane fusion. The second project tested the role of an N-terminal extension of ATL-1 that is highly conserved across vertebrate species. My results indicated that this extension was dispensable for ER structuring at least in non-neuronal cells. Therefore, the significant conservation observed within this region may reflect a regulatory role specific to neurons, an idea that remains to be

tested. Lastly, I collaborated with James McNew and his group to investigate the precise role of the cytoplasmic C-terminal tail of ATL. Together we showed that the C-terminal tail is important for both the fusion and ER network formation functions of ATL. And yet in the context of less stable lipid bilayers, the requirement for the C-terminal tail during fusion was alleviated.

Altogether, my findings reveal a discrepancy with the hypothesis that disease mutations disrupt ER morphology and highlight a gap in the understanding of the cause of ATL-1 linked SPG3A. The apparent lack of a requirement for a highly conserved N-terminal extension, as well as residues implicated in HSP, is surprising. It suggests that the ER in neurons might rely on a neuron specific factor that binds and regulates the fusion. Alternatively, ATL-1 may mediate an additional (non-ER fusion) function specific to neurons. Overall, my investigation reveals that there is more to be understood in terms of precise role (s) and regulation of ATL a well as the basis of SPG3A pathogenesis.

TABLE OF CONTENTS

LIST OF FIGURES

CHAPTER 1

INTRODUCTION

1.1 Membrane-Bound Organelles

Eukaryotic cells contain numerous membrane-bound organelles that take up a large fraction of the cell volume. The membranes serve as physical barriers that allow for segregation of diverse cellular processes occurring simultaneously within a single cell (Cohen-Fix, 2014). Each organelle, such as the endoplasmic reticulum (ER), Golgi, mitochondria, endosomes or lysosomes, is defined by its specific cellular functions and possesses a characteristic morphology. Furthermore, these organelles can change their shape and size to adjust to the needs of the cell (Voeltz and Barr, 2013). Some of these structural changes can be observed as a part of the normal cell cycle such as during cell division (Puhka et al., 2007; Lu et al., 2009). Other changes occur as a response to environmental or stress conditions (Borgese et al., 2006), presumably to help the cell adapt to physiological changes. The importance of organelle morphology and dynamics is highlighted by the large number of diseases associated with defects in organelle structuring. One such disease is Hereditary Spastic Paraplegia, a neurodegenerative disease linked to mutations in proteins responsible for establishing the proper structure of the ER (Blackstone et al., 2012).

1.2 Endoplasmic Reticulum Structure and Function

1.2.1 Distinct morphological domains contribute to function

Of all the membrane bound organelles in cells, the ER is by far the largest, occupying more than 10 % of the total cell volume. Morphologically, it is a dispersed, continuous membrane system that starts from the nuclear envelope and extends to the cell periphery spreading throughout the entire cell (Baumann and Walz, 2001). This extensive network houses a wide array of essential cellular processes. These include protein synthesis, protein folding and quality control, coat protein (COP)II-mediated secretory protein export, lipid synthesis, detoxification and regulation of intracellular Ca^{+2} (Baumann and Walz., 2001). Furthermore, the ER, perhaps due to its prevalence,

physically interacts with almost all other membrane-bound organelles including the plasma membrane, the Golgi apparatus, endosomes, lysosomes and mitochondria. These contacts have been suggested to be involved in a variety of functions such as lipid and calcium transfer (Elbaz and Schuldiner, 2011; Friedmann et al., 2011; Voeltz and Barr, 2013; Daniele and Schiaffino, 2014). Recent analyses have also suggested a regulatory role for ER in dynamics of endosomes and mitochondria. The contact sites of ER tubules on endosomes and mitochondria have been shown to predict the site and timing of endosome fission and mitochondrial division (Friedmann et al., 2011; Rowland et al., 2014).

Though a single continuous membrane network, the ER is organized into functional subdomains with different morphologies; which may help to increase the efficiency of a wide range of functions with disparate structural requirements (Baumann and Walz., 2001; Voeltz et al.,2002). Immunofluorescence staining of the ER shows two distinct subdomains: nuclear and peripheral ER. The nuclear ER (NE) surrounds the nuclear envelope and consists of two sheets of membranes with a lumen (Voeltz et al., 2002). The peripheral ER is composed of a mixture of flat sheets and highly curved tubules which are all interconnected to maintain both luminal and membrane continuity (Shibata, 2006). Although both sheets and tubules are conserved in all eukaryotes, their relative proportions vary between cell types likely resulting in the morphology most suited to the predominating ER functions in any given cell type. (Figure 1.1)

Peripheral ER sheets are often studded by ribosomes (so called rough ER, RER) and are abundant in secretory cells such as pancreatic cells to compensate for the increased requirement for protein synthesis. In contrast, highly curved tubules often devoid of ribosomes are the major site of Ca^{+2} exchange, lipid synthesis, and drug detoxification. Therefore, tubular ER predominates for example in muscle cells where the primary function of the ER is to mediate changes in Ca^{+2} during muscle contraction (Baumann and Walz, 2001; Shibata et al., 2006).

ER domains are not only complex in morphology but are also highly dynamic. As cells undergo division and differentiation, the entire ER network undergoes reorganization. In interphase cells, ER dynamics are observed in peripheral ER as sheet rearrangements and formation of new three-way junctions through fusion between ER tubules (Lee and

Chen, 1988; Prinz et al., 2000; Puhka et al., 2007). Regardless of which transition the ER undergoes, the continuous network with distinctly structured domains is always reconstructed suggesting that the mechanisms and factors that generate the shapes of distinct ER domains are always present.

1.2.2 Several factors and mechanisms shape up the ER

Nuclear Endoplasmic Reticulum

The nuclear ER (NE) is mostly made up of flat sheets. The inner and outer nuclear membranes (INM ad ONM) form the two leaflets that are connected at nuclear pores. The structure of NE is stabilized by interactions between the inner nuclear membrane proteins (such as LINC complex) and the chromatin/ nuclear lamina (Holmer and Worman, 2001; Voeltz et al, 2006). Most of the ER lumen and membrane, however, is not dedicated to the NE, but is spread out to form the peripheral ER which is continous with the ONM (Baumann and Walz., 2001).

Peripheral Endoplasmic Reticulum

The Peripheral ER, branches out from the NE and extends all the way through the cell periphery. The sites of contact between the ER and the other organelles are also a part of the peripheral ER. Peripheral ER is further reorganized into sheets and tubules and despite having these structurally distinct subregions, it is highly dynamic and interconnected via three-way junctions that maintain luminal and membrane continuity. Although highly complex in morphology, only a handful of factors have been identified as having roles in shaping the ER.

ER sheet generation

Peripheral ER sheets consist of two closely apposed membranes approximately 50nm apart. They are relatively flat except for the high curvature observed at the edges (Shibata et al., 2010). Peripheral ER sheets are enriched for ribosomes and translocation complexes. Thus studies have suggested that the presence of polyribosomes exerts enough force on the membrane to stabilize the flat sheets. The ER of cells treated with puromycin to strip off ribosomes is found to undergo a transition from a mixture of sheets and tubules to mostly tubules (Puhka et al., 2007). One other factor has been implicated in ER sheet formation. Climp-63, an integral membrane

protein, is found to be the most abundant protein in ER sheets. It has been suggested to induce sheet morphology by forming a bridge between the ER lumen and acting as a "luminal spacer" between ER membranes (Figure 1-2B) (Shibata et al., 2006; Barlowe, 2010). Its role in ER sheet formation came from studies in cultured cells where while the overexpression of Climp-63 led to dramatic proliferation of ER sheets, depletion of Climp-63 caused a reduction in the distance between the cisternal sheets (Shibata et al., 2006).

Curvature generation in ER tubules

ER membranes, like most other intracellular membranes, are composed of a largely symmetric lipid bilayer consisting predominantly of phospholipids. In the absence of protein, lipid bilayers tend to adopt a flat morphology, the lowest energy state. It has been determined that generating a fragment of a lipid tubule with a diameter of 60nm (as in ER tubules) requires around 70 kcal/mol which is much higher than the characteristic thermal energy, around 0.6 kcal/mol (Shibata et al., 2009). This suggests that curvature cannot be generated spontaneously and factors should be involved to overcome the energy requirement. Consistent with this, integral membrane proteins have been identified that generate and stabilize the specific degrees of membrane curvature.

The first protein family identified to have a role in tubule generation was the reticulons (RTN) that are conserved and expressed ubiquitously in all eukaryotes. They are specifically enriched in the tubular ER and are absent from the sheets and nuclear envelope (Voeltz et al., 2006; Shibata et al., 2006; Borgese et al., 2006). Overexpression of the reticulon isoform Rtn4a in mammalian cells leads to the proliferation of bundled ER tubules causing a reduction in the peripheral sheets. This suggests a type of "tug-of-war" between sheet and tubule formation (Shibata et al., 2006). In yeast, deletion of both isoforms of reticulons (RTN1 and 2) was found to have no effect on the morphology of the ER network suggesting additional proteins playing a role in ER tubule formation. Consistent with this, immunoprecipitation experiments with reticulons revealed another family of proteins called REEPs that also preferentially localized to ER tubules and to the highly curved edges of the ER sheets. The depletion of reticulons and Reep5/DP1 homolog Yop1 simultaneously resulted in a dramatic loss of peripheral ER tubules in yeast (Voeltz et al., 2006). More interestingly when purified yeast Yop1 and reticulons were reconstituted with lipids into proteoliposomes they were found to be sufficient to

generate tubules of about 20nm in diameter (Hu et al., 2008). This observation suggests that REEP and reticulon family proteins are not only necessary but also sufficient to generate and stabilize the ER tubules *in vitro*.

Both reticulons and the REEP family of proteins share a unique membrane topology with unusually long hydrophobic domains (~30-40 amino acids) that are hypothesized to only penetrate the outer lipid bilayer and form a hairpin in the membrane (Voeltz et al., 2006; Collins, 2006; Hu et al., 2008). This hairpin is suggested to adopt a "wedge shape" increasing the surface area of the outer lipid membrane more than the inner membrane thus generating curvature (Voeltz et al., 2006; Shibata et al., 2008). Furthermore, both reticulons and Yop1 seem to form immobile oligomers that may act as a 'scaffold' to localize other proteins necessary to stabilize the curvature seen in ER tubules and the edges of the ER sheets (Figure 1-2A) (Voeltz et al., 2006; Shibata et al., 2008, Shnyrova et al.,2008; English et al., 2009). However, it is unclear how oligomerization and disassembly of these proteins are regulated and how these processes control tubule formation.

Factors that distribute and interconnect ER

In mammalian cells, the close proximity of ER tubules to microtubules suggested a direct role of the cytoskeleton in the dynamics and distribution of the ER network. (Waterman and Salmon., 1998; Baumann and Walz., 2001). It has been shown that new ER tubules are pulled out by microtubule associated molecular motors (likely via kinesin-1) along the microtubules or they are dragged by the TAC attachment complexes at the plus ends of microtubules. In yeast ER, tubules appear to be generated along actin filaments (Toyoshima et al., 1992; Waterman and Salmon., 1998; Prinz et al., 2000; Baumann and Walz., 2001; Voeltz et al., 2002; Shibata et al., 2006). Although *in vitro* generation of the ER network did not require an intact cytoskeleton (Dreier and Rapoport, 2000), depolymerization of microtubules using nocodazole resulted in collapse of the ER as it retracted from the cell periphery further suggesting direct microtubule involvement in the network distribution (Lu et al., 2009). Consistent with this, REEP1-4 and the longer isoform of AAA ATPase spastin, all localized to ER tubules, are proposed to regulate the cytoskeleton-dependent ER dynamics by physically linking the ER membranes to microtubules through their microtubule binding domains (Sanderson et al., 2006; Evans et al., 2006; Park et al, 2010).

Upon extension on a pre-existing microtubule track, the majority of ER tubules proceed to fuse with pre-existing ER tubules, generating new three-way junctions. The three-way junctions are the key elements necessary to mediate the luminal and membrane continuity of the extensive, branched ER network (Baumann and Walz, 2001). Recent studies have revealed a conserved family of GTPases called atlastins (Orso et al, 2009) that generate three-way junctions by homotypic ER membrane fusion. Antibodies against atlastin (ATL) inhibited *in vitro* ER network formation in the Xenopus egg extract implying its critical role in ER network formation (Derier and Rapoport., 2000; Hu et al., 2009).

Although atlastins are absent in yeast and in plants, functional orthologs, Sey1 and RHD3 respectively, have been identified (Anwar et al., 2012, Zhang et al., 2013). In yeast, Ufe1p, an ER-localized t-SNARE, has also shown to be involved in ER membrane fusion based on the defects in ER fusion observed in *in vitro* studies performed with ER membranes isolated from the temperature sensitive *ufe1-1* mutant strain (Patel et al., 1998). SNAREs are known to mediate fusion between cargo vesicles and their target organelles essential for vesicle trafficking. SNARE mediated vesicle fusion is dependent upon interaction between the SNAREs on the target membrane (t-SNARE) and the SNARE on the incoming vesicle (v-SNARE). The t-SNARE and v-SNARE form a coiled-coil complex that forces the lipid membranes to come into close apposition (Sutton et al., 1988). Recent study showed that the *ufe1-1* mutant strain that also lacks SEY1, has an even slower rate of homotypic ER fusion than *ufe1-1* strain or strains lacking SEY1 alone, suggesting the two pathways to be redundant and independent (Anwar et al., 2012; Rogers et al., 2013).

Taken together, the complex morphology and dynamics of the endoplasmic reticulum are maintained as a result of cooperation between curvature generating integral membrane proteins, the cytoskeleton and ATL/Sey1/RHD3 proteins generating the three-way junctions. Generation of the ER network in neurons presents added challenges as each subdomain needs to be coordinated and distributed over the significantly long distances of axons and dendrites. Remarkably, defects in ER structure in neurons have been associated with neurodegenerative diseases including Hereditary Spastic Paraplegia (Park et al., 2010; Renvoise and Blackstone, 2010).

1.3 Significance of maintaining a continuous ER network in neurons

Not surprisingly, the ER plays crucial roles in neuronal cells. Similar to the ER network in many cell types, neurons also have a dispersed, continuous ER composed of sheets and tubules. (Dailey and Bridgman, 1989: Terasaki et al., 1994). In the cell body, or soma, the ER is mostly composed of sheets studded with ribosomes, whereas ER tubules are spread out into the cell periphery along and into axonal and dendritic processes in a microtubule dependent manner (Rolls et al., 2002: Vedrenne et al., 2005). The rough ER likely functions in the synthesis, modification and export of proteins, including the surface receptors of vital importance in neuronal development (Wang et al., 2012). Lipid synthesis and Ca^{+2} storage functions associated with ER tubules are also important in axon and dendrite formation as well as synaptic signal transmission (Collin et al., 2005, Renvoise and Blackstone, 2010).

Overall, the ER in neuronal cells appears to be closely involved in neuronal development, axon and dendrite formation and extension, regulation of Ca^{+2} dependent synaptic signaling and coordination with other organelles. Thus, it is not surprising that factors that lead to loss of ER structure, especially within neurons that can reach up to 1m in length, are implicated in Hereditary Spastic Paraplegia (HSP).

1.3.1 Hereditary Spastic Paraplegia

Hereditary spastic paraplegia (HSP) is a group of inherited disorders affecting individuals of diverse ethnic groups. Genetic mutations have been found to be the major causative factor and up-to date more than 55 genetic HSP loci have been found. The types of HSP are designated by the locus ("Spastic Paraplegia" SPG 1-56). They are associated with and numbered in order of their discovery. Regardless of the type, all affected individuals suffer from weakness and spasticity of the lower limbs but these symptoms are phenotypically variable in terms of severity, the degree of progression and the age-of-symptom onset. The variation in the mode of inheritance (dominant, recessive or X-linked) adds to the complexity of the disease (Fink, 2006).

Post mortem analysis of HSP patients revealed length dependent degeneration of axons in the corticospinal tract. Consistently, the functional categorization of the proteins encoded by HSP genes suggests pathways including axon elongation, endosomal

trafficking, myelin formation, mitochondrial function and endoplasmic reticulum morphogenesis. All these might be especially important for the maintenance of long axons. Thus defects in one or several of the pathways stated above are suggested to cause the disease pathogenesis (Fink, 2006; Blackstone et al., 2011, Noreau et al., 2014).

Among these pathways, ER morphology defects are hypothesized to be the major cause of HSP as the majority, ~60% , of affected individuals have mutations in one of the four proteins associated with ER network formation: spastin (SPG4A), Reep1 (SPG31), reticulon2 (SPG12) and atlastin1 (SPG3A) (Salinas et al., 2008).

The lack of direct evidence, such as analysis of the neuronal ER in affected individuals, leaves this hypothesis elusive. However, it suggests that a more detailed understanding of the mechanisms that generate and maintain ER morphology may lead to better understanding of why proper ER structure is important and why loss of this structure would cause disease. To this end in my thesis work, I studied atlastin mediated ER network formation specifically focusing on analyzing the possible effects of ATL-1 mutations identified in SPG3A patients.

1.3.2 SPG3A

Among HSPs, SPG3A stands out as the most common early onset (often before the age of 10) autosomal dominant form. Together with SPG4A, SPG3A make up for more than ~50% of the autosomal dominant form of HSP seen in patients. Symptoms in patients suffering from SPG3A are reported to show slow, if any, progression (Fink, 2003; Namekawa et al., 2006). SPG3A was determined to be caused by mutations in the atlastin1 gene, one of the three human atlastin isoforms that belong to the dynamin-superfamily of GTPases. Disease mutations have been identified throughout the entire protein, but mostly concentrated in the GTPase domain. Indeed some disease mutants were determined to have reduced or even abolished GTPase activity (Zhu et al., 2001).

ATL-1 is most abundant in the central nervous system though present to a lesser extent in other tissues including lung, smooth muscle, adrenal gland, kidney and testis. ATL-1 is reported to localize predominantly to neurons of the corticospinal tract as well as the cerebral cortex and hippocampus. Although the majority of atlastin family proteins,

including the yeast and plant homologues SEY1 and RHD3, are primarily known for their GTP dependent ER membrane fusion activity, several other functions have been suggested for ATL-1. For instance, the localization of ATL-1, in addition to ER, to Golgi apparatus (Zhu et al., 2003) and to vesicular structures (Namekawa et al., 2007) within neurons suggests roles in vesicle trafficking (Zhu et al., 2003). Furthermore, ATL-1 may be associated with axonal development as it is found to be enriched in axonal growth cones and varicosities. Specifically, the significant reduction in the length of axons observed in cultured neuronal cells depleted of ATL-1 suggests a role in axon outgrowth (Zhu et al., 2006). Additionally, ATL-1 has been implicated in bone morphogenetic protein (BMP) signaling. Studies in zebrafish, *Danio Rerio*, suggests reduction in BMP receptor endocytosis in addition to severe mobility defects of the larvae depleted of atlastin (Fassier et al., 2010).

The different functions associated with ATL-1 adds additional challenges to identifying the major cause of the SPG3A disease pathogenesis. Despite the other functions reported, overexpression studies of ATL-1 disease mutants in cultured mammalian cells are shown to cause long, unbranched ER tubules suggesting ER defects to be the major cause of SPG3A (Hu et al., 2009). To this end, Atlastin dependent ER structuring has been studied extensively.

1.4 Atlastin GTPases in ER network formation

Generation of one continuous network requires interconnections between the ER membranes. Maintenance of these interconnections is a dynamic process as new three-way junctions should be generated to compensate for their elimination during sliding events observed along microtubules (Friedman et al., 2010). The GTP dependence of *in vitro* ER network generation suggests the presence of a GTP dependent ER fusion machinery (Derier and Rapoport, 2000). Membrane anchored ATL GTPases that belong to the dynamin superfamily, are identified to be the GTP dependent fusion factor critical to mediate formation of the interconnected tubular network (Hu et al., 2009; Orso et al ., 2009).

Atlastin GTPases are present in all vertebrates in several isoforms unlike *Drosophila melanogaster, C.elegans* and *Danio Rerio* that contain a single isoform (Rismanchi et al., 2008). There are three isoforms of ATL (ATL-1, ATL-2 and ATL-3) in humans.

Unlike the neuronal isoform ATL-1, ATL-2 and ATL-3 are expressed ubiquitously and localized predominantly to tubular ER. All three human isoforms share a conserved domain architecture. They posses extensive homology in the GTP binding domain located in the cytosolic N-terminal portion but are more divergent in the cytoplasmic C-terminal tail and the extreme N- terminal portion that precedes the GTP binding domain (Zhu et al., 2003). The GTP binding domain is followed by a middle domain that connects the GTPase head to the two tandem transmembrane domains that anchor the protein into ER membranes. Several studies have shown the interaction between atlastins and other ER shaping proteins DP1, REEP1 and reticulon4 to be through the transmembrane domains though the functional significance of these interactions is unknown (Rismanchi et al., 2008; Hu et al., 2009; Park et al., 2010).

Atlastin`s ER structuring role was first suggested by expression studies in various cultured cells. Overexpression of a GTP binding mutant of ATL-1 in Cos-7 cells led to long, unbranched ER tubules in a dominant negative fashion suggesting a GTP binding dependent ER structuring function for ATLs (Rismanchi et al., 2008; Hu et al., 2009). In support, siRNA-mediated depletion of the ATL-2 and ATL-3 also caused defects in ER morphology characterized by dramatic reduction in the number of interconnections between the tubules in HeLa cells (Hu et al., 2009). Secretory pathway trafficking, based on ts045-VSVG, was reported to be normal under the knockdown conditions for all human atlastins suggesting a role for the atlastins primarily in ER network morphogenesis (Rismanchi et al., 2008). Separately ultrastructural analysis of ER morphology in *Drosophila melanogaster* neurons depleted of the single ATL orthologue (dAtl) they possess, showed drastic ER alterations characterized as ER fragmentation with lack of continuity. With the observation of ER membrane expansion upon overexpression of dAtl, these data collectively suggested a conserved role for the atlastins in ER network morphogenesis (Orso et al., 2009).

The similarity of the GTPase domain of atlastins to that of dynamins and mitofusins, mechanochemical enzymes that mediate membrane fission and fusion respectively (Praefcke and McMahon, 2004), suggested a direct membrane-remodeling role (Rismanchi et al., 2008). Indeed, the direct role for atlastin in membrane fusion came from the finding that the purified dAtl incorporated into synthetic lipid vesicles was sufficient to catalyze lipid bilayer fusion (Orso et al., 2009). Consistent with the

dependence of *in vitro* ER network formation assay on the presence of GTP and the conservation of the GTPase domain in all atlastin isoforms, this fusion activity was found to be GTP-hydrolysis dependent. Interestingly, only the dAtl orthologue and the more distantly related yeast SEY1 have been shown to fuse liposomes, while none of the three human ATL isoforms were fusion competent *in vitro* (Anwar et al., 2012).

Atlastin dependent homotypic membrane fusion mechanism

The recently solved crystal structures of the cytoplasmic domain of ATL-1 provided insights into the ATL catalyzed membrane fusion mechanism (Bian et al., 2011; Brynes and Sondermann, 2011). The structures revealed a GTPase head connected to a middle domain comprised of a three- helix bundle through a short linker. Strikingly all solved structures were dimeric with two distinct dimer conformations. In both structures, GTPase head domains of two ATL molecules were interacting with each other with the dimer interface near to the nucleotide binding pocket. The two different dimer forms differed with respect to the location of the three-helix bundle middle domain relative to the GTPase head. In crystal form 2, the GTPase heads of each monomer are 'engaged' with the respective three helix bundles of the middle domains that point away from the dimer interface. In crystal form 1, a similar head-to head dimerization is observed but three-helix bundles of the middle domains are 'dislodged' from the GTPase head and run parallel upon crossing over each other caused by a 90° rotation about a central conserved proline residue in the linker (Figure 1-3A, B) (Bian et al., 2011; Byrnes and Sondermann, 2011).

Although not present in the crystal structures, the crystal form 2 suggests the transmembrane domains to be anchored in apposing membranes, thus originally named as the 'pre-fusion' dimer, while in crystal form 1 the transmembrane domains are predicted to be in the same membrane, forming the 'post-fusion' dimer. These two distinct dimer conformations suggested a potential ATL mediated ER membrane fusion mechanism in which ATL monomers anchored to apposing membranes form nucleotide-dependent dimer formation initiates tethering followed by the conformational change that leads to the crossover of the middle domains brings the membranes into close apposition which then leads to fusion (Bian et al., 2011; Byrnes and Sondermann, 2011).

Despite the attempts of obtaining crystals with GTP or GTP analogues, the obtained

structures were strictly GDP bound. The lack of a GTP bound or a transition state crystal left the details of the mechanism including the role of GTP binding and hydrolysis unclear. The similarity of the GDP bound ATL-1 dimers to dimers of dynamin and GBP1, the closest relative of ATL in the dynamin superfamily, bound to GDP.ALF4 (transition state analog) helped gain insights into details of the ATL-1 dependent fusion mechanism (Chappie et al., 2010; Ghosh et al., 2010; Prakasah et al., 2000).

With the recently solved crystal structure of ATL-1 bound to GDP.ALF4 (Byrnes et al., 2013) and more detailed biochemical analysis to uncover the details of the fusion machinery, it is now known that atlastin undergoes GTP dependent head-to-head dimerization and as it catalyzes GTP hydrolysis forms a stable homodimer tethering the opposing membranes (Figure 1-3C) (Byrnes and Sondermann, 2011: Bian et al., 2011; Moss et al., 2011; Saini et al., 2014). Although still not clear, the conformational rearrangement observed with the middle domains is hypothesized to contribute to the driving force for membrane fusion (Daumke and Praefcke, 2011).

Although the crystal structures of the cytoplasmic domain of ATL revealed some information of the fusion cycle, structure-function analysis on Drosophila ATL showed involvement of the transmembrane domains and the cytoplasmic tail in fusion (Moss et al., 2011; Liu et al., 2012). In these studies, deletion of either of the two transmembrane domains inhibited the protein`s ability to fuse liposomes *in vitro* (Liu et al., 2012). Studies showing the replacement of either of the transmembrane domains with the transmembrane domain of another ER integral membrane protein (SEC61β) was still fusion incompetent, suggesting a specific role for these domains in ATL`s fusion activity rather than only serving as membrane anchor sites. Similarly, such a specific role was identified for cytoplasmic tail located on the C-terminal (Moss et al., 2011; Liu et al., 2012). The sequence alignment of atlastins among different species pointed to a highly conserved region within the cytoplasmic tail immediately following the second transmembrane domain. Thus, this region was predicted to form an amphipathic helix capable of interacting with lipid bilayer (Liu et al., 2011; Faust et al., 2015). Strikingly, a synthetic peptide corresponding to this helix rescued the fusion activity of the tailless mutant when added in trans. Further studies on this amphipathic helix uncovered its role in destabilizing the lipid bilayer which in turn facilitates the fusion process (Liu et al., 2011; Faust et al., 2015).

The pieces of the atlastin mediated ER membrane fusion are coming together at a fast-pace. However, the precise mechanism is still not known as several pieces are still missing. One such piece is the mechanism that triggers the disassembly of the dimer after completing one fusion cycle. The low abundance of atlastin proteins in cells suggests recycling of proteins for multiple cycles of fusion. How this recycling is maintained is still not known. Moreover, precisely how atlastins mediate ER morphogenesis and whether their function is regulated remain to be elucidated.

Understanding how atlastins work will not only reveal a novel fusion machinery utilized by cells but also in the big picture will contribute to information on the mechanisms that maintain and establish the overall branched ER network. Determining the role of atlastins in ER morphology in detail will also have crucial implications in the context of neurodegeneration seen in Hereditary Spastic Paraplegia patients. To this end, I investigated the precise cellular role(s) of neuronal ATL-1 focusing on the disease mutations identified in patients. Specifically, I set out to test the hypothesis that disease mutations cause HSP because they disrupt ATL-1's fusion-dependent ER structuring function. Chapter 2 describes the analysis of a panel of disease causing mutations using cell-based assays for ATL-mediated ER network formation and biochemical assays for ATL-catalyzed GTP hydrolysis, dimer formation and membrane fusion. In this study I showed that neuronal ATL-1 can fully restore a branched ER network in HeLa cells depleted of ATL-2/3, indicating a similar ER fusion function for all three isoforms. I also showed that not all the disease mutations disrupt ER morphology. Altogether, my findings revealed a discrepancy of the hypothesis that disease mutations disrupt ER morphology and highlighted the gap in the understanding of the cause of ATL-1 linked SPG3A. The effects of the mutations on the alternate non ER-fusion functions proposed for ATL-1 in neurons remain to be tested. Although my data on the Drosophila ATL with corresponding disease mutations suggest that a deficit in the membrane fusion activity may be a key contributor, but is not required, for HSP causation, the true impact of the mutations on ATL-1 mediated fusion activity also remains elusive since ATL-1 is incapable of mediating fusion between synthetic liposomes *in vitro* due to unknown reasons. One possibility is presence of regulatory elements such as binding partners necessary for ATL-1 mediated homotypic-fusion. Alternatively, it is possible that the human isoforms including ATL-1 possess structural elements that inhibit their fusion

capability *in vitro*. Consistent with the second possibility, the sequence alignment between the human isoforms and the *in vitro* fusion competent Drosophila isoform reveals high divergence only at the extreme ends consisting of the N-terminal extension prior to the GTPase domain and the C-terminal tail following the transmembrane domains. Interestingly, alignment of the N-terminal extension domains of human atlastins reveal high conservation specifically for ATL-1 among different species suggesting functional importance. Therefore, I set out to investigate the role of the N-terminal extension in ATL-1 by testing its requirement in the cell-based ER network formation assay as well as GTP hydrolysis and nucleotide dependent dimerization. Surprisingly, my results showed that the N-terminal extension was dispensable in cell based ER network formation and showed no effect on the biochemical assays, at least in the context of soluble domain of ATL-1. Additionally, in collaboration with James McNew`s lab, I analyzed the role of the C-terminal tail in atlastin-mediated membrane fusion. As described in Chapter 3, supportive to the *in vitro* data of McNew`s group revealing the role of the amphipathic helix within the tail in facilitating fusion by destabilizing the membranes, my data shows the requirement of this helix in ER network formation *in vivo*. Remarkably, the replacement of Drosophila ATL tail with ATL-1 tail in this study show partial rescue of the abolished *in vitro* fusion activity observed with tailless Drosophila ATL suggesting the conserved role for the amphipathic helix for all isoforms.

FIGURES

Figure 1-1 Different structural subdomains of the Endoplasmic Reticulum

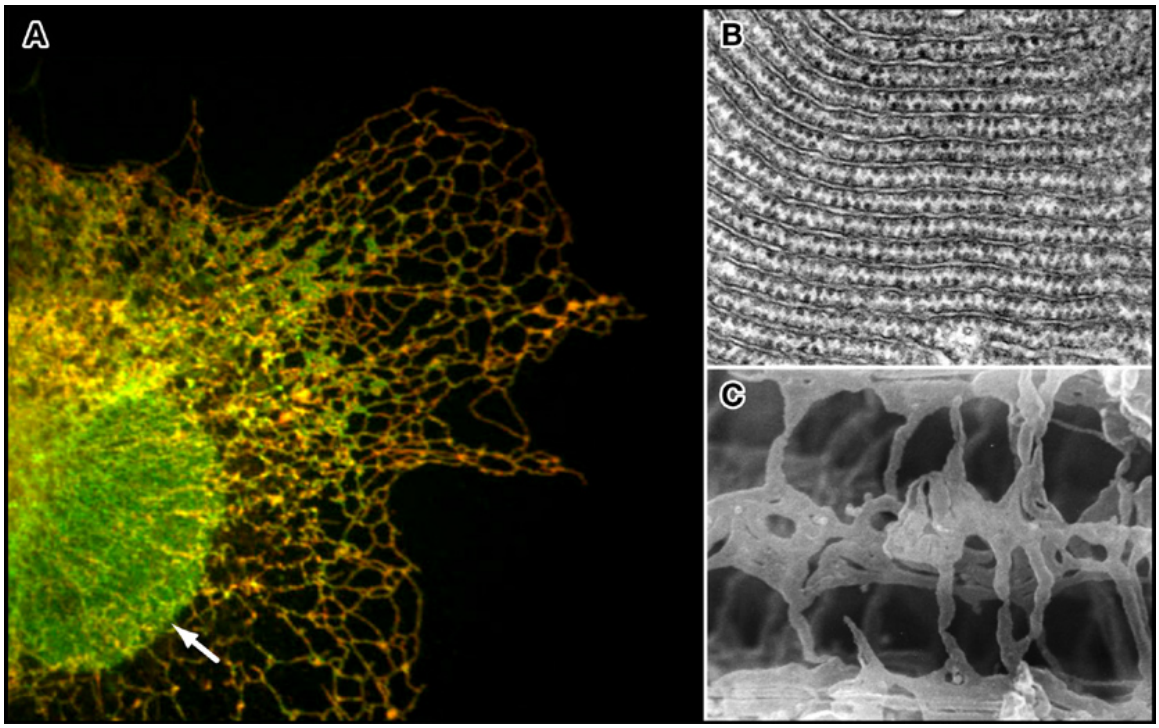

A) A cultured cell line coexpressing two ER markers shows the low-curvature domains of the nuclear envelope (arrow) and the cisternal sheets (green), as well as the high curvature domains of the peripheral tubules (red). **B)** Thin-section electron micrograph of the RER in secretory cells from the silk glands of the silkworm. **C)** Scanning electron micrograph of the SER in the sarcoplasmic reticulum of rat white skeletal muscle fibers. Note that the ER in (B) appears as sheets, whereas the SER in (C) is tubular. Figure is taken from *Shibata et al., 2006*.

Figure 1-2 Schematic diagram of factors that shape up Endoplasmic Reticulum

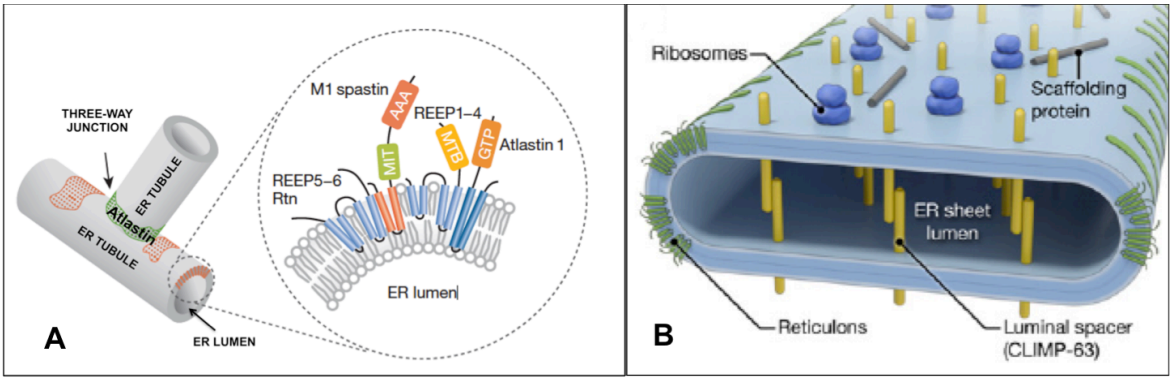

A) DP1/Reeps/Yop1 family proteins form oligomers that maintain and stabilize the curvature of ER tubules. Atlastin/RHD3/Sey1 proteins are shown at three-way junctions. Figure adapted from *Park et al., 2010.* **B)** Factors involved in the formation and stabilization of ER sheets. Climp-63. Figure taken from *Goyal et al., 2013*.

Figure 1-3 Crystal structures of ATL reveal insights into ATL-mediated fusion

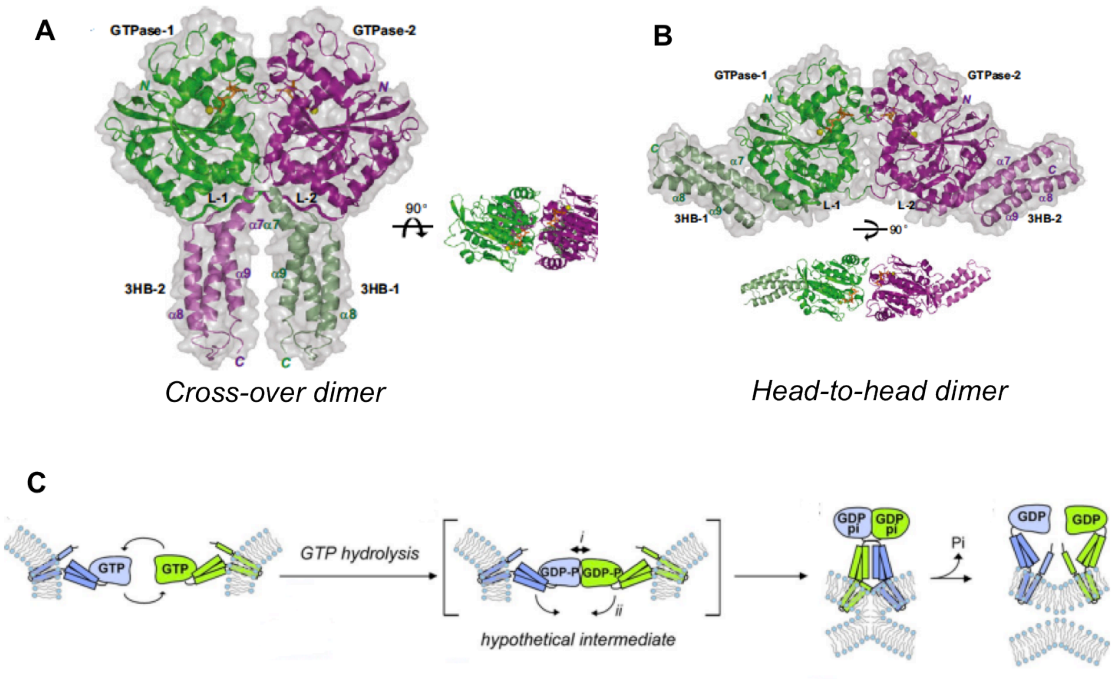

The crystal structures of Atlastin reveal two distinct dimer conformations where GTPase head domains of two ATL molecules interact with each other with the dimer interface near to the nucleotide binding pocket. **A)** In cross-over dimer form, the GTPase heads of each monomer are tightly 'engaged' with the respective three helix bundles (3HB) of the middle domains that pointing away from the dimer interface. **B)** In head-to-head dimer form, the three-helix bundles of the middle domains are 'dislodged' from the GTPase head running parallel upon crossing over each other (Crystal structures taken from Bian et al., 2011). **C)** Working model ATL catalyzed membrane tethering and fusion. Interaction between the GTP-bound head domain of two ATL monomers trigger GTP hydrolysis. 3HB are released upon GTP hydrolysis for cross-over. Stable trans pairing tethers opposing membranes to one another, while cross-over, with assistance from the tail, powers fusion. After fusion, Pi release may trigger dimer disassembly for subunit recycling (Panel C taken from *Saini et al., 2014*).

REFERENCES

Anwar, K., R.W. Klemm, A. Condon, K.N. Severin, M. Zhang, R. Ghirlando, J. Hu, T.A. Rapoport, and W.A. Prinz. (2012). The dynamin-like GTPase Sey1p mediates homotypic ER fusion in S. cerevisiae. J Cell Biol. 197:209-217.

Baumann, O. and Walz, B. (2001). Endoplasmic Reticulum of Animal Cells and Its Organization into Structural and Functional Domains. Int.REV.Cytol. 205, 149-214.

Blackstone, C. (2012). Cellular pathways of hereditary spastic paraplegia. Annu Rev Neurosci 35, 25-47.

Borgese, N., Francolini, M. and Snapp, E. (2006). Endoplasmic Reticulum Architecture: Structures in flux. Curr. Opin. Cell Biol 18, 358-364.

Byrnes , L.J. , and H. Sondermann. (2011). Structural basis for the nucleotide-dependent dimerization of the large G protein atlastin-1/SPG3A . Proc. Natl. Acad. Sci. 108 : 2216 – 2221

Chappie , J.S. , S. Acharya , M. Leonard , S.L. Schmid , and F. Dyda . (2010) . G domain dimerization controls dynamin's assembly-stimulated GTPase activity. Nature. 465 : 435 – 440

Daniele, T. and Schiaffino, M.V (2014) Organelle biogenesis and interorganella connections: Better in contact than in isolation. Commun Integr Biol. 23; 7

Daumke , O. , and G.J. Praefcke . (2011). Structural insights into membrane fusion at the endoplasmic reticulum . Proc. Natl. Acad. Sci. USA . 108 : 2175 – 2176

Dreier, L. Rapoport, ,T.A. (2000). In vitro formation of the endoplasmic reticulum occurs independently of microtubules by a controlled fusion reaction. J. Cell Biol. 148 883–898.

Elbaz, Y. and Schuldiner, M. (2011) Staying in touch: the molecular era of organelle contact sites. Trends Biochem Sci. 36(11):616-23

Evans, K., Keller, C., Pavur., K., Glasgow, K., Conn, B., Lauring B., (12006) Interaction of two hereditary spastic paraplegia gene profucts, spastin and atlastin, suggest a common pathway for axonal maintance. Pros Natl Acad Sci USA. 103(28):10666-71

Fassier, C., J.A. Hutt, S. Scholpp, A. Lumsden, B. Giros, F. Nothias, S. Schneider-Maunoury, C. Houart, and J. Hazan. (2010). Zebrafish atlastin controls motility and spinal motor axon architecture via inhibition of the BMP pathway. Nat

Neurosci. 13:1380-1387.

Faust, J.E., T. Desai, A. Verma, I. Ulengin, T.L. Sun, T.J. Moss, M.A. Betancourt, H.W. Huang, T. Lee, and J.A. McNew. (2015). The Atlastin C-terminal Tail is an Amphipathic Helix that Perturbs Bilayer Structure during Endoplasmic Reticulum Homotypic Fusion. J Biol Chem. 290(8):4772-83.

Fink, J.K. 2006. Hereditary spastic paraplegia. Curr Neurol Neurosci Rep. 6:65-76.

Friedman, J.R., Webster, B.M., Mastronarde, D.N., Verhey, K.J., Voeltz, G.K. (2010) ER sliding dynamics and ER-mitochondrial contacts occur on acetylated microtubules. J. Cell Biol. 190, 363–375

Ghosh , A. , G.J. Praefcke , L. Renault , A. Wittinghofer , and C. Herrmann . (2006). How guanylate-binding proteins achieve assembly-stimulated processive cleavage of GTP to GMP. Nature . 440 : 101 – 104

Goyal, U. and Blackstone, C. (2013). Untangling the web: Mechanisms underlying ER network formation. Biochimica et Biophysica Acta. 1833(11):2492-8.

Holmer, L., Worman, H.J. (2001). Inner nuclear membrane proteins: functions and targeting Cell Mol Life Sci. 58(12-13); 1741-7.

Hu, J., Shibata, Y.,Voss, C., Shemesh, T., Li, Z., Coughlin, M., Kozloc, M.M., Rapoport, T.A., Prinz, W.A. (2008) Membrane Proteins of the Endoplasmic reticulum Induce High Curvature Tubules. Science 319, 1247-50.

Hu, J., Shibata, Y., Zhu, P., Voss, Christiane, V., Rismanchi, N., Prinz, W.A., Rapoport, T. A., Blackstone, C. (2009) A Class of Dynamin-like GTPases Involved in the Generation of the Tubular ER Network. Cell 138, 549-561.

Lee, C., and Chen, L. B. (1998) Dynamic behavior of endoplasmic reticulum in living cells. Cell. 54:37–46.

Liu, T.Y., Bian, X., Sun, S., Hu, X., Klemm, R. W., Prinz, W.A., Rapoport, T. A., Hu, J. (2012). Lipid interaction of the C terminus and association of the transmembrane segments facilitate atlastin-mediated homotypic endoplasmic reticulum fusion. Proc. Natl. Acad. Sci. USA. 109(32);E2146-54.

Lu, L., Ladinsky, M.S. and Kirchhausen T., (2009) Cisternal Organization f the Endoplasmic Reticulum During Mitosis. Mol.Biol.Cell 20, 3471-3480.

McMahon, H.T. and Gallop, J.L. (2005)Membrane Curvature and Mechanisims of Dynamic Cell Membrane Remodelling. Nature 438, 590-6.

Morin-Leisk, J., Saini S.G., Meng, X., Makhov, A. M., Zhang, P., Lee, T. H. (2011) An intramolecular salt bridge drives the soluble domain of GTP-bound atlastin into the postfusion conformation. J. Cell Biol 195, 605-615.

Moss, T.J., C. Andreazza, A. Verma, A. Daga , and J.A. McNew. (2011).Membrane fusion by the GTPase atlastin requires a conserved C-terminal cytoplasmic tail and dimerization through the middle domain . Proc. Natl. Acad. Sci. 108 : 11133 – 11138

Namekawa, M., P. Ribai, I. Nelson, S. Forlani, F. Fellmann, C. Goizet, C. Depienne, G. Stevanin, M. Ruberg, A. Dürr, and A. Brice. (2006). SPG3A is the most frequent cause of hereditary spastic paraplegia with onset before age 10 years. Neurology. 66:112-114.

Orso, G., D. Pendin, S. Liu, J. Tosetto, T.J. Moss, J.E. Faust, M. Micaroni, A. Egorova, A. Martinuzzi, J.A. McNew, and A. Daga. (2009). Homotypic fusion of ER membranes requires the dynamin-like GTPase atlastin. Nature. 460:978-983.

Park, S.H. and Blackstone, C. (2010) Further Assembly Required: Construction and Dynamics of the Endoplasmic Reticulum Network. EMBO reports. 11, 515-21.

Patel, S.K., Indig, F.E., Olivieri, N., Levine, N.D., Latterich, M. (1998) Organelle membrane fusion: a novel functionfor the syntaxin homolog Ufe1p in ER membrane fusion. Cell. 92(5): 611-20

Praefcke , G.J. , and H.T. McMahon . (2004). The dynamin superfamily: universal membrane tubulation and fission molecules? Nat. Rev. Mol. Cell Biol. 5 : 133 – 147.

Prakash, B., G.J. Praefcke , L. Renault, A. Wittinghofer , and C. Herrmann. (2000). Structure of human guanylate-binding protein 1 representing a unique class of GTP-binding proteins. Nature . 403 : 567 – 571

Prinz,W.A., Grzyb, L., Veenhuis,M.,Kahana, J.A., Silver, P.A.,Rapoport,T.A. (2000) Mutants Affecting the Structure of the Cortical Endoplasmic Reticulum in *Saccharomyces cerevisiae*. The Journal of Cell Biology 150, 461-74.

Puhka, M., Vihinen, H., Joensuu, M. And Jokitalo, E. (2007) Endoplasmic Reticulum Remains Continuous and Undergoes sheet-to-tubule Transformation During Cell Division in Mammalian Cells. The Journal of Cell Biology 179, 895-909.

Renvoise, B. and Blackstone, C. (2010) Emerging Themes of ER Organization in the Development and Maintenance of Axons. Curr. Opin. Neur. 20, 531-7.

Rismanchi , N. , C. Soderblom , J. Stadler , P.P. Zhu , and C . Blackstone. (2008).

Atlastin GTPases are required for Golgi apparatus and ER morphogenesis . Hum. Mol. Genet. 17 : 1591 –1604.

Rowland, A.A., Chitwood, P.J., Phillips, M. J., Voeltz, G.K. (2014). ER contact sites define the position and timing of endosome fission. Cell 159(5): 1027-41

Saini, S.G., C. Liu, P. Zhang, and T.H. Lee. (2014). Membrane tethering by the atlastin GTPase depends on GTP hydrolysis but not on forming the crossover configuration. *Mol Biol Cell*. 25(24):3942-53.

Salinas, S., C. Proukakis, A. Crosby, and T.T. Warner. (2008). Hereditary spastic paraplegia: clinical features and pathogenetic mechanisms. *Lancet Neurol*. 7:1127-1138.

Sanderson CM, Connell J, Edwards TL, Bright NA, Duley S, Thompson A, Luzio P, Reid E. (2006). Spastin and atlastin, two proteins mutated in autosomal dominant hereditary spastic paraplegia, are binding partners. Hum Mol Genet. 15(2): 307-318.

Shibata,Y., Voeltz ,G.K. and Rapoport,T.A. (2006). Rough Sheets and Smooth Tubules. Cell. 126, 435-9.

Shibata,Y., Voss, C., Rist, J.M., Hu, J., Rapoport,T.A.,Prinz,W.A., Voeltz, G.K. (2008) The Reticulon and DP1/Yop1p Proteins Form Immobile Oligomers in the Tubular Endoplasmic Reticulum. The Journal of Biological Chemistry 283, 18892-18904.

Shibata, Y., Hu, J., Kozlov, M.M and Rapoport, T.A. (2009) Mechanisms Shaping the Membranes of Cellular Organelles Annu Rev Cell Dev Biol. 25, 329-54.

Shnyrova, A., Frolov, V.A. and Zimmerberg, J. (2008) ER Biogenesis: Self-Assembly of Tubular Topology by Protein Hairpins. Current Biology 18.

Sidrauski C and Walter P. (1997).The Transmembrane Kinase Ire1p Is a Site-Specific Endonuclease That Initiates mRNA Splicing in the Unfolded Protein Response. Cell. 90, 1031–1039

Terasaki, M., L.B. Chen, and K. Fujiwara. (1986). Microtubules and the endoplasmic reticulum are highly interdependent structures. J Cell Biol. 103:1557-1568.

Terasaki M and Jaffe LA. (1991).Organization of the sea urchin egg endoplasmic reticulum and its reorganization at fertilization. J. Cell Biol., 114, 929–940

Terasaki, M., N.T. Slater, A. Fein, A. Schmidek, and T.S. Reese. (1994). Continuous network of endoplasmic reticulum in cerebellar Purkinje neurons. Proc Natl Acad Sci U S A. 91:7510-7514.

Vedrenne,C., Hauri, H.P. (2006). Morphogenesis of the endoplasmic reticulum: beyond active membrane expansion, Traffic 639–646

Voeltz, G.K., Rolls, M.M. and Rapoport, T.A. (2002). Sturctural Organization of the Endoplasmic Reticulum. EMBO reports 3, 944-950.

Voeltz, G.K., Prinz, W.A., Shibata, Y., Rist, J.M and Rapoport, T.A. (2006). A Class of Membrane Proteins Shaping the Tubular Endoplasmic Reticulum. Cell 124, 573-586.

Voeltz, G.K. and Barr, F.A. (2013). Cell organelles. Curr Opin Cell Biol 25(4):403-5

Waterman-Storer, C.M. and E.D. Salmon. (1998). Endoplasmic reticulum membrane tubules are distributed by microtubules in living cells using three distinct mechanisms. Curr. Biol. 8:798-806.

Zhang, M., F. Wu, J. Shi, Y. Zhu, Z. Zhu, Q. Gong, and J. Hu. (2013). ROOT HAIR DEFECTIVE3 family of dynamin-like GTPases mediates homotypic endoplasmic reticulum fusion and is essential for Arabidopsis development. *Plant Physiol*. 163:713-720.

Zhao, X., D. Alvarado, S. Rainier, R. Lemons, P. Hedera, C.H. Weber, T. Tukel, M. Apak, T. Heiman-Patterson, L. Ming, M. Bui, and J.K. Fink. (2001). Mutations in a newly identified GTPase gene cause autosomal dominant hereditary

Zhu, P.P., A. Patterson, B. Lavoie, J. Stadler, M. Shoeb, R. Patel, and C. Blackstone. (2003). Cellular localization, oligomerization, and membrane association of the hereditary spastic paraplegia 3A (SPG3A) protein atlastin . J. Biol. Chem. 278 : 49063– 49071

Zhu, P.P., Soderblom, C., Tao-Cheng, J.H., Stadler, J. (2006). SPG3A protein atlastin-1 is enriched in outgrowth cones and promotes axon elongation during neuronal development. Human Molecular Genetics. 15(8) : 1343-1353.

CHAPTER 2

ER Network Formation and Membrane Fusion by atlastin1/SPG3A Disease Variants

ABSTRACT

At least 38 distinct missense mutations in the neuronal atlastin1/SPG3A GTPase are implicated in an autosomal dominant form of hereditary spastic paraplegia (HSP), a motor-neurological disorder manifested by lower limb weakness and spasticity and length dependent axonopathy of corticospinal motor neurons. Because the atlastin GTPase is sufficient to catalyze membrane fusion and required to form the ER network, at least in non-neuronal cells, it is logically assumed that defects in ER membrane morphogenesis due to impaired fusion activity are the primary drivers of SPG3A associated HSP. Here we analyzed a subset of established atlastin1/SPG3A disease variants using cell-based assays for atlastin-mediated ER network formation and biochemical assays for atlastin-catalyzed GTP hydrolysis, dimer formation and membrane fusion. As anticipated, some variants exhibited clear deficits. Surprisingly however, at least two disease variants, one of which represents that most frequently identified in SPG3A HSP patients, displayed wild type levels of activity in all assays.The same variants were also capable of co-redistributing ER-localized REEP1, a recently identified function of atlastins that requires its catalytic activity. Altogether, these findings indicate that a deficit in the membrane fusion activity of atlastin1 may be a key contributor, but not required, for HSP causation.

*This manuscript appeared as an article in the Molecular Biology of the Cell, and is reprinted here. **Ulengin, I**., Park, J., Lee, T.H. (2014). MBoC 25 (24).: 3942-3953. All experiments were performed by Ulengin, I and analyzed by Ulengin, I and Lee, TH. The manuscript was written by Ulengin, I and Lee, T.H.

INTRODUCTION

HSP is an uncommon but not rare disorder (afflicting ~3-9 per 100,000) that causes weakness and spasticity in the lower limbs of affected individuals while largely sparing the upper extremities (Blackstone, 2012; Depienne et al., 2007; Fink, 2006; Salinas et al., 2008). Post mortem analysis of HSP patients revealed a length dependent degeneration of the longest axons in the corticospinal tract (Deluca et al., 2004). Over 55 distinct spastic paraplegia genes (SPGs) have been identified (Lo Giudice et al., 2014) and the products can be grouped into functions having to do with axon pathfinding, myelination, receptor trafficking, organelle movement, mitochondrial function and ER morphogenesis (Blackstone et al., 2011). Consequently, a deficit in one or more cellular pathways necessary for long axon maintenance has been proposed to underlie the symptoms of HSP (Blackstone, 2012).

The original identification of atlastin1/SPG3A occurred through genetic analysis of three independent kindreds (ADHSP-P, ADHSP-T and ADHSP-S) each presenting with an early onset autosomal dominant form of HSP (Zhao et al., 2001). In each case, the disease segregated with a single genetic locus termed SPG3A (Gispert et al., 1995; Hazan et al., 1993) , which was ultimately narrowed to a 2.7 cM region on chromosome 14 (Rainier et al., 2001). Sequencing the open reading frames within the mapped region uncovered a point mutation in the atlastin1 gene in all three kindreds (Zhao et al., 2001). Each kindred had a distinct mutation, but within each kindred, the affected members were invariably positive for the same mutation at one of two alleles. None of the asymptomatic individuals had the mutation, indicating a high degree of penetrance (Zhao et al., 2001). Since its original identification, more than 30 additional atlastin1/SPG3A mutations, mostly mis-sense mutations within the GTPase domain, have been identified in early onset HSP patients (Guelly et al., 2011).

Atlastin1/SPG3A expression in vertebrates is enriched in the central nervous system (Zhao et al., 2001; Zhu et al., 2006). Accordingly, the first studies aimed at elucidating function utilized a neuronal cell culture model, in which, silencing of atlastin1 impaired axonal outgrowth (Zhu et al., 2006). Concurrent studies showed over-expression of an atlastin1/SPG3A mutant variant, localized to the ER in HeLa cells, perturbing ER network morphology in a dominant negative fashion, suggesting a possible role in ER

morphogenesis (Rismanchi et al., 2008). In support, siRNA-mediated depletion of the more ubiquitously expressed atlastin2 and atlastin3 isoforms also caused ER morphological abnormalities (Hu et al., 2009). Collectively, the data suggested a role for the atlastins in ER network morphogenesis.

Precisely how atlastins mediate ER morphogenesis remains to be elucidated. The similarity of the GTPase domain of atlastin to that of dynamins and mitofusins, mechanochemical enzymes that mediate membrane fission and fusion respectively (Praefcke and McMahon, 2004), led investigators early on to hypothesize a direct membrane-remodeling role (Rismanchi et al., 2008). Soon thereafter, purified Drosophila *melanogaster* atlastin was demonstrated sufficient to catalyze lipid bilayer fusion when incorporated into synthetic lipid vesicles (Orso et al., 2009). Fusion was GTP hydrolysis-dependent, prompting the idea that atlastin might represent the long sought GTP-dependent fusion machinery for the ER (Dreier, 2000). It is now known that atlastin, similar to dynamin (Chappie et al., 2010), and other GTPases that undergo nucleotide-dependent head-to-head dimerization (Gasper et al., 2009), forms a trans homodimer as it catalyzes GTP hydrolysis (Byrnes et al., 2013). Trans dimerization in atlastin is further accompanied by a rigid body rotation of a 3-helix bundle (3HB) connecting each GTPase head domain to its membrane anchor. This rotation causes the 3HB's to cross over one another and is proposed to bring the 3HBs, pointing away from the dimer interface and anchored in opposing membranes initially, into close parallel alignment such that they come to reside within the same membrane (Bian et al., 2011; Byrnes and Sondermann, 2011). Crossover is hypothesized to constitute the driving force for membrane fusion (Daumke and Praefcke, 2011).

The long axon degeneration associated with SPG3A-linked HSP could be explained simply by the inability of atlastin1/SPG3A disease variants to catalyze ER membrane fusion and network formation. While compelling, a clear demonstration of this hypothesis has remained elusive. In particular, the idea that a reduction in the membrane fusion activity of atlastin1/SPG3A causes HSP lacks strong support. This may be due in part to the lack of an ideal assay system: whereas the Drosophila orthologue (Orso et al., 2009), and more recently other atlastin counterparts in more distantly related organisms (Anwar et al., 2012; Zhang et al., 2013), have been shown to catalyze the fusion of synthetic membranes, the human proteins have not yet been demonstrated to possess

this activity for unknown reasons (Wu et al., 2015). Consequently, assessment of the fusion capability of atlastin1/SPG3A mutant variants has relied on transfer of point mutations to the Drosophila orthologue and only a few have been analyzed in this manner (Bian et al., 2011). Also, a large number of truncated atlastin1/SPG3A mutant variants were analyzed in the soluble phase for their ability to hydrolyze GTP and to dimerize in a nucleotide dependent manner (Byrnes and Sondermann, 2011). Surprisingly, no clear correlation between disease causing mutations and biochemical activity emerged from that analysis. For many variants, the impairment of GTP hydrolysis and dimer formation was modest at best (Byrnes and Sondermann, 2011).

The idea that SPG3A HSP is caused by ER morphology defects similarly lacks strong support. Simply put, the status of the ER in neurons expressing the SPG3A disease mutations remains unknown. This is due in part to the lack of an appropriate animal model for the disease. It may also be due to the peculiarities of neuronal cell shape, which renders the details of the branched tubular ER network a challenge to image (Dailey and Bridgman, 1989; Terasaki et al., 1994). In any case, further investigation is needed to determine whether atlastin1/SPG3A mutations invariably perturb ER network structure.

Our lab previously established a functional replacement assay which demonstrated the capacity of an exogenously introduced non-neuronal atlastin2 to mediate ER network formation in HeLa cells depleted of endogenous atlastins (Morin-Leisk et al., 2011). We recently showed that Drosophila atlastin was also capable of functionally replacing human atlastins in this system (Faust et al., 2015). Because Drosophila atlastin can catalyze membrane fusion in a robust fashion (Orso et al., 2009) and shares 66% amino acid identity with atlastin1 in its GTPase domain, we reasoned that analysis of the atlastin1/SPG3A mutations transferred to the Drosophila orthologue afforded a unique opportunity to simultaneously assess individual atlastin1/SPG3A mutations both for their effects on ER morphogenesis and on membrane fusion catalysis. Based on the current thinking in the field, we started with the hypothesis that each atlastin1/SPG3A mutant variant would exhibit a measurable deficit both in its ability to mediate network formation and in its ability to catalyze membrane fusion. Surprisingly, our results indicated that while this was the case for some of the variants, it was not the case for others. In particular, two of the three mutations (in the ADHSP-T and –S kindreds) that led to the

original identification of atlastin1/SPG3A (Zhao et al., 2001) caused no measurable deficit in any assay. Our findings lead us to question whether impaired ER membrane fusion is the sole driver of SPG3A HSP.

MATERIALS AND METHODS

Cell culture, constructs, transfections and reagents

HeLa and Cos-7 cells were maintained in MEM (Sigma-Aldrich). and DMEM (Sigma-Aldrich), respectively, containing 10% fetal bovine serum (Atlanta Biologicals) and 1% penicillin/streptomycin (Thermo Fisher Scientific) at 37°C in a 5% CO_2 incubator. PC12 cells were maintained on collagen IV (Sigma-Aldrich) coated plates in F12K media (Sigma-Aldrich) supplemented with 10% fetal bovine serum and 5% horse serum (Atlanta Biologicals). Transient plasmid DNA transfection of HeLa cells was performed using 1 µg DNA and 2 µl jetPEI™ (Polyplus) per 1 mL media according to the manufacturer's protocol. Cos-7 cell transfections were performed using 200 ng DNA and 1.5 µl Lipofectamine 2000 (Life Technologies) per 0.5 ml media, and PC12 transfections were performed using 1 µg DNA and 7.5 µl Lipofectamine in 1.5 ml OptiMEM (Life Technologies). Atlastin2/3 siRNA transfections, using atlastin2 (#1) and atlastin3 (#2) siRNAs identical in sequence to those previously published (Rismanchi et al., 2008) , were performed using 20 pmol siRNA (10 pmol of each) and 2 µl Oligofectamine (Life Technologies) in 0.5 ml media. eYFP-tagged *Drosophila melanogaster* atlastin (Faust et al., 2015), the 6xHis-tagged full length Drosophila atlastin (Saini et al., 2014), and the 6xHis-tagged soluble domain of Drosophila atlastin encoding amino acids 1 to 415 have been described previously (Saini et al., 2014). The N-terminally HA-tagged atlastin1 was constructed by substituting the atlastin2 coding sequence in HA-tagged atlastin2 within XbaI and EcoRI sites (Morin-Leisk et al., 2011) with a PCR amplified fragment encoding amino acids 1 to 558 of atlastin1. The REEP1-flag construct was generated by inserting the coding sequence of human REEP1 into the BamHI and ClaI sites of the Cs2+MT vector. Subsequently, the Myc tag at the C-terminus was replaced with the Flag epitope (DYKDDDDK) following a short linker sequence (HRFKA). The Myc-REEP5/DP1/TB2 construct was previously described (Morin-Leisk et al., 2011). All point mutations were generated using QuikChange site-directed mutagenic PCR (QIAGEN) and fully verified by sequencing (Genewiz). All lipids were purchased (Avanti Polar Lipids).. GTP, GDP, and GMPPNP were purchased (Sigma-Aldrich), reconstituted to 100 mM stocks in 10 mM Tris, 1 mM EDTA pH 8.0, and stored at -80°C. Antibodies used include a mouse monoclonal antibody (mAb) against the HA-epitope (Sigma-Aldrich); the 9E10 mAb against the Myc-epitope (gift from A. Linstedt); a Flag epitope mAb (Sigma-Aldrich); a

polyclonal antibody (pAb) against calnexin (Abcam); a pAb against REEP5 (Proteintech), and a pAb against tubulin (Abcam). Alexa 568-conjugated goat anti-mouse and FITC-conjugated goat anti-rabbit secondary antibodies, as well as BODIPY 493/503 were purchased (Life Technologies).

Knockdown replacement assay

Cells plated on 60-mm dishes were transfected with 5 µg of the indicated HA-atlastin1 or eYFP-Drosophila atlastin constructs using transfection reagent jetPEI™ (Polyplus). Myc-tagged ER resident protein REEP5/DP1/TB2, which did not affect either the percentage of cells showing the unbranched ER phenotype or the extent of loss of network branching relative to siRNA treatment alone (Morin-Leisk et al., 2011), served as a negative control. 24 h after DNA transfection, cells were trypsinized and replated onto 12-mm glass coverslips in a 24-well plate. siRNA treatment targeting both atlastin2 and atlastin3 was performed the next day. 72 h after knockdown, cells were fixed in ice-cold methanol and processed for immunofluorescence (Morin-Leisk et al., 2011). For quantification of functional replacement, the percentage of cells expressing the indicated HA-atlastin1 or eYFP-Drosophila atlastin that showed a loss of ER network branching (among ≥100 cells in there independent experiments) was counted. Nocodazole washout experiments were performed as follows: 72 h after the second transfection (siRNA treatment), cells were incubated in 1 ml media containing 1 µg/ml nocodazole for 3 h followed by washes with fresh media without nocodazole. Cells were fixed at the indicated times following washout and processed for immunofluorescence (Morin-Leisk et al., 2011).

Confocal microscopy

Cells were viewed using a spinning-disk confocal scanhead (Yokagawa; PerkinElmer) mounted on an Axiovert 200 microscope (Zeiss) with a 100x 1.4 NA objective (Zeiss) and acquired using a 16-bit ORCA-ER camera (Hamamatsu Photonics). Maximal value projections of sections at 0.2 µm spacing were acquired using Micro-manager open source software (UCSF) and imported either as 16-bit or 8-bit images in ImageJ open source software (NIH) or Adobe Photoshop (Adobe). For quantification of network branch points (Fig 2-1B), images of either control, eYFP-Drosophila atlastin or HA-atlastin1 expressing cells, acquired using identical acquisition parameters, were imported into ImageJ, where they were thresholded using a constant threshold value

and skeletonized. The average number of three-way junctions in each of five 10 μm x 10 μm boxed peripheral regions was then manually counted. Quantification of functional replacement was performed manually on a wide-field Axioplan fluorescence microscope (Carl Zeiss) with a 40x 1.4 NA objective.

REEP1 and atlastin1 co-redistribution assay

Cos-7 cells transfected with REEP1-Flag alone, eYFP-atlastin1 variants alone, or both, were fixed and stained using the Flag antibody 48 h after transfection and viewed by confocal microscopy. To determine whether the large structures to which REEP1 and atlastin1 redistributed to when co-expressed were lipid droplets, cells were co-transfected with REEP1-Flag and HA-atlastin1 variants, fixed 48 h later, and co-stained using either the Flag or HA antibody with BODIPY 493/503. The BODIPY 493/503 was dissolved in DMSO at 1 mg/ml and added to the secondary antibody incubation at 1 μg/ml as previously described (Klemm et al., 2013). Quantification of the number of large lipid droplet-like structures per cell was performed by importing confocal images, acquired as described above, into ImageJ and obtaining a count of particles >0.7 μm in diameter after thresholding. 5-10 fields were analyzed per atlastin1 variant.

Measurement of protein stability in PC12 cells

10 cm dishes of PC12 cells were each transfected with 5 μg HA-atlastin1 DNA and 30 μl Lipofectamine 2000 in 10 ml OptiMEM. Transfection media was replaced with growth media after 4 h. 24 h following transfection, cells on each dish were trypsinized and passed onto individual 3.5 cm dishes. Cycloheximide at a concentration of 0.1 mg/ml in growth media, well documented to block protein synthesis (Gilden and Carp, 1966) , was added 48 h following transfection for 0, 1, 2 or 4 h. Cells were harvested by scraping into ice cold PBS, collected by centrifugation at 6k rpm for 5 min, resuspended in RSB, resolved by SDS-PAGE, blotted onto nitrocellulose and probed using antibodies against the HA epitope to detect HA-atlastin1 and antibodies to detect endogenous calnexin. Longer incubation times (6-8 h or longer) with cycloheximide led to cell death as previously reported (Geier et al., 1992).

Protein expression and purification

Full length Drosophila atlastin protein expression was induced with 0.2 mM IPTG in BL21(DE3)pLysS cells at 16°C for 2.5 h. Cells were lysed in 4% Triton-X 100 (Roche) in

a standard lysis buffer (50 mM Tris-HCl pH 8.0, 5 mM $MgCl_2$, 500 mM NaCl, 10 mM Imidazole, 10% glycerol, 2 mM 2-mercaptoethanol, 1 µg/ml leupeptin and 1 µg/ml pepstatin) and 6xHis-tagged proteins purified using standard protocols on Ni^{+2} agarose beads (QIAGEN). Bound protein was eluted in 50 mM Tris, pH 8.0, 250 mM imidazole, 100 mM NaCl, 5 mM $MgCl_2$, 10% glycerol, 2 mM 2-mercaptoethanol, 0.1% Anapoe-X 100 (Affymetrix)., 1mM EDTA. Protein yields were typically 3–8 mg/ml (~1 mg per liter of culture), >85% pure, flash frozen in liquid N_2, and stored at -80°C. The 6His-tagged cytoplasmic domain of Drosophila atlastin protein expression was induced with 0.5 mM IPTG in BL21(DE3)pLysS cells at 20°C for 16 h, and purified using standard protocols for purification of 6His-tagged proteins on Ni^{+2} agarose beads (QIAGEN). Proteins, eluted in 50 mM Tris, pH 8.0, 250 mM imidazole, 100 mM NaCl, 5 mM $MgCl_2$, and 10% glycerol, were typically 10–24 mg/ml, >95% pure, flash frozen in liquid N_2, and stored at −80°C.

GTPase assay

Purified 6xHis-tagged Drosophila atlastin soluble domain (residues 1 to 415) and variant proteins were dialyzed into 50 mM Tris-HCl, pH 7.5, 100 mM NaCl, 1 mM $MgCl_2$ at 4°C and pre-cleared by centrifugation at 100,000 rpm (TLA100, Beckman) at 4°C for 15 min. GTPase activity was measured using the Enzchek Phosphate Assay kit (Life Technologies). A standard reaction for GTPase measurements involved mixing 1 U/ml purine nucleoside phosphorylase (PNP), 0.2 mM 2-amino-6-mercapto-7-methylpurine riboside (MESG) in the provided buffer (50 mM Tris–HCl, pH 7.5, 1 mM $MgCl_2$, 0.1 mM sodium azide) supplemented with 100 mM NaCl and 0.5 mM GTP in a total volume of 200 ml. After 10 min at 37°C, reactions were transferred to a 96-well plate (Costar) and started by addition of either buffer or 6xHis-tagged Drosophila atlastin variants at a final concentration of 1 or 2 mM. Absorbance at 360 nm was monitored at 30 s intervals for 30 min at 37°C in a plate reader (Tecan, Safire 2). Data were normalized to a phosphate standard and initial velocities calculated using the early linear portion of each curve.

Cross-linking

Purified 6xHis-tagged Drosophila atlastin soluble domain (residues 1 to 415) and variant proteins were dialyzed into SEC buffer (25 mM Tris-HCl pH 7.0, 100 mM NaCl, 5 mM $MgCl_2$, 2 mM EGTA). at 4°C and pre-cleared by centrifugation at 100,000 rpm for 15 min (TLA100). 5µM of each protein was incubated at RT in SEC buffer, pH 7.0, in the

absence or presence of 2 mM GMPPNP, GDP, GTP, GDP-AlF_4^- (2 mM GDP/2 mM $AlCl_3$/20 mM NaF) or AlF_4^- only (2 mM $AlCl_3$/20 mM NaF). After 30 min at RT, the reaction was diluted 2.5-fold into SEC (to 2 µM D-ATL) in the absence or presence of 6 µM BMOE (Thermo Fisher Scientific) and incubated for 1 h at RT. Samples were then quenched with 20 mM DTT for 15 min, mixed with reducing sample buffer, resolved by SDS-PAGE and stained with Coomassie Blue.

Proteoliposome production

Lipids in chloroform dried down by rotary evaporation were hydrated by resuspension in A100 Buffer (25 mM HEPES pH 7.4, 100 mM KCl, 10% glycerol, 2 mM b-mercaptoethanol, 1 mM EDTA) (Moss et al., 2011), final lipid concentration ~10 mM, and subjected to 12 freeze thaw cycles in liquid N_2 and room temperature water. 100-300 nm diameter liposomes were formed by extrusion through 100 nm polycarbonate filters using the LipoFast LF-50 extruder (Avestin). Unlabeled liposomes consisted of POPC:DOPS (85:15) and labeled liposomes had POPC:DOPS:NBD-DPPE:rhodamine-DPPE (82:15: 1.5:1.5). Drosophila atlastin in 0.1% Anapoe-X 100 was reconstituted into pre-formed 100 nm liposomes as previously described (Moss et al., 2011). In brief, reconstitutions were carried out at a protein to lipid ratio of 1:300 or 1:1000 at a constant lipid concentration and an effective detergent-to-lipid ratio of ~0.7 as previously described (Moss et al., 2011). Protein and lipid were incubated at 4°C for 1 h. Detergent was removed by SM-2 Bio-Beads (BioRad) at 70 mg Triton-X 100 per 1 g of beads. Insoluble protein aggregates were pelleted by centrifugation of the samples in a microcentrifuge for 10 min at 16,000 x g. Thereafter, reconstituted Drosophila atlastin proteoliposomes were adjusted to 50% Nycodenz and separated from unincorporated protein by flotation of proteoliposomes through a (50%/45%/0%) Nycodenz (Axis-Shield). 5 ml step gradient. All Nycodenz solutions were made in A100 Buffer without glycerol. After centrifugation at 40 k rpm for 16 h at 4°C in a SW-50.1 rotor, the gradient was fractionated and analyzed by SDS-PAGE stained with Coomassie Blue to assess insertion efficiency (Fig S2-3 and Fig S2-4). The proteoliposomes typically migrated to the 45%/0% Nycodenz interface. Finally, the floated fraction was desalted over a 2.4 ml Sephadex A (GE Healthcare) column into A100 Buffer, stored at 4°C and used within 72 h.

Fusion Assay

Fusion assays were performed as previously described (Moss et al., 2011; Orso et al., 2009). Donor (0.2 mM) and acceptor proteoliposomes were mixed at varying molar ratios of 1:1, 1:2 and 1:3 in A100 Buffer in the presence of 5 mM $MgCl_2$ in a total volume of 200 µl per reaction. The reaction mixture was transferred into a clear, flat-bottomed polystyrene 96-well plate (Corning) and incubated at 37°C for 10 min. The fusion reaction was started by addition of 2 mM GTP (final concentration) or buffer. NBD fluorescence (excitation 460 nm, emission 538 nm) was measured at 1-min intervals with a 1 sec shaking after every read. After 60 min, 10 µl of 10% Anapoe-X 100 was added to determine the total fluorescence in the sample. All measurements, reported as the percent of total fluorescence after solubilization in Anapoe-X 100, were acquired on a Tecan Safire II fluorescence plate reader using Microsoft Excel.

RESULTS

Atlastin1/SPG3A mutations

Atlastins consist of a large globular cytoplasmic GTPase domain followed by a 3HB, which is in turn anchored to ER membranes by a pair of trans-membrane helices and a cytoplasmic tail (Bian et al., 2011; Byrnes and Sondermann, 2011; Rismanchi et al., 2008). Fig 2-1 shows the identity and location of the 38 distinct atlastin1/SPG3A mutations identified at the time of a recent report (Guelly et al., 2011) and further updated on the Human Gene Mutation Database (www.hgmd.cf.ac.uk/ac/search.php). A number of variants were previously produced in truncated form and analyzed in the soluble phase (Byrnes and Sondermann, 2011). Some were insoluble when expressed in *E. coli*, consistent with protein folding or stability issues (Fig 2-1, underlined mutations) (Byrnes and Sondermann, 2011); others, including R217Q and Q191R, were stably expressed but strongly defective in dimerization and/or GTP hydrolysis (Byrnes and Sondermann, 2011). The basis for disease causation for those variants seemed clear. Interestingly however, a substantial number of the remaining variants showed only modest impairment in dimerization and/or GTP hydrolysis (Byrnes and Sondermann, 2011). To better understand the basis for disease for these mildly impaired variants, we set out to analyze them using broader functional assays encompassing ER network formation and membrane fusion catalysis.

Not all SPG3A/atlastin1 mutations impair ER network formation

To assess ER network formation, we used HeLa cells because their relatively flat shape renders imaging of the branched tubular morphology of the ER network straightforward. As previously reported (Hu et al., 2009; Morin-Leisk et al., 2011), RNAi-mediated atlastin2/3 knockdown perturbed the ER in HeLa. Whereas the ER in nearly all control cells consisted of a densely branched network of polygons (Fig 2-2A and inset; quantified in Fig 2-2E,F), ER tubules ran largely parallel to one another in 57% of knockdown cells, and there was a significant reduction in three-way junctions in those cells (Fig 2-2B and inset; quantified in Fig 2-2E,F). Expression of either eYFP-tagged Drosophila atlastin (Fig 2C and inset; quantified in Fig 2-2E,F), or HA-tagged atlastin1 (Fig 2-2D and inset; quantified in Fig 2-2E,F), maintained normal network branch point density after endogenous atlastin depletion, and the percent of cells with an unbranched ER phenotype fell from 57% to 1% or 0.8% of cells expressing eYFP-Drosophila atlastin

or HA-atlastin1, respectively. To monitor ER morphology in untreated and control RNAi-treated cells (Fig 2-2A,B), we used a Myc-tagged version of the tubular ER marker REEP5/DP1/TB2 (Hashimoto et al., 2014), which by itself had no discernable impact on ER morphology in either control or knockdown cells (Morin-Leisk et al., 2011). Overall, our observations were consistent with recent reports of phenotypic rescue of RNAi-induced ER defects by Drosophila atlastin in HeLa (Faust et al., 2015) and by atlastin1 and Drosophila atlastin in Cos-7 cells (Wu et al., 2015). The similarity of morphological rescue by these distinct atlastins underscored the conservation of atlastin function in ER network morphogenesis.

We next assessed individual atlastin1/SPG3A mutant variants that previously showed only modest impairment in soluble phase assays (Fig 2-1, highlighted in green). As a control, we included R217Q, reported to lack both GTP hydrolysis and dimerization ability due to mutation of a key GTP binding residue (Byrnes and Sondermann, 2011; Rismanchi et al., 2008). As anticipated, the R217Q atlastin1 variant was unable to maintain a branched ER network, similar to the negative control (Fig 2-3A, quantified in 3B). Lack of function was also observed for Y196C and L250P atlastin1 (Fig 2-3A, quantified in 2-3B). Y196C atlastin1 exerted such a strong dominant negative effect that it further increased the fraction of knockdown cells with abnormal ER morphology, from 57% in the control, to 98% (Fig 2-3B). Likely, this variant perturbed ER network formation even in cells with only partial atlastin2/3 knockdown. Co-staining for the tubular ER marker REEP5/DP1/TB2 indicated that all three non-functional variants retained ER-localization (Fig S2-1). In sum, even though Y196C and L250P showed only modest deficits when analyzed in the soluble phase (Byrnes and Sondermann, 2011), they exhibited strong defects in our functional replacement assay. Surprisingly however, and in clear contrast, several atlastin1/SPG3A variants scored as well as the wild type (Fig 2-3A, quantified in 2-3B). Notably, these functional variants included R239C, H258R and S259Y atlastin1, corresponding to the ADHSP-S, ADHSP-T and ADHSP-P familial mutations that originally led to the identification of atlastin1/SPG3A.

We wondered whether the apparent functionality of these prominent disease variants might be due to the order of manipulations in our replacement assay. As expression of the test atlastin1 variant was typically induced prior to RNAi treatment, it was possible that these “functional” variants might be capable of sustaining an ER network already

established prior to knockdown, but incapable of mediating network formation de novo. To address this possibility, we carried out a nocodazole washout regime. Nocodazole treatment abolishes the microtubule tracks upon which ER membranes extend (Friedman et al., 2010; Waterman-Storer, 1998) thereby inducing a near complete retraction of the ER towards the cell center and loss of the peripheral tubular network (Lu et al., 2009; Terasaki et al., 1986). Upon drug washout, microtubule reassembly provides new tracks for ER network reformation (Terasaki et al., 1986). As shown (Fig S2-2) and quantified (Fig 2-3C), there was no significant difference in re-establishing an ER network between cells rescued with wild type or R239C atlastin1. The percent of cells displaying a branched tubular ER network decreased in dramatic fashion after nocodazole treatment, from 99% to 13% for wild type and 12% for R239C atlastin1. By 30 min after drug washout, the percent of cells with branched ER rose to 44% for both wild type and R239C atlastin1. By 120 min, 72% (± 7.8 S.D.) of wild type and 68% (± 8 S.D.) of R239C atlastin1 cells displayed network branching (Fig 2-3C, Fig S2-2), indicating similar and substantial network reformation in both. Therefore, R239C atlastin1, and likely the other functional SPG3A variants, were capable of supporting de novo ER network formation.

SPG3A/atlastin1 variants that are functional in ER network formation are also functional in co-redistribution of ER-localized REEP1

A recent study has suggested a conserved role for atlastins in the formation of large lipid droplets. Atlastin depletion caused a reduction in lipid droplet size in the intestinal cells of C. elegans, as well as in the fat bodies of Drosophila (Klemm et al., 2013). Conversely, atlastin1 over-expression induced the appearance of large lipid droplet like structures in Cos-7 cells, though the enlargement required joint over-expression of REEP1, an ER structuring protein that binds and bundles microtubules (Klemm et al., 2013; Park et al., 2010). In this instance, the atlastin1 and REEP1 were largely redistributed from ER and ER/microtubule structures, respectively, to structures coincident with BODIPY 493/503 staining, an accepted marker of lipid droplets (Listenberger and Brown, 2007). This ability of atlastin1 to co-redistribute REEP1 was not seen with several atlastin1 variants defective for membrane fusion (Klemm et al., 2013), suggesting that both the ER network formation and lipid droplet enlargement functions of atlastins depended on membrane fusion catalysis. Whether the apparent atlastin requirement for lipid droplet enlargement reflected a direct or indirect

requirement for atlastin's fusion function remains to be clarified (Klemm et al., 2013). Nevertheless, it seemed reasonable that analysis of disease variants for their functionality in this new assay might reveal deficits not detectable in our ER network formation assay.

As reported previously (Klemm et al., 2013), exogenous atlastin1 localized to the ER when expressed in Cos-7, and exogenous REEP1 accumulated in microtubule-associated ER structures (Fig S2-3). In contrast, co-expression drove both atlastin1 and REEP1 into enlarged lipid droplet like structures similar to those seen previously (Fig 2-4A, quantified in 2-4B). Curiously, these structures did not co-localize with the lipid droplet marker BODIPY 493/503 (Fig S2-4). The basis for our inability to detect BODIPY staining in these structures remains to be clarified. It could reflect differences in the ratios and/or levels of atlastin1 and REEP1 used; or it could reflect a difference in the staining procedure. Nevertheless, the R217Q atlastin1 variant was altogether unable to induce co-redistribution of REEP1 (Fig 2-4A,B), consistent with the previous report (Klemm et al., 2013). The Y196C and L250P variants had significantly reduced activity in this assay, as anticipated, but still induced some redistribution (Fig 2-4A,B). In contrast, both the R239C and H258R atlastin1 variants co-redistributed REEP1 to large structures to an extent indistinguishable from the wild type (Fig 2-4A,B).

Select atlastin1/SPG3A mutations do not impair ER network formation by either atlastin1 or Drosophila atlastin

Based on the unexpected functionality of certain atlastin1/SPG3A disease variants in ER network formation as well as REEP1 co-redistribution, it was imperative that they be characterized in terms of their effects on membrane fusion catalysis. As mentioned above, few if any Drosophila counterparts of atlastin1/SGP3A variants had been characterized previously. Therefore, we set out to analyze the effects of these mutations when transferred to the Drosophila orthologue. Our overall plan was to first assess Drosophila versions of the variants in ER network formation, then to determine their ability to hydrolyze GTP and form crossover dimers, and finally to measure their ability to catalyze membrane fusion.

The R239C and S259Y atlastin1 variants were constructed in Drosophila atlastin simply by substituting the identical residues in Drosophila atlastin, after sequence alignment, to

R214C and S234Y, respectively. For H258R and S398Y, where the corresponding residue in Drosophila atlastin was similar but not identical, the Drosophila residue was converted to that present in the disease variant. When the eYFP-tagged Drosophila atlastin variants were tested, one, A373Y (S398Y in atlastin1) was clearly non-functional (Fig 2-5A, quantified in 2-5B), as would have been expected for its atlastin1 counterpart. However, in contrast to this variant, the three other Drosophila atlastin variants (R214C, S233R, S234Y corresponding to R239C, H258R, S259Y in atlastin1) were again indistinguishable from the wild type (Fig 2-5A,B). Notably, these were the same variants present in the ADHSP-S, ADHSP-T and ADHSP-P kindreds, respectively (Zhao et al., 2001).

Atlastin1/SPG3A mutations R239C, H258R and S259Y, do not impair Drosophila atlastin GTPase activity

Our results thus far established that, contrary to our initial expectations, three prominent atlastin1/SPG3A variants, whether in the context of atlastin1 or Drosophila atlastin, lacked any detectable deficit in cell-based assays. To biochemically characterize the *Drosophila* versions, we first transferred each mutation to the truncated Drosophila atlastin soluble domain (aa 1-415) and performed a standard GTPase assay (Orso et al., 2009). As points of reference, we also included two variants that were incompetent for ER network formation: Y171C and A373Y (Y196C and S398Y in atlastin1). Consistent with their lack of ER network formation functionality (Fig 2-5A,B), both the Y171C and A373Y variants had reduced GTPase activity (Fig 2-6A). In contrast, the other three variants were indistinguishable from the wild type (Fig 2-6A).

Atlastin1/SPG3A mutations R239C, H258R and S259Y, do not impair Drosophila atlastin crossover dimer formation

The same soluble domain variants were next subjected to an assay for nucleotide dependent crossover dimer formation, which is essential for membrane fusion catalysis (Bian et al., 2011; Pendin et al., 2011; Saini et al., 2014). The assay, developed originally in our lab for atlastin2 (Morin-Leisk et al., 2011) , relies on the conjugation of two 3HB cysteines to one another by the short (8Å) spacer arm sulfhydryl cross-linking reagent bismaleimidoethane (BMOE) when atlastin is in the crossover dimer configuration, but not when it is either monomeric or in the extended dimer configuration. Because Drosophila atlastin lacked a cysteine at the same position, the corresponding

glycine residue was cysteine-substituted to generate G343C Drosophila atlastin. Prior analysis had indicated that the cysteine substitution did not at all impair membrane fusion functionality (Saini et al., 2014). As anticipated and recently reported (Saini et al., 2014), cross-linked wild type (G343C) crossover dimers were recovered after incubation with GMPPNP, GTP or GDP-AlF_4^-, but not with GDP, AlF_4^- alone, or in the absence of nucleotide (Fig 2-6B). This behavior largely mirrored that previously observed for atlastin2 (Morin-Leisk et al., 2011). It was also consistent with a FRET-based stopped flow kinetic analysis of the atlastin1 soluble domain showing rapid though transient crossover dimer formation with GTP, slower but irreversible crossover dimer formation with either GMPPNP or GDP-AlF_4^-, and no activity with GDP or in the absence of nucleotide (Byrnes et al., 2013). Consistent with their reduced GTPase activity (Fig 2-6A), neither the Y171C nor A373Y variant was captured in the crossover dimer conformation under any nucleotide incubation condition (Fig 2-6B). Thus, each of the variants that showed defects in our cell-based network formation assay (Fig 2-5A,B) also had strong defects in crossover dimer formation. In striking contrast, R214C, S233R and S234Y were each fully capable of forming the crossover dimer and did so in a nucleotide-dependent manner mirroring that of the wild type protein (Fig 2-6B).

Drosophila atlastin variants, with R239C, H258R and S259Y SPG3A equivalent mutations, are fusion competent

The three functional variants were finally expressed in the context of the full-length Drosophila protein, purified, incorporated into proteoliposomes and subjected to an established assay for atlastin-catalyzed membrane fusion (Bian et al., 2011; Orso et al., 2009). Again as a point of reference, we included the Y171C variant (Y196C in atlastin1), expected to lack fusion activity due to its inability to mediate ER network formation (Fig 2-5A,B) as well as its reduced ability to hydrolyze GTP (Fig 2-6A) and inability to form crossover dimers (Fig 2-6B). All variants were purified in similar quantities, indicative of comparable protein stabilities, and incorporated into donor and acceptor vesicles with similar efficiencies (Fig S2-5). As expected (Fig 2-7), the wild type protein catalyzed fusion robustly, with similar kinetics and to a similar extent as previously reported (Bian et al., 2011; Moss et al., 2011; Orso et al., 2009). Also as expected, the Y171C variant had no fusion activity (Fig 2-7). Remarkably though, all three variants R214C, S233R and S234Y (R239C, H258R and S259Y in atlastin1) were clearly competent for fusion catalysis. S234Y appeared slightly less active, but both

R214C and S233R appeared indistinguishable from the wild type (Fig 2-7). To obtain a more quantitative comparison of the activities of R214C and S233R relative to wild type, fusion was monitored at a lower protein to lipid ratio (1:1000), at which, the efficiency of incorporation into donor and acceptor vesicles was again similar between variants (Fig S2-6). As expected, the lower protein to lipid ratio resulted in slightly slower and less efficient fusion for the wild type protein (Fig 2-8). Even under these conditions however, both R214C and S233R were at least as active as the wild type in their ability to catalyze membrane fusion (Fig 2-8). In sum, neither disease variant could be distinguished from the wild type in any of our assays for atlastin functionality.

FIGURES

Figure 2-1 Atlastin1/SPG3A mutations

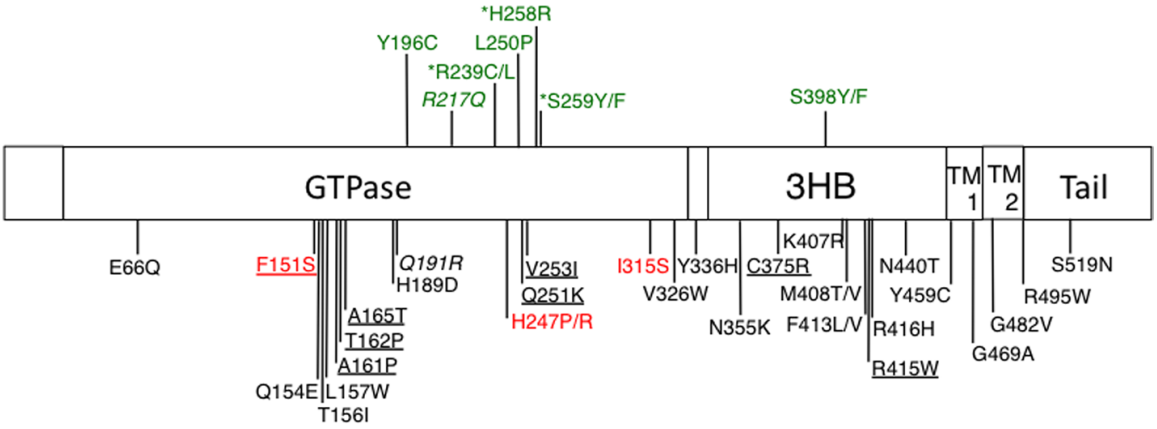

The positions of known atlastin1/SPG3A mutations as of a recent report (Guelly at al, 2011) and further updated (www.hgmd.cf.ac.uk/ac/search.php). are indicated on an atlastin1 primary sequence map. Mutations that caused insolubility when expressed in the context of the atlastin1 soluble domain are underlined (Byrnes et al, 2011); mutations that greatly reduced GTPase activity or dimer formation are italicized; mutations that inhibited fusion activity when transferred to Drosophila atlastin are in red (Bian et al, 2011); mutations occurring in the families ADHSP-P, ADHSP-T and ADHSP-S are indicated by an asterisk (Zhao et al, 2011); and the mutations analyzed within this study are in green.

Figure 2-2 Atlastin1 and Drosophila atlastin maintain a normal branched ER network in HeLa cells in the absence of atlastin2/3

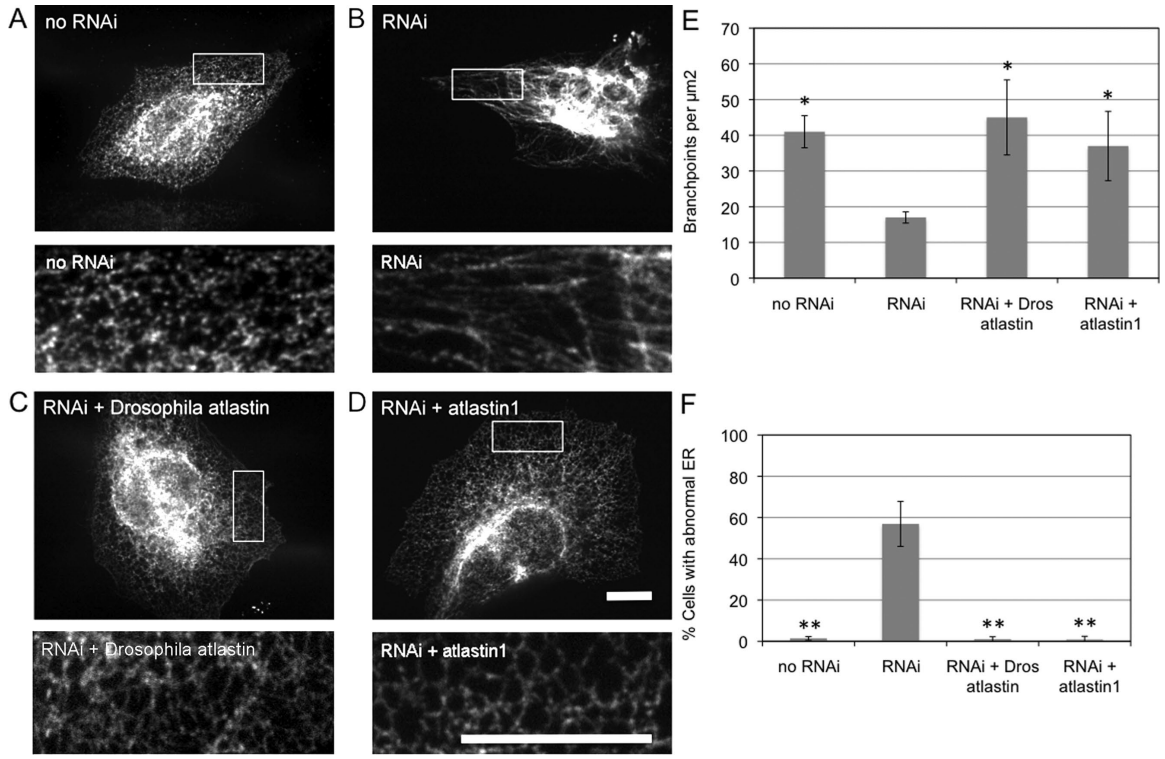

48 h after transfection with Myc-tagged REEP5/DP1/TB2 (neg con) **(A, B).**, eYFP-tagged Drosophila atlastin **C)** or HA-tagged atlastin1 **D)**, cells were either left untreated **A)** or further transfected using siRNAs targeting atlastin2/3 **(B-D)** 72 h after knockdown, cells were fixed and stained using an antibody against the Myc or HA epitope and viewed by confocal microscopy. Scale bars, 10 µm. The insets in each **(A-D)** show magnified views of a boxed region of the peripheral ER. **E)** Quantification of the average number of network branchpoints (+/- S.D.) in 5 representative 100 μm^2 boxed peripheral regions of the ER under each condition. **F)** Quantification of the percent of cells, expressing Myc-REEP5/DP1/TB2 (with or without RNAi), eYFP-Drosophila atlastin (with RNAi), or HA-atlastin1 (with RNAi), that displayed an abnormal unbranched ER morphology. Values represent the means of 3 independent experiments (>100 cells each) +/- S.D. *$p<0.001$ and **$p<0.0001$ (unpaired student's t-test) relative to the RNAi-treated negative control.

Figure 2-3 Some but not all atlastin1/SPG3A variants are defective in forming a branched ER network

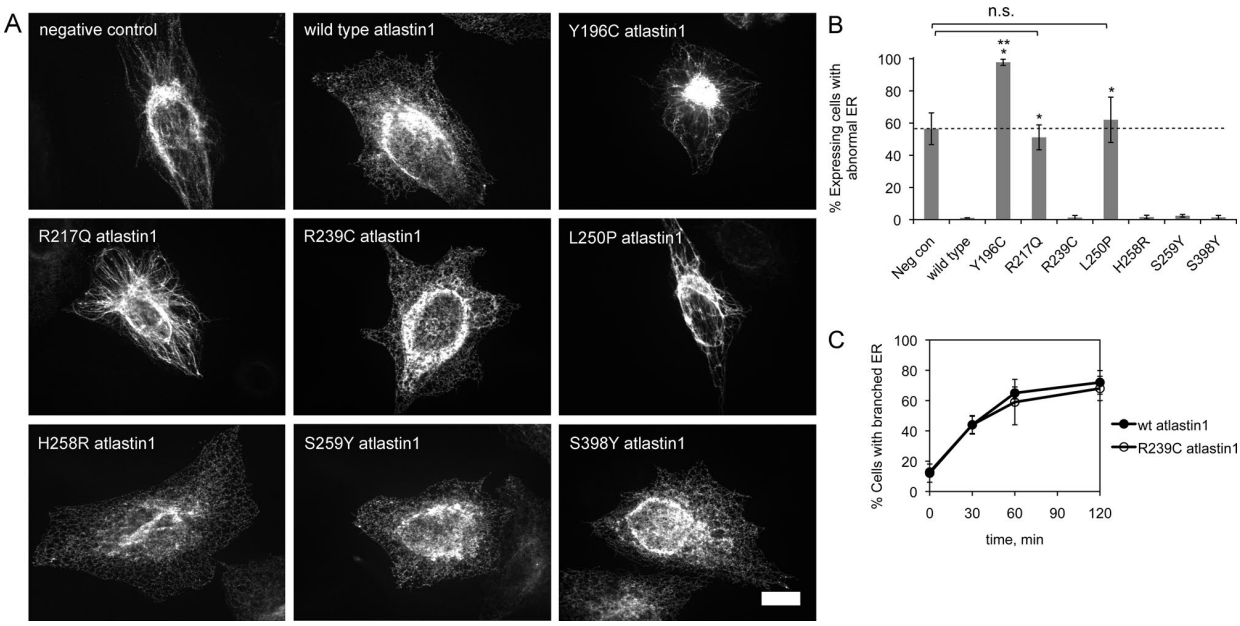

A) 48 h after transfection with the indicated HA-tagged atlastin1 variant constructs, HeLa cells were further transfected using siRNAs targeting endogenous atlastin2/3. 72 h after knockdown, cells were fixed and stained using an antibody against the HA epitope and viewed by confocal microscopy. The negative control was Myc-tagged REEP5/DP1/TB2 stained with an antibody against the Myc epitope. Scale bar, 10 μm. **B)** Quantification of the percent of cells, expressing the HA-or Myc-tagged construct, showing an abnormal unbranched ER morphology. Values represent the means of 3 independent experiments (>100 cells each) +/- S.D. *p<0.0001 with respect to the wild type and **p<0.0001 with respect to the negative control. R217Q and L250P were not significantly different from the negative control (unpaired Student's t-test). **C)** Quantification of de novo branched ER network formation. After knockdown and replacement with either HA-tagged wild type or R239C atlastin1 as in **(A)**, cells were treated for 3 h with nocodazole to induce microtubule depolymerization and ER collapse, followed by drug washout. At the indicated times, cells were fixed and stained with antibodies against HA and tubulin (Fig S2-2). The percent of cells expressing the HA-tagged construct and displaying a normal branched ER morphology was quantified. Values represent the means of 3 independent experiments (>100 cells each) +/- S.D.

Figure 2-4 Some but not all atlastin1/SPG3A variants are defective in co-redistributing REEP1

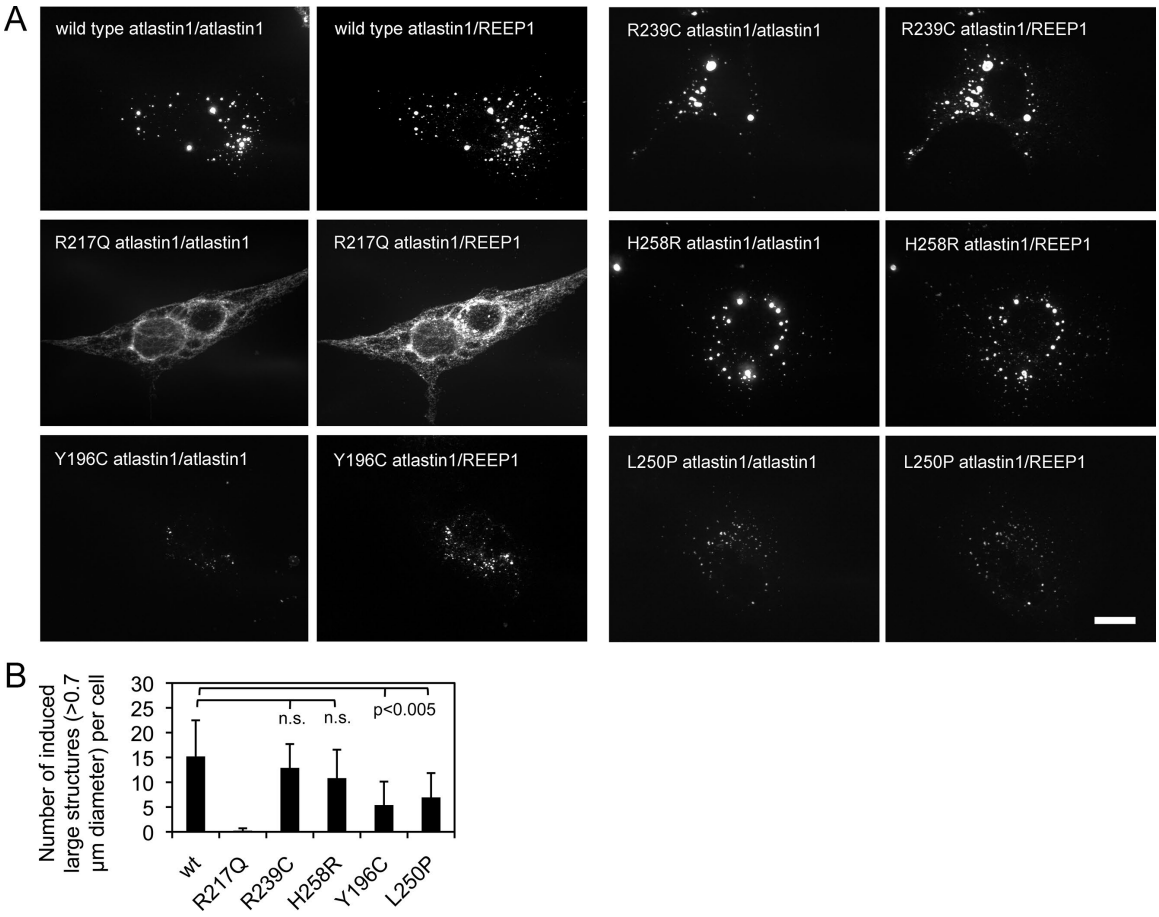

A) The indicated eYFP-atlastin1 and variants were transfected into Cos-7 cells together with Flag-tagged REEP1. 48 h after transfection, cells were fixed and stained with the Flag epitope antibody and viewed by confocal microscopy. Scale bar, 10 µm. **B)** The average number of large structures containing both REEP1 and atlastin1 (>0.7 µm diameter) per cell +/- S.D. (>10 cells) were quantified in ImageJ. Both the wild type and each of the variants were clearly different from the nucleotide binding defective R217Q variant ($p=0.007$ for L250P and $p<0.0001$ for all others). Y196C and L250P had reduced activity compared to the wild type ($p<0.005$) whereas R239C and H258R were not significantly different (n.s.) from the wild type ($p=0.41$ and 0.14 respectively).

Figure 2-5 Some but not all SPG3A mutations impair ER network formation when expressed in Drosophila atlastin

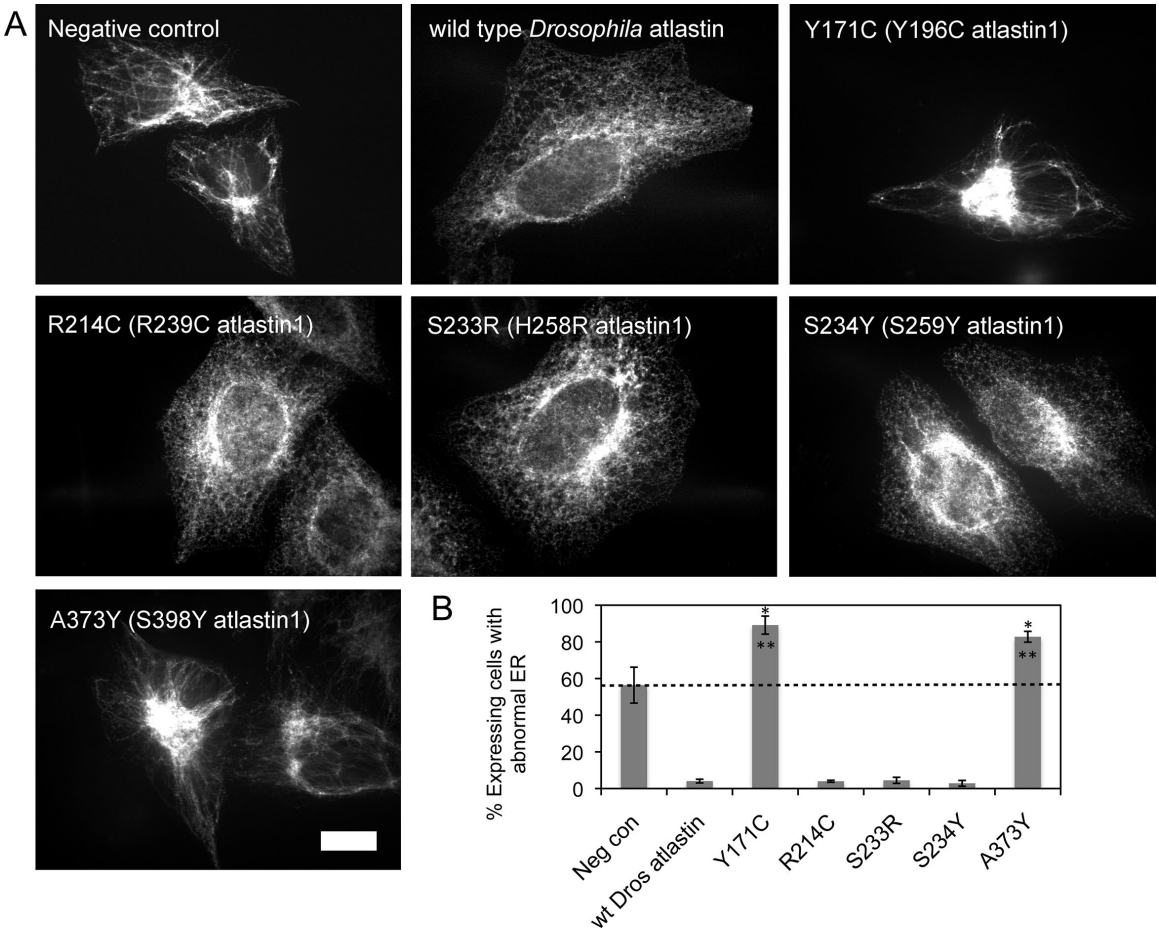

A) 48 h after transfection with the indicated eYFP-tagged Drosophila atlastin variant constructs, HeLa cells were further transfected using siRNAs targeting endogenous atlastin2 and atlastin3. 72 h after knockdown, cells were fixed and viewed by confocal microscopy. The negative control Myc-tagged REEP5/DP1/TB2 was stained with an antibody against the Myc epitope. Scale bar, 10 µm. **B)** Quantification of the percent of cells, expressing either the Myc-tagged or eYFP-tagged construct, showing an abnormal unbranched ER morphology. Values represent the means of 3 independent experiments (>100 cells each) +/- S.D. *$p<0.0001$ with respect to the wild type and **$p<0.004$ with respect to the negative control (unpaired Student's t-test).

Figure 2-6 GTP hydrolysis and crossover dimer formation capabilities of SPG3A variants in the context of the Drosophila atlastin soluble domain

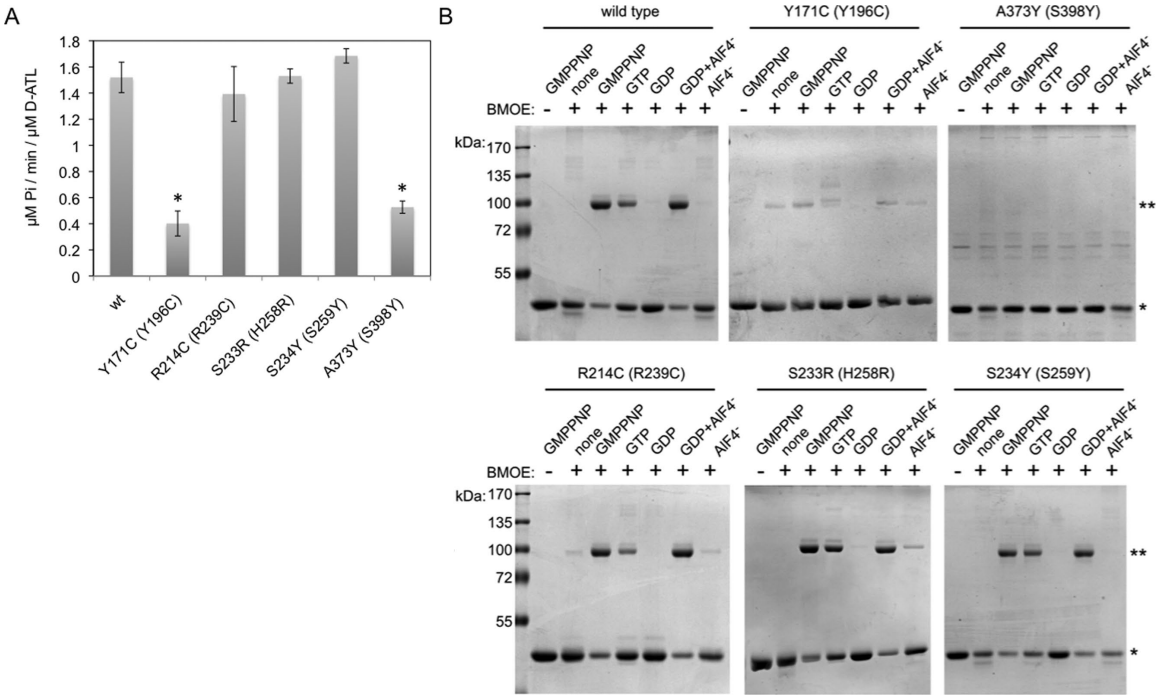

A) GTPase activity. Purified soluble domain versions of Drosophila atlastin (aa 1-415) with the indicated SPG3A equivalent mutations were assayed for GTPase activity. Values represent the means of 3 independent measurements +/- S.D. *p<0.0001 with respect to the wild type (unpaired Student's t-test). All others were not significantly different from the wild type. **B)** Crossover dimer formation. The same purified proteins (from A) were incubated at RT in the absence or presence of the indicated nucleotides and then subjected to BMOE cross-linking. The single asterisk marks the soluble domain monomer and the double asterisk marks the cross-linked dimer. Results shown are representative of at least 2 independent experiments for each variant. All variants also had the G343C substitution, which enabled crossover specific sulfhydryl cross-linking by BMOE. For clarity, the corresponding SPG3A mutation is also indicated in parentheses.

Figure 2-7 R214C, S233R and S234Y but not Y171C Drosophila atlastin (R239C, H258R and S259Y but not Y196C atlastin1) are fusion competent

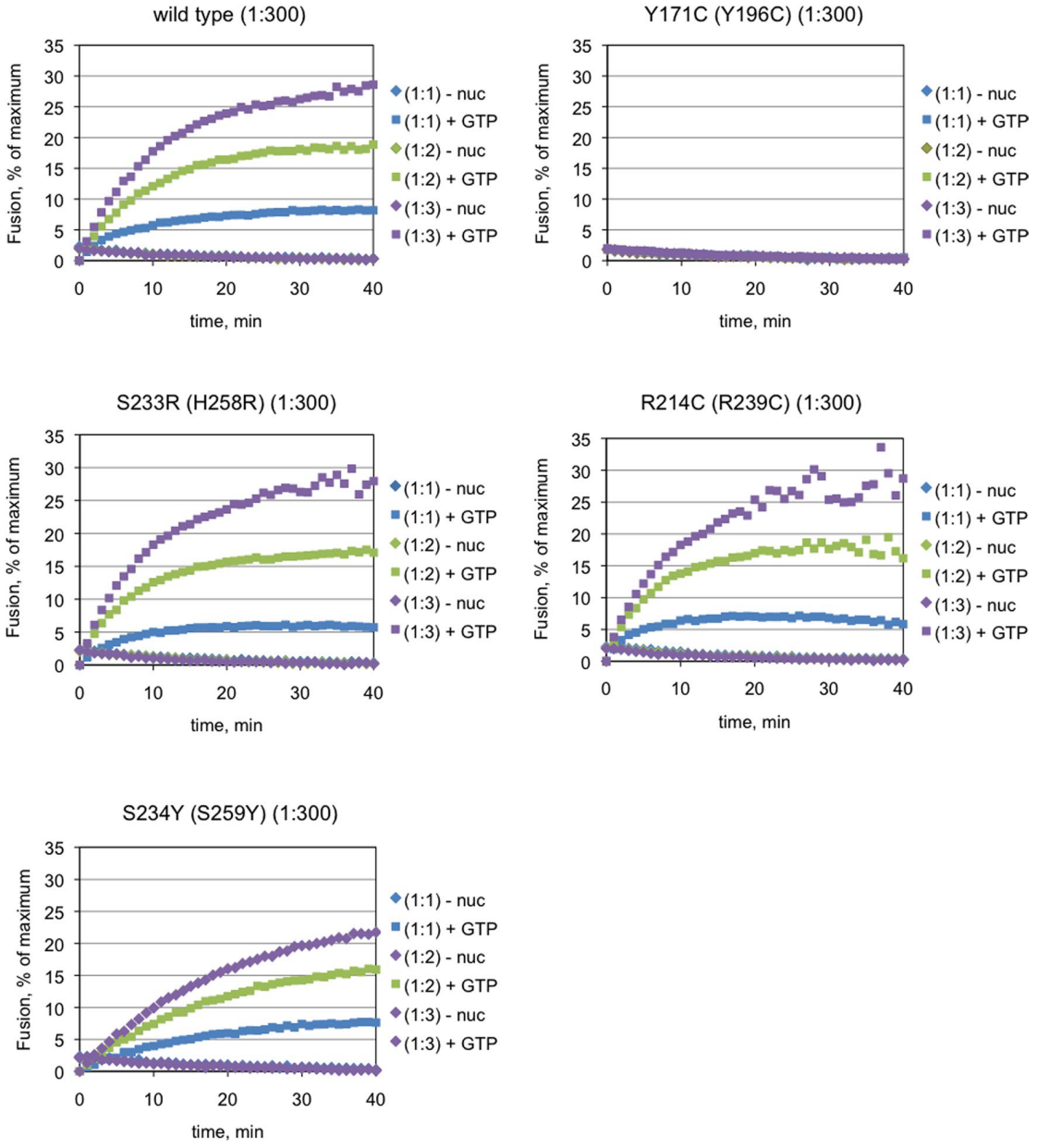

Each of the indicated Drosophila atlastin variants was reconstituted into donor (labeled) and acceptor (unlabeled) vesicles at a 1:300 protein to lipid ratio. Fusion was monitored as the de-quenching of fluorescent NBD-labeled lipid in donor vesicles after the addition of either GTP or buffer. For each variant, the reaction at 3 distinct donor-to-acceptor vesicle ratios is shown. The results shown are representative of at least two independent protein preparations.

Figure 2-8 R214C and S233R Drosophila atlastin (R239C and H258R atlastin1) are similar to the wild type in their fusion activity

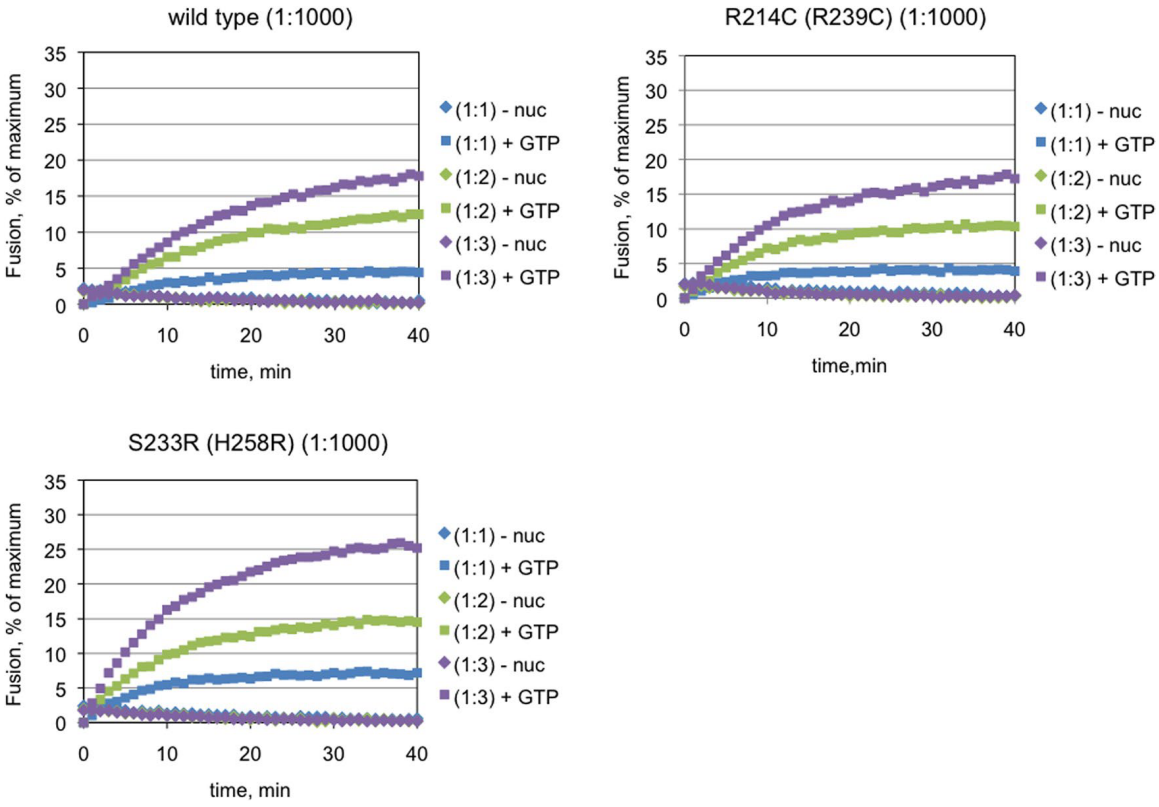

Each of the indicated Drosophila atlastin variants was reconstituted into donor (labeled) and acceptor (unlabeled) vesicles at a 1:1000 protein to lipid ratio. Fusion was monitored as the de-quenching of fluorescent NBD-labeled lipid in donor vesicles after the addition of either GTP or buffer. For each variant, the reaction at 3 distinct donor-to-acceptor vesicle ratios is shown. The results shown are representative of at least two independent protein preparations.

SUPPLEMENTARY FIGURES

Figure S2-1 Atlastin1/SPG3A variants co-localize with the tubular ER marker REEP5/DP1/TB2

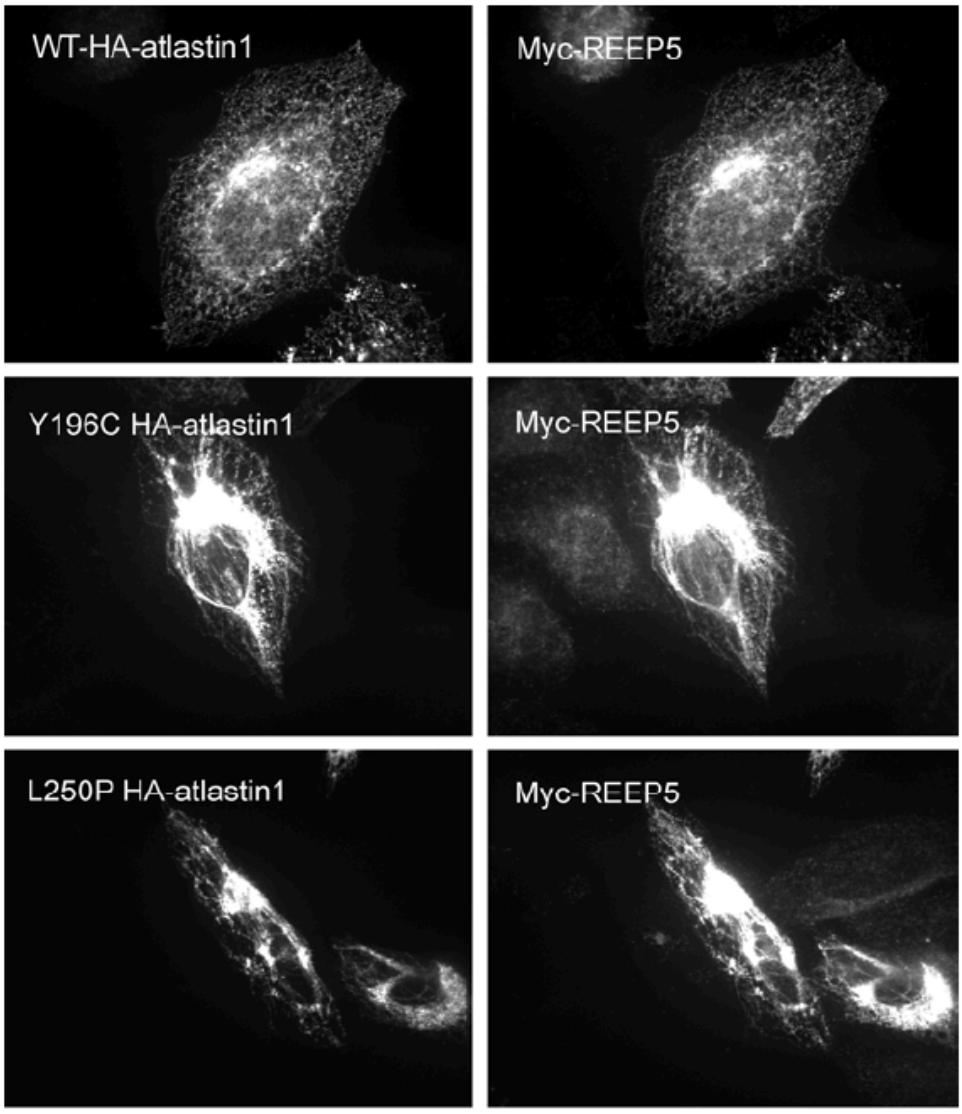

HeLa cells co-transfected with HA-tagged versions of the indicated atlastin1 variants and Myc-tagged REEP5/DP1/TB2 were fixed, co-stained with antibodies against HA and REEP5 and viewed by confocal microscopy. Scale bar, 10 μm.

Figure S2-2 ER network formation by R239C atlastin1

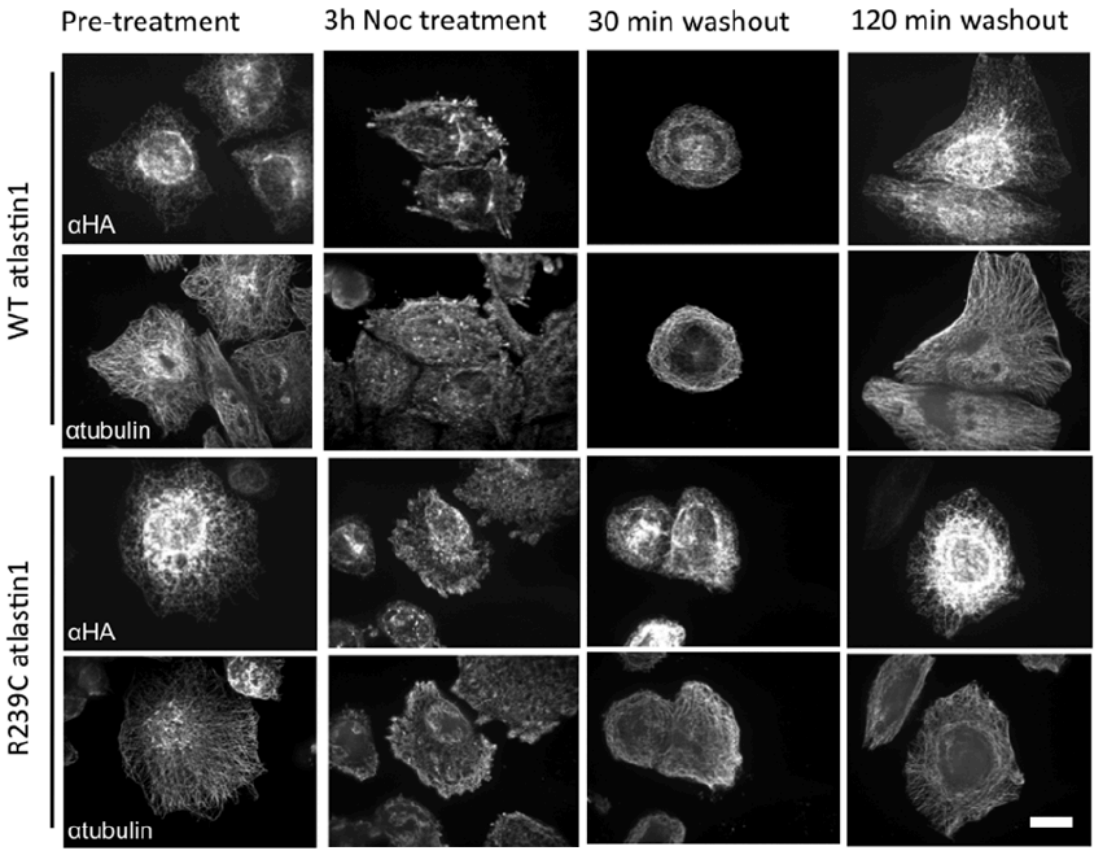

After knockdown and replacement with either HA-tagged wild type or R239C atlastin1, cells were either left untreated or treated for 3 h with nocodazole to induce microtubule depolymerization and ER collapse, followed by drug washout. At the indicated times following drug washout, cells were fixed and co-stained with antibodies against HA and tubulin, and viewed by confocal microsopy. Scale bar, 10 μm. Quantification of this experiment is shown in Fig 2-3C.

Figure S2-3 Distribution of singly transfected REEP1 and atlastin1 in Cos-7

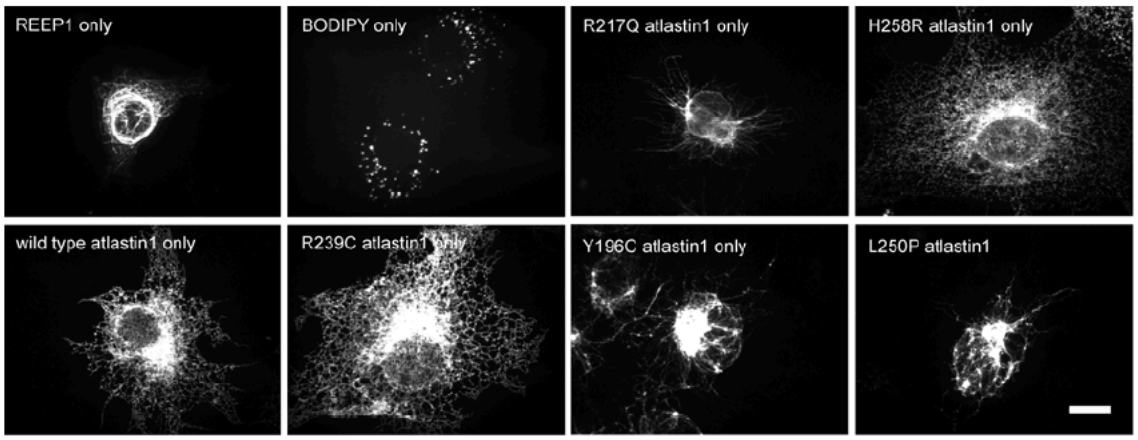

Cos-7 cells transfected with either REEP1-Flag or the indicated wild type or disease variants of HA-atlastin1 were fixed 48 h later, stained with Flag or HA antibodies and viewed by confocal microscopy. Scale bar, 10 μm. Untransfected cells stained with BODIPY 493/503 are also shown.

Figure S2-4 Large lipid droplet like structures induced by atlastin1 and REEP1 co-expression do not co-localize with lipid droplets

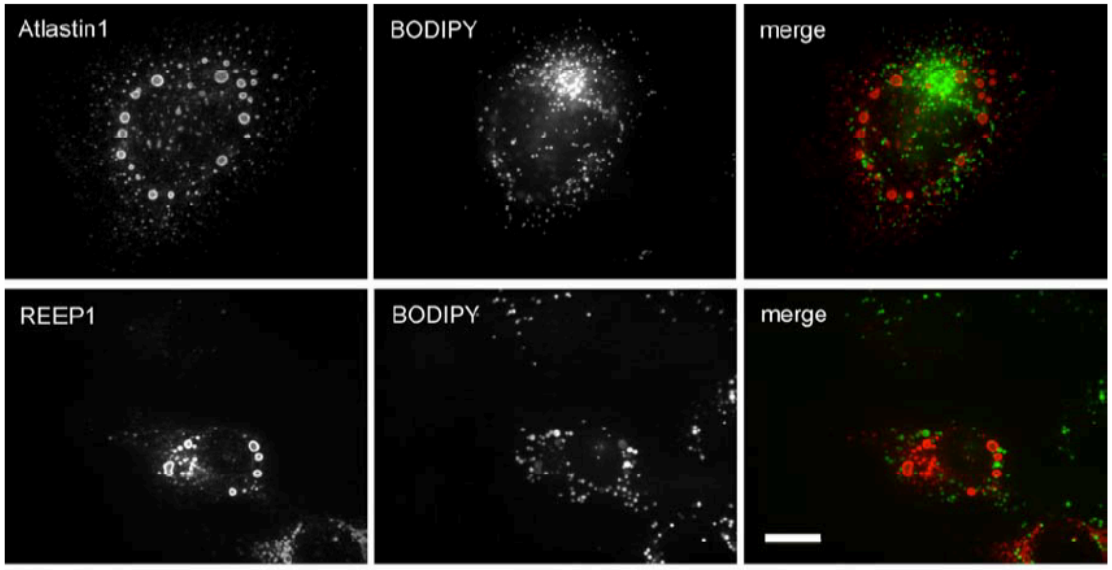

Cos-7 cells co-transfected with REEP1-Flag and HA-atlastin1 were fixed 48 h later and stained either with the HA antibody or Flag antibody followed by BODIPY 493/503 staining. The merge shows absence of overlap between atlastin1 and lipid droplets. Scale bar, 10 μm.

Figure S2-5 Incorporation of Drosophila atlastin variants into proteoliposomes at 1:300

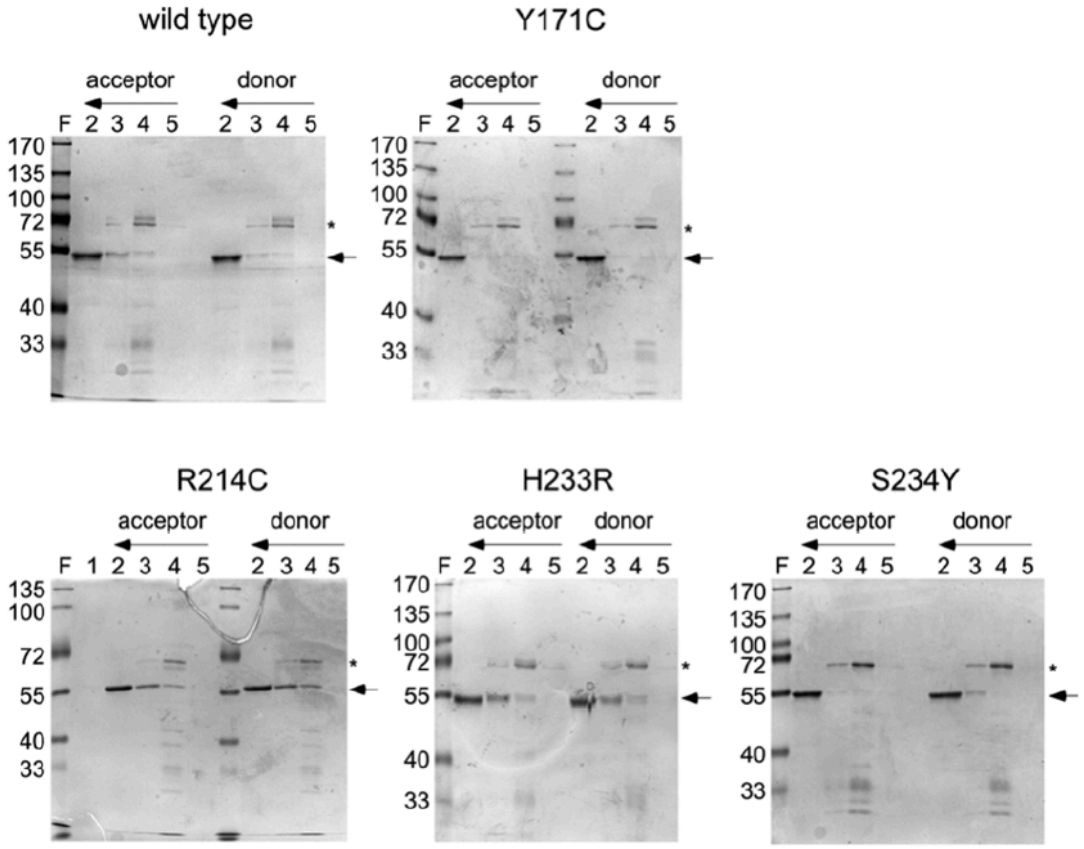

The indicated Drosophila atlastin proteins, purified and incorporated into labeled (donor) and unlabelled (acceptor) vesicles at a 1:300 protein to lipid ratio, were subjected to a (50%/45%/0%) Nycodenz step membrane flotation gradient. Fractions were resolved by SDS-PAGE and stained with Coomassie Blue. The vesicles were recovered from fraction 2 corresponding to the 45%/0% interface. The arrow just below the 55 kD marker indicates the position of full-length His-tagged Drosophila atlastin.

Figure S2-6 Incorporation of Drosophila atlastin variants into proteoliposomes at 1:1000

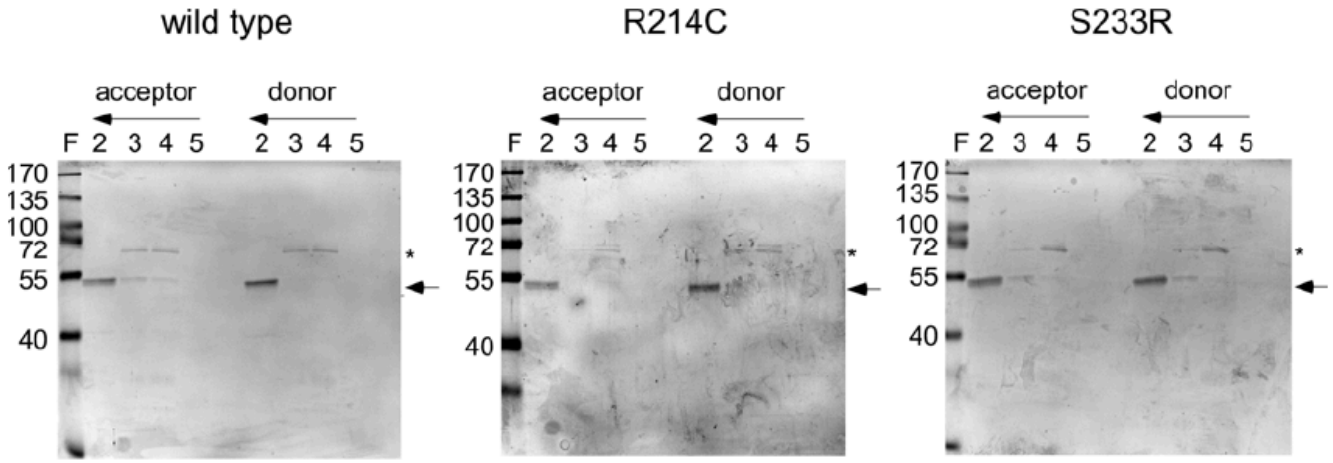

The indicated Drosophila atlastin proteins, purified and incorporated into labeled (donor) and unlabelled (acceptor) vesicles at a 1:1000 protein to lipid ratio, were subjected to a (50%/45%/0%) Nycodenz step membrane flotation gradient. Fractions were resolved by SDS-PAGE and stained with Coomassie Blue. The vesicles were recovered from fraction 2 corresponding to the 45%/0% interface. The arrow just below the 55 kD marker indicates the position of full-length His-tagged Drosophila atlastin.

Figure S2-7 R239C and H258R atlastin1 variants are stable when expressed in neuroblast-derived PC12 cells

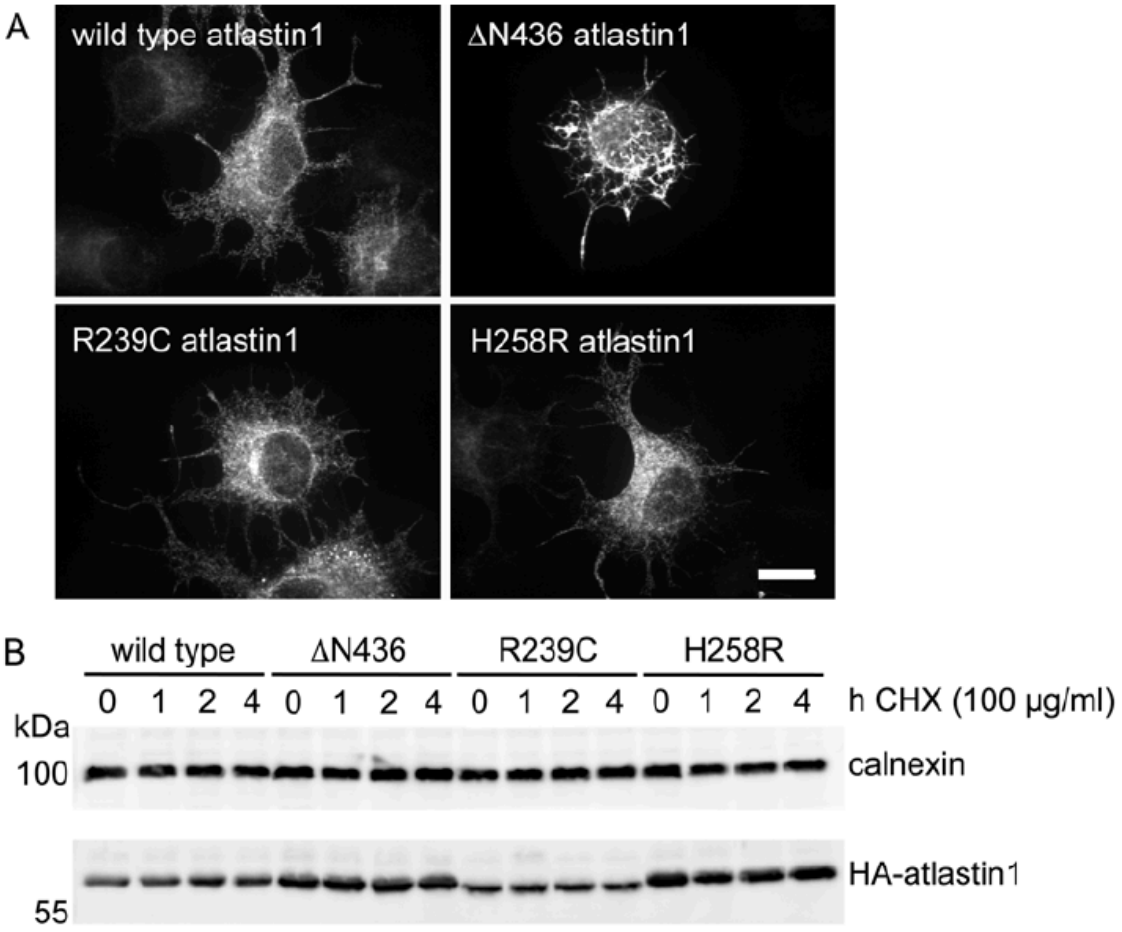

PC12 cells transfected with the indicated HA-atlastin1 constructs were **A)** fixed and stained 48 h later using HA antibodies. Only ΔN436 atlastin1 perturbed ER morphology. Scale bar, 10 μm. **B)** Protein stability of each variant was assessed by treating cells 100 μg/ml cycloheximide (CHX) for the indicated times 48 h after transfection. Cell were harvested, resolved by SDS-PAGE and subjected to immunoblotting with the HA antibody. All variants including ΔN436 were stable over the course of treatment.

DISCUSSION

Our study has uncovered two distinct categories of atlastin1/SPG3A mutations. Disease mutations of the first category impaired activity in functional assays for ER network formation, REEP1 co-redistribution, and membrane fusion catalysis, though they were reported to reduce activity only modestly in soluble phase biochemical assays (Byrnes and Sondermann, 2011). In contrast, little or no impact on either ER network formation, REEP1 co-redistribution, or on membrane fusion catalysis could be detected for disease mutations of the second category. The behavior of the first group was anticipated and consistent with perturbation of the ER network as the root cause of the disease. The behavior of the second group was entirely unexpected. Overall, our findings reveal a notable gap in understanding of how atlastin function and dysfunction contributes to health and disease.

The Y196C, L250P and S398Y atlastin1/SPG3A mutations impaired activity in multiple assays. The precise structure function relationship of each of these mutations remains to be understood. Y196C and S398Y strongly inhibited GTP-dependent crossover dimer formation when transferred to the Drosophila soluble domain. For these mutations, inspection of the atlastin1 crystal structures reveals potential explanations for functional perturbation. For instance, the side chain of Y196, a residue within the globular GTPase head, contacts a residue outside the head specifically in the crossover dimer configuration (Bian et al., 2011; Byrnes and Sondermann, 2011). The residue that it contacts, P342, resides within the linker connecting the head to the 3HB, and constitutes the pivot point of 3HB rotation (Bian et al., 2011; Byrnes and Sondermann, 2011). Based on this information, we speculate that the Y196C substitution hinders crossover dimer formation, which in turn inhibits fusion. Notably, a mutation in P342 has recently been identified in an HSP patient (Zhu et al., 2014). Closer study of this and the other nonfunctional atlastin1/SPG3A variants may uncover new insights into the conformational dynamics of 3HB rotation and crossover.

Our discovery of disease mutations with no apparent effect on atlastin activity was a surprise. Two variants, R239C and H258R (R214C and S233R in Drosophila), showed no measurable deficit either in the context of atlastin1 or Drosophila atlastin, and whether in the context of cells or in pure protein assays. A third variant S234Y (S259Y in atlastin1) had only a slight reduction in fusion activity. The apparent functionality of these

variants was of note because the mutations they harbor correspond to the very mutations in the kindreds, ADHSP-P (S259Y), ADHSP-T (H258R) and ADHSP-S (R239C), originally analyzed towards the identification of SPG3A as atlastin1 (Zhao et al., 2001). As mentioned above, R239C is the most commonly occurring SPG3A mutation in patients, identified ten times more frequently than the others and in unrelated families (Namekawa et al., 2006). In each of the original families, the disease was tightly linked to the SPG3A locus, with LOD scores of 4.63, 5.59 and 2.28 for ADHSP-P, ADHSP-T and ADSP-S, respectively (Zhao et al., 2001). Many subsequently identified SPG3A alleles have been uncovered solely on the basis of sequencing the SPG3A gene in patients after exclusion of a mutation in SPG4/spastin, the other common autosomal dominant HSP locus (Abel et al., 2004; Muglia et al., 2002; Rainier et al., 2006; Sauter et al., 2004). Consequently, some of the latter cases could, in principle, be attributable to a secondary mutation outside of the SPG3A locus. But this seems unlikely for the originally characterized mutations (Zhao et al., 2001).

The atlastin1 levels in the neurons of patients heterozygous for the R239C and H258R mutations are unknown; therefore we cannot rule out the possibility they might be low enough to cause a fusion defect. However, neither the R239C nor H258R protein was unstable upon expression in neuroblast-derived PC12 cells (Fig S2-7A,B). This is in agreement with the previously reported wild type level of thermostability of these variants in the soluble phase (Byrnes and Sondermann, 2011). Loss of atlastin1 has been reported in the lymphocytes of adult patients heterozygous for the DN436 mutation, a deletion of a single amino acid from the 3HB (Meijer et al., 2007); though, the atlastin1 level in patients' neurons was not examined. We speculate that the loss of protein observed in the lymphocytes may have occurred as a secondary long-term consequence of ER structural perturbation. Indeed, we observed strong dominant negative ER perturbation on expression of the DN436 variant in pC12 cells (Fig S2-7A); whereas, the R239C and H258R variants did not perturb ER morphology in any cell type analyzed (Fig S2-7A, Fig 2-3). Consequently, protein loss would not be predicted for the latter.

The true impact of the R239C and H258R mutations on atlastin1 fusion activity remains unknown because the fusion assay in this study was carried out, by necessity, on Drosophila atlastin. Interestingly, the histidine at position 258 in atlastin1, though highly conserved in vertebrate atlastins, is replaced by a serine and arginine in the Drosophila

and C. elegans orthologue, respectively. The lack of conservation across the vertebrate/invertebrate divide may, in and of itself, argue against the residue serving an evolutionarily conserved core fusion function. Moreover, the H258R disease mutation converts the histidine to a residue already present in the C. elegans orthologue. Thus the H258R mutation would not have been predicted, a priori, to impair fusion. In contrast, R239 is at the dimer interface and conserved across all atlastin orthologues, thus expected to serve a conserved and essential function. Still, we found no impairment in fusion or in any other biochemically assayable activity for the R239C variant. Despite the potential caveats pertaining to the use of the Drosophila orthologue, it is remarkable that no impairment could be discerned, at least within the confines of our assay conditions, for two of the three most prominent SPG3A disease variants. It might be argued that a slight reduction in fusion activity, within the margin of error in our assays, is sufficient to cause disease. But a counter argument is that the majority of atlastin1/SPG3A mutations are autosomal dominant, causing disease even in the presence of a wild type copy of the gene (Zhao et al., 2001). It is difficult to envision a scenario in which disease is caused by a slight, difficult to detect, reduction in the fusion activity in one of two atlastin1 alleles. Collectively, our findings question the idea that SPG3A mutations cause HSP solely by disrupting the minimal machinery that catalyzes membrane fusion and ER morphogenesis.

Why then do these mutations cause disease? One possible explanation is that the ER in neurons is specialized and therefore relies on a neuron specific factor that binds and regulates the fusion activity of atlastin1. In this case, R239 and H258, both surface exposed on the monomer, might constitute a binding interface for such a regulator. Another plausible explanation is that atlastin1 carries out an alternate non-ER fusion function in neurons and this alternate function is perturbed by the R239C and H258R mutations. In this context, it is noteworthy that atlastin1 has separately been implicated in bone morphogenetic protein (BMP) signaling (Fassier et al., 2010). In the zebrafish *Danio rerio*, atlastin1 knockdown caused severe larval mobility defects accompanied by alterations in spinal motor neuron architecture and a reduction in BMP receptor endocytosis (Fassier et al., 2010). Remarkably, the mobility defects were rescued with an inhibitor of BMP signaling, suggesting that atlastin1 may normally down regulate the BMP signaling pathway in neurons by directly or indirectly modulating BMP receptor internalization. Furthermore, spinal neurons, isolated from atlastin1 morphants lacking

atlastin1, and possibly relying on atlastin3 for ER membrane fusion (Rismanchi et al., 2008) , were reported to have normal ER morphology, implying that the mobility defects might not stem from ER morphological perturbations. Though, the imaging methods used would not necessarily have enabled detection of branch point density changes (Fassier et al., 2010).

In sum, a significant level of uncertainty remains pertaining to the precise cellular role(s) of neuronal atlastin1. While the behavior of some of the atlastin1/SPG3A variants analyzed herein remains consistent with loss of ER membrane fusion as the root cause of HSP, the behavior of at least two disease variants is at odds with this hypothesis. The role and regulation of atlastin1 in the maintenance of long axons of the corticospinal tract may be complex, involving interplay between ER remodeling, microtubule interactions, receptor endocytosis and signaling. Further investigation of the cellular role, mechanism and regulation of atlastin1 in neurons will be necessary to better understand the pathophysiology of SPG3A mutations.

REFERENCES

Abel, A., N. Fonknechten, A. Hofer, A. Dürr, C. Cruaud, T. Voit, J. Weissenbach, A. Brice, S. Klimpe, G. Auburger, and J. Hazan. (2004). Early onset autosomal dominant spastic paraplegia caused by novel mutations in SPG3A. *Neurogenetics*. 5:239-243.

Anwar, K., R.W. Klemm, A. Condon, K.N. Severin, M. Zhang, R. Ghirlando, J. Hu, T.A. Rapoport, and W.A. Prinz. (2012). The dynamin-like GTPase Sey1p mediates homotypic ER fusion in S. cerevisiae. *J Cell Biol*. 197:209-217.

Bian, X., R.W. Klemm, T.Y. Liu, M. Zhang, S. Sun, X. Sui, X. Liu, T.A. Rapoport, and J. Hu. (2011). Structures of the atlastin GTPase provide insight into homotypic fusion of endoplasmic reticulum membranes. *Proc Natl Acad Sci U S A*. 108:3976-3981.

Blackstone, C. (2012). Cellular pathways of hereditary spastic paraplegia. *Annu Rev Neurosci*. 35:25-47.

Blackstone, C., C.J. O'Kane, and E. Reid. (2011). Hereditary spastic paraplegias: membrane traffic and the motor pathway. *Nat Rev Neurosci*. 12:31-42.

Byrnes, L.J., A. Singh, K. Szeto, N.M. Benvin, J.P. O'Donnell, W.R. Zipfel, and H. Sondermann. (2013). Structural basis for conformational switching and GTP loading of the large G protein atlastin. *EMBO J*. 32:369-384.

Byrnes, L.J., and H. Sondermann. (2011). Structural basis for the nucleotide-dependent dimerization of the large G protein atlastin-1/SPG3A. *Proc Natl Acad Sci U S A*. 108:2216-2221.

Chappie, J.S., S. Acharya, M. Leonard, S.L. Schmid, and F. Dyda. (2010). G domain dimerization controls dynamin's assembly-stimulated GTPase activity. *Nature*. 465:435-440.

Dailey, M.E., and P.C. Bridgman. (1989). Dynamics of the endoplasmic reticulum and other membranous organelles in growth cones of cultured neurons. *J Neurosci*. 9:1897-1909.

Daumke, O., and G.J. Praefcke. (2011). Structural insights into membrane fusion at the endoplasmic reticulum. *Proc Natl Acad Sci U S A*. 108:2175-2176.

Deluca, G.C., G.C. Ebers, and M.M. Esiri. (2004). The extent of axonal loss in the long tracts in hereditary spastic paraplegia. *Neuropathol Appl Neurobiol*. 30:576-584.

Depienne, C., G. Stevanin, A. Brice, and A. Durr. (2007). Hereditary spastic paraplegias: an update. *Curr Opin Neurol*. 20:674-680.

Dreier, L. and T.A. Rapoport. (2000). In vitro formation of the endoplasmic reticulum occurs independently of microtubules by a controlled fusion reaction. *J. Cell Biol.* 148:883-898.

Fassier, C., J.A. Hutt, S. Scholpp, A. Lumsden, B. Giros, F. Nothias, S. Schneider-Maunoury, C. Houart, and J. Hazan. (2010). Zebrafish atlastin controls motility and spinal motor axon architecture via inhibition of the BMP pathway. *Nat Neurosci*. 13:1380-1387.

Faust, J.E., T. Desai, A. Verma, I. Ulengin, T.L. Sun, T.J. Moss, M.A. Betancourt, H.W. Huang, T. Lee, and J.A. McNew. (2015). The Atlastin C-terminal Tail is an Amphipathic Helix that Perturbs Bilayer Structure during Endoplasmic Reticulum Homotypic Fusion. *J Biol Chem*. 290(8).:4772-83.

Fink, J.K. (2006). Hereditary spastic paraplegia. *Curr Neurol Neurosci Rep*. 6:65-76.

Friedman, J.R., B.M. Webster, D.N. Mastronarde, K.J. Verhey, and G.K. Voeltz. (2010). ER sliding dynamics and ER-mitochondrial contacts occur on acetylated microtubules. *J Cell Biol*. 190:363-375.

Gasper, R., S. Meyer, K. Gotthardt, M. Sirajuddin, and A. Wittinghofer. (2009). It takes two to tango: regulation of G proteins by dimerization. *Nat Rev Mol Cell Biol*. 10:423-429.

Geier, A., R. Beery, M. Haimshon, R. Hemi, and B. Lunenfeld. (1992). Serum and insulin inhibit cell death induced by cycloheximide in the human breast cancer cell line MCF-7. *In Vitro Cell Dev Biol*. 28A:415-418.

Gilden, R.V., and R.I. Carp. (1966). Effects of cycloheximide and puromycin on synthesis of simian virus 40 T antigen in green monkey kidney cells. *J Bacteriol*. 91:1295-1297.

Gispert, S., N. Santos, R. Damen, T. Voit, J. Schulz, T. Klockgether, G. Orozco, F. Kreuz, J. Weissenbach, and G. Auburger. (1995). Autosomal dominant familial spastic paraplegia: reduction of the FSP1 candidate region on chromosome 14q to 7 cM and locus heterogeneity. *Am J Hum Genet*. 56:183-187.

Guelly, C., P.P. Zhu, L. Leonardis, L. Papić, J. Zidar, M. Schabhüttl, H. Strohmaier, J. Weis, T.M. Strom, J. Baets, J. Willems, P. De Jonghe, M.M. Reilly, E. Fröhlich, M. Hatz, S. Trajanoski, T.R. Pieber, A.R. Janecke, C. Blackstone, and M. Auer-Grumbach. (2011). Targeted high-throughput sequencing identifies mutations in

atlastin-1 as a cause of hereditary sensory neuropathy type I. *Am J Hum Genet*. 88:99-105.

Hashimoto, Y., M. Shirane, F. Matsuzaki, S. Saita, T. Ohnishi, and K.I. Nakayama. (2014). Protrudin regulates endoplasmic reticulum morphology and function associated with the pathogenesis of hereditary spastic paraplegia. *J Biol Chem*. 289:12946-12961.

Hazan, J., C. Lamy, J. Melki, A. Munnich, J. de Recondo, and J. Weissenbach. (1993). Autosomal dominant familial spastic paraplegia is genetically heterogeneous and one locus maps to chromosome 14q. *Nat Genet*. 5:163-167.

Hu, J., Y. Shibata, P.P. Zhu, C. Voss, N. Rismanchi, W.A. Prinz, T.A. Rapoport, and C. Blackstone. (2009). A class of dynamin-like GTPases involved in the generation of the tubular ER network. *Cell*. 138:549-561.

Klemm, R.W., J.P. Norton, R.A. Cole, C.S. Li, S.H. Park, M.M. Crane, L. Li, D. Jin, A. Boye-Doe, T.Y. Liu, Y. Shibata, H. Lu, T.A. Rapoport, R.V. Farese, C. Blackstone, Y. Guo, and H.Y. Mak. (2013). A conserved role for atlastin GTPases in regulating lipid droplet size. *Cell Rep*. 3:1465-1475.

Listenberger, L.L., and D.A. Brown. (2007). Fluorescent detection of lipid droplets and associated proteins. *Curr Protoc Cell Biol*. Chapter 24:Unit 24.22.

Lo Giudice, T., F. Lombardi, F.M. Santorelli, T. Kawarai, and A. Orlacchio. (2014). Hereditary spastic paraplegia: clinical-genetic characteristics and evolving molecular mechanisms. *Exp Neurol*. 261:518-539.

Lu, L., M.S. Ladinsky, and T. Kirchhausen. (2009). Cisternal organization of the endoplasmic reticulum during mitosis. *Mol Biol Cell*. 20:3471-3480.

Meijer, I.A., P. Dion, S. Laurent, N. Dupré, B. Brais, A. Levert, J. Puymirat, M.F. Rioux, M. Sylvain, P.P. Zhu, C. Soderblom, J. Stadler, C. Blackstone, and G.A. Rouleau. (2007). Characterization of a novel SPG3A deletion in a French-Canadian family. *Ann Neurol*. 61:599-603.

Morin-Leisk, J., S.G. Saini, X. Meng, A.M. Makhov, P. Zhang, and T.H. Lee. (2011). An intramolecular salt bridge drives the soluble domain of GTP-bound atlastin into the postfusion conformation. *J Cell Biol*. 195:605-615.

Moss, T.J., C. Andreazza, A. Verma, A. Daga, and J.A. McNew. (2011). Membrane fusion by the GTPase atlastin requires a conserved C-terminal cytoplasmic tail and dimerization through the middle domain. *Proc Natl Acad Sci U S A*. 108:11133-11138.

Muglia, M., A. Magariello, G. Nicoletti, A. Patitucci, A.L. Gabriele, F.L. Conforti, R. Mazzei, M. Caracciolo, G. Casari, B. Ardito, M. Lastilla, A. Gambardella, and A. Quattrone. (2002). A large family with pure autosomal dominant hereditary spastic paraplegia from southern Italy mapping to chromosome 14q11.2-q24.3. *J Neurol*. 249:1413-1416.

Namekawa, M., P. Ribai, I. Nelson, S. Forlani, F. Fellmann, C. Goizet, C. Depienne, G. Stevanin, M. Ruberg, A. Dürr, and A. Brice. (2006). SPG3A is the most frequent cause of hereditary spastic paraplegia with onset before age 10 years. *Neurology*. 66:112-114.

Orso, G., D. Pendin, S. Liu, J. Tosetto, T.J. Moss, J.E. Faust, M. Micaroni, A. Egorova, A. Martinuzzi, J.A. McNew, and A. Daga. (2009). Homotypic fusion of ER membranes requires the dynamin-like GTPase atlastin. *Nature*. 460:978-983.

Park, S.H., P.P. Zhu, R.L. Parker, and C. Blackstone. (2010). Hereditary spastic paraplegia proteins REEP1, spastin, and atlastin-1 coordinate microtubule interactions with the tubular ER network. *J Clin Invest*. 120:1097-1110.

Pendin, D., J. Tosetto, T.J. Moss, C. Andreazza, S. Moro, J.A. McNew, and A. Daga. (2011). GTP-dependent packing of a three-helix bundle is required for atlastin-mediated fusion. *Proc Natl Acad Sci U S A*. 108:16283-16288.

Praefcke, G.J., and H.T. McMahon. (2004). The dynamin superfamily: universal membrane tubulation and fission molecules? *Nat Rev Mol Cell Biol*. 5:133-147.

Rainier, S., P. Hedera, D. Alvarado, X. Zhao, K.A. Kleopa, T. Heiman-Patterson, and J.K. Fink. (2001). Hereditary spastic paraplegia linked to chromosome 14q11-q21: reduction of the SPG3 locus interval from 5.3 to 2.7 cM. *J Med Genet*. 38:E39.

Rainier, S., C. Sher, O. Reish, D. Thomas, and J.K. Fink. (2006). De novo occurrence of novel SPG3A/atlastin mutation presenting as cerebral palsy. *Arch Neurol*. 63:445-447.

Rismanchi, N., C. Soderblom, J. Stadler, P.P. Zhu, and C. Blackstone. (2008). Atlastin GTPases are required for Golgi apparatus and ER morphogenesis. *Hum Mol Genet*. 17:1591-1604.

Saini, S.G., C. Liu, P. Zhang, and T.H. Lee. (2014). Membrane tethering by the atlastin GTPase depends on GTP hydrolysis but not on forming the crossover configuration. *Mol Biol Cell*. 25(24).:3942-53.

Salinas, S., C. Proukakis, A. Crosby, and T.T. Warner. (2008). Hereditary spastic paraplegia: clinical features and pathogenetic mechanisms. *Lancet Neurol*. 7:1127-1138.

Sauter, S.M., W. Engel, L.M. Neumann, J. Kunze, and J. Neesen. (2004). Novel mutations in the Atlastin gene (SPG3A). in families with autosomal dominant hereditary spastic paraplegia and evidence for late onset forms of HSP linked to the SPG3A locus. *Hum Mutat*. 23:98.

Terasaki, M., L.B. Chen, and K. Fujiwara. (1986). Microtubules and the endoplasmic reticulum are highly interdependent structures. *J Cell Biol*. 103:1557-1568.

Terasaki, M., N.T. Slater, A. Fein, A. Schmidek, and T.S. Reese. (1994). Continuous network of endoplasmic reticulum in cerebellar Purkinje neurons. *Proc Natl Acad Sci U S A*. 91:7510-7514.

Waterman-Storer, C.M. and E.D. Salmon. (1998). Endoplasmic reticulum membrane tubules are distributed by microtubules in living cells using three distinct mechanisms. *Curr. Biol.* 8:798-806.

Wu, F., X. Hu, X. Bian, X. Liu, and J. Hu. (2015). Comparison of human and Drosophila atlastin GTPases. *Protein Cell*. 6:139-146.

Zhang, M., F. Wu, J. Shi, Y. Zhu, Z. Zhu, Q. Gong, and J. Hu. (2013). ROOT HAIR DEFECTIVE3 family of dynamin-like GTPases mediates homotypic endoplasmic reticulum fusion and is essential for Arabidopsis development. *Plant Physiol*. 163:713-720.

Zhao, X., D. Alvarado, S. Rainier, R. Lemons, P. Hedera, C.H. Weber, T. Tukel, M. Apak, T. Heiman-Patterson, L. Ming, M. Bui, and J.K. Fink. (2001). Mutations in a newly identified GTPase gene cause autosomal dominant hereditary spastic paraplegia. *Nat Genet*. 29:326-331.

Zhu, P.P., K.R. Denton, T.M. Pierson, X.J. Li, and C. Blackstone. (2014). Pharmacologic rescue of axon growth defects in a human iPSC model of hereditary spastic paraplegia SPG3A. *Hum Mol Genet*. 23(21).:5638-48.

Zhu, P.P., C. Soderblom, J.H. Tao-Cheng, J. Stadler, and C. Blackstone. (2006). SPG3A protein atlastin-1 is enriched in growth cones and promotes axon elongation during neuronal development. *Hum Mol Genet*. 15:1343-1353.

CHAPTER 3

Analysis of the N-terminal Extension In Human Atlastin GTPases

ABSTRACT

Atlastin (ATL) is a dynamin-related membrane-anchored GTPase that undergoes GTP-dependent dimerization and conformational change to catalyze membrane fusion. Depletion of the ubiquitous ATL-2/3 isoforms in HeLa cells results in long, un-branched ER tubules with a dramatic loss of interconnections, leading to the idea that atlastin mediates homotypic fusion of ER tubules to form the characteristic branched ER network. Mutations in the neuron specific Atlastin isoform, ATL-1 (SPG3A), are the second most common cause of hereditary spastic paraplegia (HSP), a group of inherited neurodegenerative disorders. The cause of HSP has been attributed to deficits in maintenance of the ER network in the affected motor neurons. To better understand the role of ATL-1, we analyzed its ability to function in ER network formation in cells. Here we show that atlastin1 can fully restore a branched ER network in HeLa cells depleted of ATL-2/3, indicating a similar ER fusion function for all three isoforms. To identify new structural requirements for atlastin1 function, we tested the role of a conserved N-terminal extension unique to the neuronal isoform. Our results indicate that the N-terminal extension of ATL-1 is dispensable for its ER structuring function at least in HeLa cells. The apparent lack of a general requirement for a highly conserved N-terminal extension suggests that the extension may specifically regulate the ability of ATL-1 to catalyze ER fusion in neurons; or alternatively, ATL-1 might use the extension to mediate an additional (non-ER fusion) function specific to neurons.

INTRODUCTION

My work on HSP causing mutations in ATL-1, detailed in chapter 2, revealed that the fusion dependent ER network formation function of ATL-1 is not always perturbed by the mutations. One plausible explanation suggested by my work is that ATL-1 might have additional roles in neurons, dependent or independent of its ER network formation activity, and this function might be perturbed by some of the disease causing mutations. Alternatively, it is possible that network formation in neurons depends on neuron specific factors that bind and regulate the fusion activity of ATL-1. In this case, ATL-1 might have structural determinants that mediate interaction with the binding partner. Indeed, the disease causing mutations in R239 and H258, both surface exposed, might be disrupting a potential binding interface.

A potential structural element in ATL-1 that might be important for its function is the N-terminal extension domain. Sequence alignment of ATLs across species reveals the presence of a divergent N-terminal extension that precedes the highly conserved GTPase domain. This cytosolic N-terminal extension although present in all species, varies in length and lacks sequence conservation. In species with only one ATL paralog, such as Drosophila, this extension tends to be shorter than in organisms with multiple ATL paralogs such as human. Moreover, in contrast to invertebrate ATLs or ATL-2 and 3, this extension of ATL-1 is particularly conserved across vertebrate species suggesting a more critical involvement of this domain in neuronal ATL function(s). One such role of this cytosolic N-terminal extension might be to provide surface for interactions with factors such as proteins important for regulation of ATL-1 function in neurons. Alternatively, this domain might have a direct role in ATL-1 mediated fusion machinery.

To investigate the possible roles of the N-terminal extension, I performed mutational analysis on both ATL-1 and ATL-2 where I truncated the extension to the length seen in Drosophila ATL. These truncated constructs were subjected to existing assays for ATL activity. My results indicate that the N-terminal extensions of ATL-2 and ATL-1 are dispensable for all the assays used. Therefore, this extension is unlikely to be required for fusion dependent ER network formation of ATL-1.

MATERIALS AND METHODS

Cell culture, constructs, transfections and reagents

HeLa cells were maintained in minimal essential medium (Sigma-Aldrich, St. Louis, MO) containing 10% fetal bovine serum (Atlanta Biologicals, Norcross, GA) and 1% penicillin/streptomycin (Thermo Fisher Scientific) at 37°C in a 5% CO_2 incubator. Transient plasmid DNA transfection of HeLa cells was performed with jetPEI™ (Polyplus transfection, Illkirch, France), according to the manufacturer's specifications using 1 µg DNA and 2µl JetPEI per 1 mL media. Transient siRNA transfections of siRNAs against Atl2/3 were performed using Oligofectamine (Invitrogen) using 20pmol siRNA and 2µl Oligofectamine per 0.5 mL media. GST-tagged Atl1 were kindly provided by James McNew (Rice University, TX). The 6His-tagged cytoplasmic domain of ATL2 was generated using PCR amplification of nucleotides encoding amino acids 1–467 from HA-ATL2 and cloned into the pRSETB vector at NheI and EcoRI sites. Variants were generated using QuikChange mutagenesis and sequence verified. Protein expression was induced with 0.5 mM IPTG in BL21(DE3)pLysS cells at 23°C for 16 h, and purification used standard protocols for purification of 6His-tagged proteins on Ni+2 agarose beads (QIAGEN). Proteins, eluted in 50 mM Tris, pH 8.0, 250 mM imidazole, 100 mM NaCl, 5 mM MgCl 2 , and 10% glycerol, were typically 8–24 mg/ml, >95% pure, flash frozen in liquid N_2 , and stored at -80°C.The N-terminally HA-tagged ATL-1 was constructed through substituting ATL2 coding sequence in HA-tagged ATL-2 described in Morin-Leisk *et al* (2011) with PCR amplified nucleotides encoding amino acids 1- 558 from GST-ATL1 within XbaI and EcoRI sites. Point mutations and deletions were generated using QuikChange PCR and fully verified by sequencing (Genewiz).

Knockdown replacement assay

Cells plated on 60-mm culture dishes were transfected with ~5 µg of the indicated HA ATL-1 or HA-Delta N ATL-1; or HA-ATL-2 or HA-Delta N ATL-2 constructs using transfection reagent (jetPEI; Polyplus). Myc-tagged ER resident protein DP1, served as a negative control. 24 h after DNA transfection, cells were trypsinized and replated onto 12-mm glass coverslips in a 24-well plate. siRNA treatment targeting both ATL2 and ATL3 was performed the next day using transfection reagent (Oligofectamine; Invitrogen) according to manufacturer's recommendations. The ATL-2 (#1) and ATL-3 (#2) siRNAs used, were identical in sequence to those previously published (Rismanchi

et al., 2008). 72 h after knockdown, cells were fixed in ice-cold methanol and processed for immunofluorescence. For quantification of functional replacement, the fraction of cells expressing the indicated ATL constructs that showed a loss of ER network branching (among ≥100 cells in there individual experiments) was counted. This percentage was normalized to the negative control for that experiment. An efficiency of 1 reflects a complete non-rescue and 0 is a full-rescue. Nocodazole washout experiments were performed as follows: 72h after siRNA treatment, cells were incubated with 1ml media with 2X Nocodazole for 3h followed by washes with fresh media without Nocodazole. Cells were fixed at the indicated time points and processed for immunofluorescence.

Immunofluorescence and Confocal imaging

Cells were fixed in ice-cold methanol followed by 30 min incubation in the blocking solution (1X PBS + 2.5% calf serum + 0.1% Triton X-100 + 0.2 M Glycine). Primary (1 h at RT) and secondary (30 min at RT) antibody incubations were performed in the blocking solution, and washes were with 5× 1 ml PBS. Antibodies used include mouse monoclonal antibody (mAb) against the HA-epitope (Sigma-Aldrich, St. Louis, MO); a mAb against protein disulfide isomerase (PDI), a polyclonal antibody against tubulin (Both Abcam, Cambridge, MA); monoclonal antibody against MYC-epitope (9E10 mAB, Sigma - Aldrich) and Alexa 568-conjugated secondary antibody (Invitrogen). Images were viewed using a spinning-disk confocal scanhead (Yokagawa; PerkinElmer) mounted on an Axiovert 200 microscope (Zeiss) with a 100x 1.4 NA objective (Zeiss) and acquired using a 12-bit ORCA-ER camera (Hamamatsu Photonics). Maximal value projections of sections at 0.2-µm spacing were acquired using Micro-manager open source software (UCSF) and imported as 8-bit images. Quantification of functional replacement was performed manually on a wide-field fluorescence microscope (Axioplan; Carl Zeiss) with a 40× 1.4 NA objective.

GTPase assay

Purified 6His-tagged cytoplasmic domain of ATL-1 or ATL-2 variant proteins, dialyzed into GTPase buffer, pH 7.5 (50mM Tris, 1mM $MgCl_2$, 100mM NaCl) for 16h and pre-cleared by centrifugation in a rotor (TLA-100; Beckman Coulter) at 100,000 rpm for 15 min. GTPase activity was determined by measuring the release of inorganic phosphate from GTP using the EnzChek Phosphate Assay Kit (Molecular Probes) according to the manufacturer's instructions with few changes. 1U ml^{-1} purine nucleoside phosphorylase

(PNP), 200 mM 2-amino-6-mercapto-7-methylpurine riboside (MESG) and 500 mM GTP were mixed with reaction buffer to obtain a 200µl volume per reaction and incubated at 37°C for 10 min. The reaction was transferred into a clear, flat-bottomed polystyrene 96-well plate (Corning) warmed to 37 °C in a Tecan Safire II fluorescence microplate reader, recombinant D-ATL protein was added to start the reaction. In brief, PNP catalyzes the conversion of MESG to ribose 1-phosphate and 2-amino-6-mercapto-7-methylpurine in the presence of inorganic phosphate, resulting in a spectrophotometric shift in absorbance from 330 to 360 nm. The absorbance increase at 360nm was measured in real-time every 30 s over 30 min. Absorbance was normalized to phosphate standards ran parallel with the experiment and initial rates were calculated.

Nucleotide dependent cross-linking

Purified 6His- cytoplasmic domain of ATL-1 or ATL-2 variant proteins were dialyzed into SEC buffer (25mM Tris, 100mM NaCl, 5mM MgCl2, 2mm EGTA), pH 7.0 at 4°C and pre-cleared by centrifugation in a rotor (TLA-100) at 100,000 rpm for 15 min. 5 µM of each protein was incubated at RT in SEC buffer, in the absence or presence of 2 mM GMPPNP, GDP, GTP or GDP-ALF_4^- in a total reaction volume of 10µl. After 30 min at RT, the reaction was diluted two and a half folds with SEC buffer (to 2 µM D-ATL) in the absence or presence of 10µM BMOE (Thermo Fisher Scientific) and incubated for 1 h at RT. Samples were then quenched with 20 mM DTT for 15 min, mixed with reducing sample buffer, resolved by SDS-PAGE and stained with Coomassie Blue.

RESULTS

N-terminal extension prior to GTPase domain is highly conserved in ATL-1

The cytosolic N-terminal extension of ATLs is not only highly divergent in sequence but also varies in length. Schematic in Figure 3-1 represents the length of this extension in human isoforms compared to the Drosophila ATL, dAtl, (42 amino acids for ATL-1, 69 amino acids for ATL-2, 36 amino acids for ATL-3 and only 14 amino acids for dAtl). Interestingly as shown by the alignment in Figure 3-2, among the Human ATL isoforms, the extension in ATL-1 stands out with significant level of sequence conservation suggesting a role in ATL-1 function. To investigate the potential role of this domain in ATL function, I performed mutational analysis where I truncated the N-terminal extension in ATL-1 and in ATL-2 to the length seen in Drosophila atlastin (Figure 3-1) and analyzed these truncated constructs using functional assays testing ER network formation, GTP hydrolysis and nucleotide dependent dimerization activities.

N-terminal extension domain is dispensable for ER network formation

To assess ER network formation, we used HeLa cells because their relatively flat shape allows visualization of the branched tubular morphology of the ER network in detail. As previously reported (Hu et al., 2009; Morin-Leisk et al., 2011), HeLa cells depleted of endogenous ATL (ATL-2 and -3) using RNAi showed perturbed ER where ER tubules run parallel to one another due to significant loss of three-way junctions (branchpoints) interconnecting the ER tubules. Figure 3-3 panels B, B` shows that cells expressing either HA-tagged ATL-1 or RNAi immune ATL-2 maintain normal network interconnections with similar efficiency after endogenous ATL depletion. Expression of a Myc-tagged version of the tubular ER marker REEP5/DP1/TB2 (Hashimoto et al., 2014), which by itself had no discernable impact on ER morphology in either control or knockdown cells (Morin-Leisk et al., 2011), failed to rescue, as expected, with ~57% of the cells showing abnormal ER network.

Next, I assessed the ATL-1 and ATL-2 with truncated N terminal extensions. Surprisingly, both constructs were as functional as wildtype suggesting no significant role for the long N-terminal extension in ER network formation (Figure 3-3).

N- terminal extension is not required for GTP hydrolysis

My results thus far showed that whether in the context of ATL-1 or ATL-2, the N-terminal extension is dispensable in cell based ER network maintenance assays. To biochemically characterize these constructs, I performed the same truncation of the N-terminal extension on the ATL-1 and ATL-2 soluble domains and performed a standard GTPase assay. Figure 3-4A shows that soluble domains of ATL-1 and ATL-2 lacking the N-terminal extension are capable of hydrolyzing GTP at similar levels as wildtype ATL-1 and wildtype ATL-2. It should be mentioned that a slight increase in GTPase activities was observed for both deletion constructs but was not statistically significant.

Truncation of N-terminal extension does not impair nucleotide dependent crossover dimer formation

The soluble domains of ATL-1 and ATL-2 with truncated N-terminal extensions were next subjected to an assay for nucleotide dependent crossover dimer formation, a critical step in the membrane fusion mechanism (Bian et al., 2011; Pendin et al., 2011; Saini et al., 2014). The assay was originally developed in our lab (Morin-Leisk et al., 2011) for ATL-2 and relies on linking the cysteines (shown in figure 4-3B) on the 3-helix bundles of each ATL monomer, to each other by the cross-linking reagent bismaleimidoethane (BMOE). The short spacer arm of the crosslinker (8Å) enables capturing specifically of the crossover dimers and not the monomers or the extended dimers. Because ATL-1 lacked a cysteine at the same position, the corresponding asparagine residue was replaced with cysteine to generate N368C ATL-1. As shown previously, crosslinked-wildtype ATL-2 crossover dimers were observed after incubation with GMPPNP but not with GDP or in the absence of nucleotide (Morin-Leisk et al., 2011). The wildtype ATL-1 (N368C) behaved similarly but much less cross-over dimers were captured even though the same concentration of protein and nucleotide was used suggesting lower efficiency in ATL-1 monomers to undergo cross-over dimerization due to reasons that need to be determined (Figure 4-3C).

ATL-2 with a truncated N terminal extension was fully capable of forming nucleotide dependent cross-over dimers. Similarly, the N-terminal extension did not effect the dimer formation of ATL-1. In sum, neither ATL variant with truncated N-terminal extension could be distinguished from the wild type in any of our assays for atlastin functionality.

FIGURES

Figure 3-1 N-terminal extension varies in length and sequence conservation

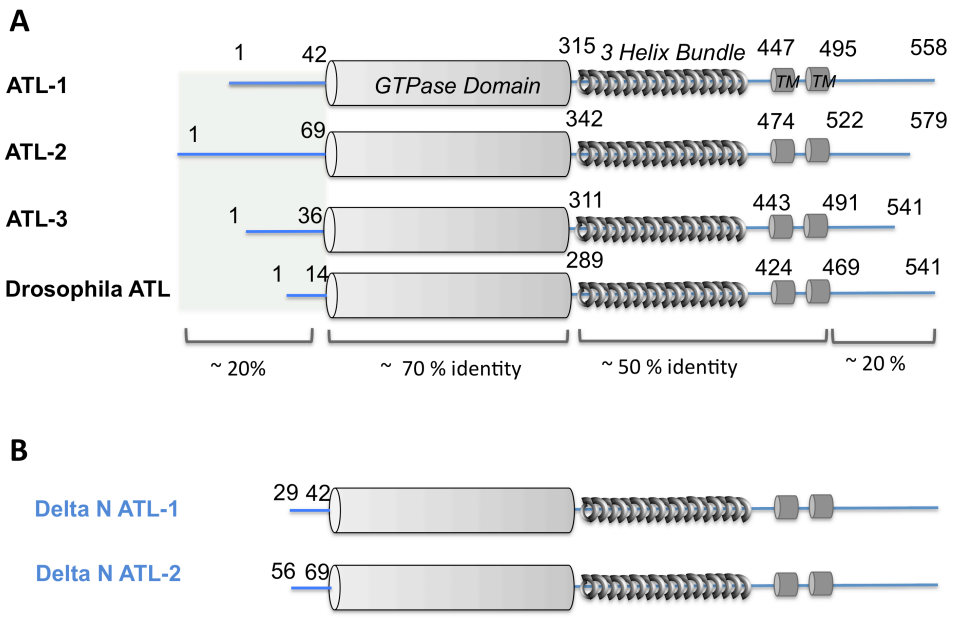

Atlastin GTPases (ATL) possess a similar domain architecture across species. **A)** Comparison of the length and sequence conservation of the domains between Human ATL-1 , Human ATL-2 and Drosophila ATL is schematized. The N terminal extensions are highlighted in blue. **B)** The truncation constructs where the N-terminal extension in ATL-1 and in ATL-2 is shortened to the length seen in Drosophila ATL, are used to test the effect of N terminal extension in ER network formation, GTP hydrolysis and nucleotide dependent dimerization activities. Adapted from *Moss et al., 2011* figure 1.

Figure 3-2 N-terminal extension in ATL-1 stands out with significant level of sequence conservation

Sequence alignment of ATL-1/2 and 3 across species reveals signification sequence conservation of N terminal extension of ATL-1.

Figure 3-3 Neuronal ATL-1 can functionally replace ATL-2 and ATL-3 to mediate ER network formation in Hela cells independent of its N terminal extension

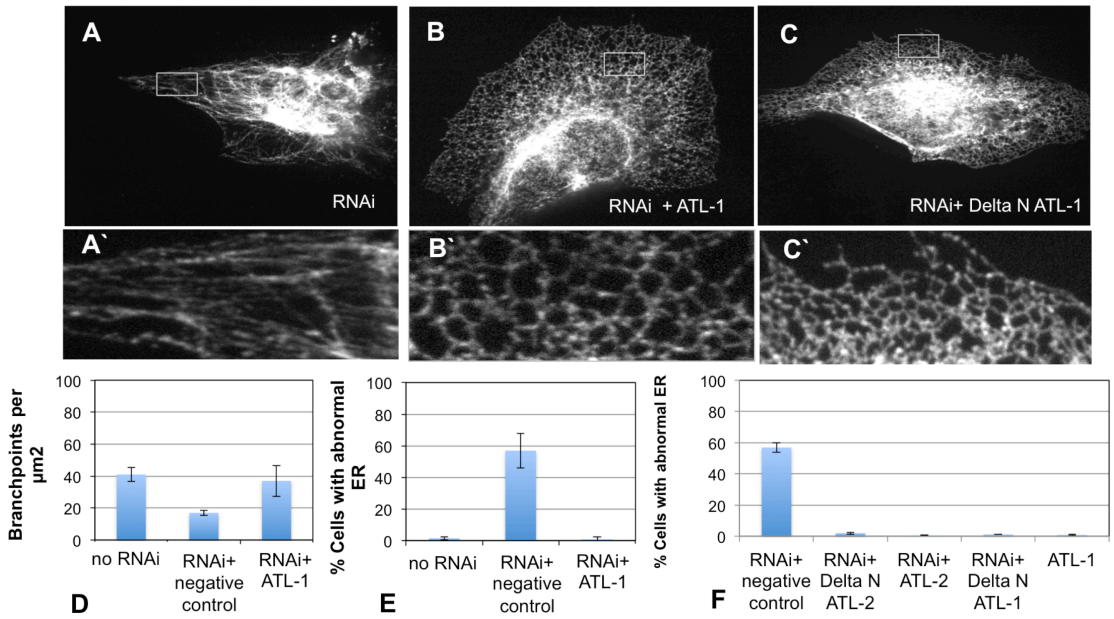

ATL-1 maintains a normal branched ER network in HeLa cells in the absence of ATL-2/3. At 48 h after transfection with Myc-tagged REEP5/DP1/TB2 (neg con; **A, A`**), HA-tagged ATL-1 (**B, B`**), Ha-tagged delta N atlastin1 (**C, C`**), HA-tagged ATL-2 or Ha-tagged delta N ATL-2 (not shown), cells were further transfected using siRNAs targeting ATL-2/3 (**A-C**). At 72 h after knockdown, cells were fixed and stained using an antibody against the Myc or HA epitope and viewed by confocal microscopy. Scale bars, 10 µm. The insets in **A`–C`** show magnified views of a boxed region of the peripheral ER. **D)** Quantification of the average number of network branch points (±SD) in five representative 100-µm^2 boxed peripheral regions of the ER under each condition. **E)** Quantification of the percentage of cells expressing Myc-REEP5/DP1/TB2 (with or without RNAi), or HA-ATL-1 (with RNAi) that displayed an abnormal unbranched ER morphology. **F)** Same as **E**, including the cells expressing atlastin1 or atlastin2 with or without N terminal extension. Values represent the means of three independent experiments (>_100 cells each) ± _SD.

Figure 3-4 N-terminal extension is dispensable for nucleotide dependent dimerization and GTP hydrolysis

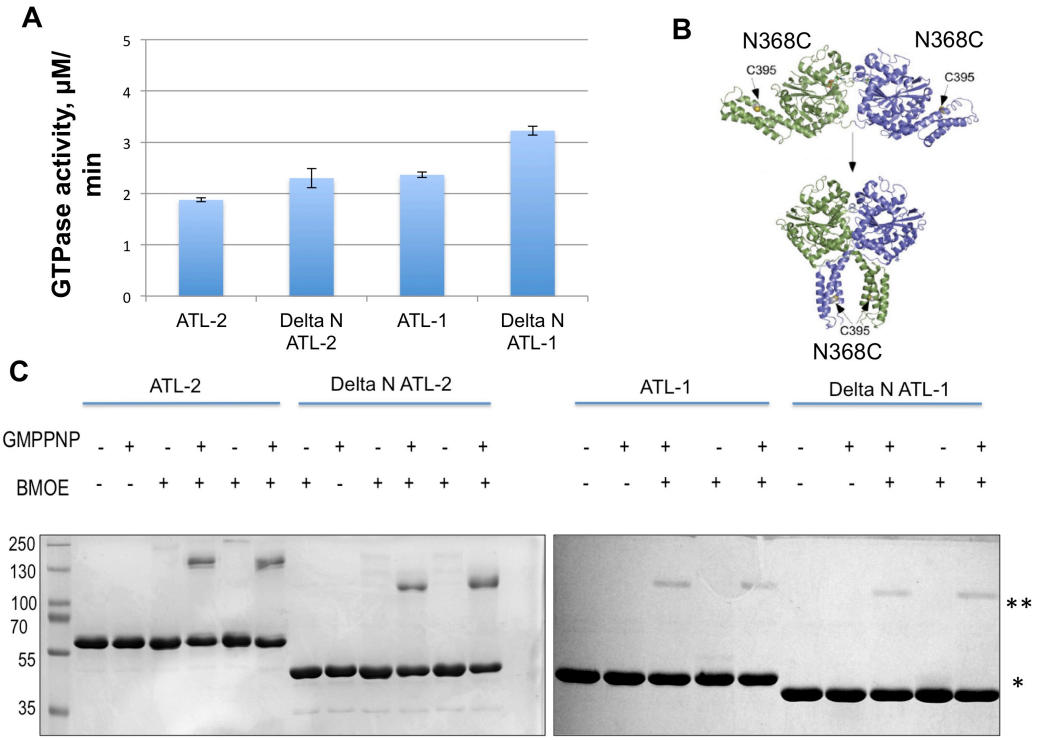

A) *In vitro* GTP hydrolysis assay. Purified soluble domain versions of ATL-1 or ATL-2 with or without N terminal extension truncation were assayed for GTPase activity. Values represent the means of three independent measurements ± _SD. **B)** ATL-1 had a N368C substitution, which enabled crossover-specific sulfhydryl cross-linking by BMOE. ATL-2 utilized an endogenous cysteine C395. **C)** Crossover dimer formation. The same purified proteins (from A) were incubated at room temperature in the absence or presence of the nonhydrolyzable GTP analog, GMPPNP, and then subjected to BMOE cross-linking. The single asterisk marks the soluble-domain monomer, and the double asterisk marks the cross-linked dimer. Results shown are representative of at least two independent experiments for each variant.

DISCUSSION

My results indicate that the N-terminal extensions of ATL-2 and ATL-1 are dispensable for their ER structuring function. Furthermore, the biochemical assays done with the soluble domains of ATL-1 and ATL-2 with or without the N terminal extension show no apparent difference on the proteins ability to hydrolyze GTP or to undergo nucleotide dependent crossover dimer formation, both required for fusion activity. Although this extension is unlikely to be required for fusion dependent ER network formation of ATL-1, a direct test needs to be established to assay ER network formation in neurons.

To date, no HSP mutations have been identified within the N-terminal extension. While it is possible that N-terminal extension might be important in another neuronal function of ATL-1, it also possible that it is mediating a unique spatial and temporal regulation of fusion dependent ER network formation activity of ATL-1 in neurons. One such role of this cytosolic N-terminal extension might be to provide surface for interactions with factors important for regulation of ATL-1 function. Further work is required to determine the presence of such a regulatory binding partner as currently there are no known interactions through this region. Additionally, the long N-terminal extension in ATL-1 might have a role in increasing the stability of ATL-1 which in turn would make the protein longer lived. Finally, it is also plausible that this extension mediates cis interactions with other ATL monomers on the same membrane to enable concerted fusion reactions between groups of ATL monomers on opposing membranes. On the other hand, excessive cis interactions might also inhibit dimerization of ATL monomers on the opposing membranes; therefore inhibition of excessive cis interactions by regulatory factors might be needed. Though speculative, this type of complex regulation could explain why ATL-1 is inactive in mediating fusion between synthetic liposomes *in vitro* (Wu et al., 2015).

REFERENCES

Morin-Leisk, J., Saini S.G., Meng, X., Makhov, A. M., Zhang, P., Lee, T. H. (2011). An intramolecular salt bridge drives the soluble domain of GTP-bound atlastin into the postfusion conformation. J. Cell Biol 195: 605-615.

Moss, T. J., Daga, A., McNew., J.A. (2011). Fusing a lasting relationship between ER tubules. Trends in Cell Biology 21(7): 416-423.

Rismanchi , N. , C. Soderblom , J. Stadler , P.P. Zhu , and C . Blackstone . (2008). Atlastin GTPases are required for Golgi apparatus and ER morphogenesis. Hum. Mol. Genet. 17: 1591-1604.

Saini, S.G., C. Liu, P. Zhang, and T.H. Lee. (2014). Membrane tethering by the atlastin GTPase depends on GTP hydrolysis but not on forming the crossover configuration. *Mol Biol Cell*. 25(24): 3942-53.

Wu F., Hu, X., Bian X., Liu, X., Hu, J. (2015). Comparison of human and Drosophila atlastin GTPases. Protein Cell. 6(2): 139-46.

CHAPTER 4

Analysis of the Cytoplasmic C- terminal Tail in Atlastin GTPases

ABSTRACT

Atlastin is a membrane-anchored GTPase that catalyzes ER membrane fusion to generate the interconnections between ER tubules characteristic of the branched ER network. Crystal structures of ATL-1 together with biochemical studies revealed a requirement for GTP hydrolysis dependent dimerization of ATL monomers followed by a conformational change that brings the membranes into close proximity for fusion. Among the mutations in the neuron specific Atlastin isoform, ATL-1 (SPG3A) identified in patients suffering from Hereditary Spastic Paraplegia (HSP), two frameshift mutations that truncate the cytosolic C-terminal tail of ATL-1 suggested its role in ATL mediated fusion activity. However, the precise role of the tail is still unknown. James McNew and his group found that the tail binds directly to membranes, binding in turn destabilizes the membrane to facilitate fusion. The activity of the tail was dependent on a membrane proximal amphipathic helix and mutations designed to disrupt the hydrophobic face lead to decreased fusion *in vitro*. Consistent with these results, I have shown that the C-terminal tail is important *in vivo* for the ER network formation function of ATL. However, in the context of less stable lipid bilayers, the requirement for the C-terminal tail during fusion may be alleviated. Regardless, the conserved function of the C-terminal tail between Drosophila ATL and human ATL isoforms might explain the disease pathogenesis seen in patients with mutations that truncate the tail of ATL-1.

***** *This work was a collaboration with James McNew`s group and appeared in their article in Journal of Biological Chemistry cited below. Ulengin I's contribution to this work involved expanding the cell based gene replacement assay to Drosophila atlastin which enabled testing the requirement of the structural elements in C-terminal tail both in vivo and in vitro. Additionally, Ulengin I performed the mutational analysis on residues predicted to disrupt the amphipathic helix in the C- terminal Tail.*

Faust, J.E., T. Desai, A. Verma, **I. Ulengin**, T.L. Sun, T.J. Moss, M.A. Betancourt, H.W. Huang, T. Lee, and J.A. McNew. (2015). The Atlastin C-terminal Tail is an Amphipathic Helix that Perturbs Bilayer Structure during Endoplasmic Reticulum Homotypic Fusion. J Biol Chem. 290(8):4772-83.

INTRODUCTION

The importance of the cytoplasmic C-terminal tail of ATL was first suggested by the identification of two distinct frameshift mutations in patients suffering from Hereditary Spastic Paraplegia. In both cases, the frameshift was caused by a base insertion that resulted in mistranslation and a premature stop codon that truncated the tail (Tessa et al., 2002; Loureiro et al., 2009). The C-terminal tail following the second transmembrane domain is present in all ATL isoforms but similar to N-terminal extension, there is very little sequence conservation across species.

Unlike the N terminal extension, the C-terminal tail of ATL has been studied extensively. Two different studies showed a requirement for the C-terminal tail in Drosophila ATL for mediating liposome fusion *in vitro* (Moss et al, 2011; Liu et al., 2012). Although there is little sequence conservation across species, a predicted membrane proximal amphipathic helical structure at the start of the tail is conserved in all ATL isoforms. The sufficiency of this amphipathic helix in ATL mediated membrane fusion is suggested by the ability of a Drosophila ATL construct lacking almost the entire tail but retaining the amphipathic helix, to mediate fusion *in vitro* (Moss et al., 2011). More strikingly, a synthetic peptide corresponding to this helix rescued the fusion activity of the tailless Drosophila ATL mutant when added in trans (Liu et al., 2011).

In order to understand the precise role of the C-terminal tail, James McNew and his group investigated the characteristics and the functional relevance of this amphipathic helix within the tail. In their recent paper (Faust et al., 2015), they show that 1) the first 23 amino acids of the Drosophila ATL tail folds into an amphipathic helix that can directly interact with the membrane through its hydrophobic face (schematized in Figure 4-1), 2) this interaction destabilizes the lipid bilayer, and 3) the destabilization of the membrane facilitates the ATL mediated fusion of the membranes. Although the *in vivo* studies suggest the requirement of the tail in ATL mediated membrane fusion its importance in ER network formation in cells was unclear. In this work, I performed the *in vivo* studies to analyze the requirement of the C- terminal tail in ATL dependent ER network formation in HeLa cells. My results show that Drosophila ATL can function in mammalian cells and rescue defects of the branched ER network in Hela cells depleted of the endogenous ATL-2 and -3. Consistent with the *in vitro* data, this activity of Drosophila ATL is

dependent on the cytoplasmic tail, more specifically on the hydrophobic face of the amphipathic helix within the tail. Overall, our results suggest that the C-terminal tail is important for ATL dependent fusion machinery but the highly curved ER tubules with much more complex lipid composition might be less sensitive to the changes in C-terminal tail.

MATERIALS AND METHODS

Cell culture, constructs, transfections and reagents

HeLa cells were maintained in minimal essential medium (Sigma-Aldrich, St. Louis, MO) containing 10% fetal bovine serum (Atlanta Biologicals, Norcross, GA) and 1% penicillin/streptomycin (Thermo Fisher Scientific) at 37°C in a 5% CO_2 incubator. Transient plasmid DNA transfection of HeLa cells was performed with jetPEI™ (Polyplus transfection, Illkirch, France), according to the manufacturer's specifications using 1 µg DNA and 2µl JetPEI per 1 mL media. Transient siRNA transfections of siRNAs against Atl2/3 were performed using Oligofectamine (Invitrogen) using 20pmol siRNA and 2µl Oligofectamine per 0.5 mL media. eYFP tagged *Drosophila melanogaster* atlastin (dAtl) and GST-tagged Atl1 were kindly provided by James McNew (Rice University, TX). Point mutations were generated using QuikChange PCR and fully verified by sequencing (Genewiz).

Knockdown replacement assay

Cells plated on 60-mm culture dishes were transfected with ~5 µg of the indicated eYFP tagged dAtl constructs using transfection reagent (jetPEI; Polyplus). Myc-tagged ER resident protein DP1, served as a negative control. 24 h after DNA transfection, cells were trypsinized and replated onto 12-mm glass coverslips in a 24-well plate. siRNA treatment targeting both ATL2 and ATL3 was performed the next day using transfection reagent (Oligofectamine; Invitrogen) according to manufacturer's recommendations. The ATL2 (#1) and ATL3 (#2) siRNAs used, were identical in sequence to those previously published (Rismanchi et al., 2008). 72 h after knockdown, cells were fixed in ice-cold methanol and processed for immunofluorescence. For quantification of functional replacement, the fraction of cells expressing the indicated HA-ATL1 or eYFP-D-ATL that showed a loss of ER network branching (among ≥100 cells in there individual experiments) was counted. This percentage was normalized to the negative control for that experiment. An efficiency of 1 reflects a complete non-rescue and 0 is a full-rescue. Nocodazole washout experiments were performed as follows: 72h after siRNA treatment, cells were incubated with 1ml media with 2X Nocodazole for 3h followed by washes with fresh media without Nocodazole. Cells were fixed at the indicated time points and processed for immunofluorescence.

Immunofluorescence and Confocal imaging

Cells were fixed in ice-cold methanol followed by 30 min incubation in the blocking solution (1X PBS + 2.5% calf serum + 0.1% Triton X-100 + 0.2 M Glycine). Primary (1 h at RT) and secondary (30 min at RT) antibody incubations were performed in the blocking solution, and washes were with 5× 1 ml PBS. Antibodies used include mouse monoclonal antibody (mAb) against the HA-epitope (Sigma-Aldrich, St. Louis, MO); a mAb against protein disulfide isomerase (PDI), a polyclonal antibody against tubulin (Both Abcam, Cambridge, MA); monoclonal antibody against MYC-epitope (9E10 mAB, Sigma - Aldrich) and Alexa 568-conjugated secondary antibody (Invitrogen). Images were viewed using a spinning-disk confocal scanhead (Yokagawa; PerkinElmer) mounted on an Axiovert 200 microscope (Zeiss) with a 100x 1.4 NA objective (Zeiss) and acquired using a 12-bit ORCA-ER camera (Hamamatsu Photonics). Maximal value projections of sections at 0.2-μm spacing were acquired using Micro-manager open source software (UCSF) and imported as 8-bit images. Quantification of functional replacement was performed manually on a wide-field fluorescence microscope (Axioplan; Carl Zeiss) with a 40× 1.4 NA objective.

RESULTS

Drosophila ATL is functional in mammalian cells

The branched ER network of mammalian cells is established by ATL dependent membrane fusion of ER tubules. The requirement for the C-terminal tail in ATL mediated fusion predicted that the ER network formation activity of ATL would also depend on the tail. To test this hypothesis, I set out to analyze the functional importance of the tail in HeLa cells. Because the *in vitro* work had been done using Drosophila ATL, I first had to show the functionality of the Drosophila ATL orthologue in maintaining the ER network in HeLa cells since it was not shown previously. As seen in Figure 4-2, in the gene replacement assay described previously, the expression of the wildtype full length Drosophila ATL protected the ER network from losing its branchpoints upon depletion of endogenous ATL. The rescue by Drosophila ATL was similar to rescue by both ATL-1 and ATL-2, suggesting a conserved function among all ATL isoforms.

The C-terminal tail of Drosophila ATL is required for its ER network formation function in mammalian cells

In vitro studies suggest the requirement of the C-terminal tail of Drosophila ATL in membrane fusion. Because the ER network formation function of ATL is dependent on its fusion ability, a construct that lacked the tail was expected to inhibit the *in vivo* gene replacement activity. Figure 4-2 shows that as expected, the Drosophila ATL mutant (1-471) that lacks the entire C-terminal tail is nonfunctional in restoring the branched ER network similar to the GTP binding mutant (K51A) used as a control.

Mutations altering the hydrophobic face of the amphipathic helix affect the functionality

To further analyze the importance of the amphipathic helix within the tail, I performed mutagenesis to disrupt the hydrophobic face of the helix. Surprisingly, single charge mutations, inhibitory to the *in vitro* fusion assay were largely without effect *in vivo* (Figure 4-3). I further expanded the mutations and determined that loss of function required four charge replacements down the length of the hydrophobic face. Overall my results revealed that mutations altering the hydrophobic face of ATL affect the functionality *in vivo* but to a lesser degree compared to *in vitro*. More significant perturbation seemed to be required within the hydrophobic face to inhibit function.

The degree of the requirement of the C-terminal tail of ATL is determined by lipid composition

One possible explanation for the difference seen in the degree of susceptibility to changes in the amphipathic helix within of the C-terminal tail is the difference in the lipid composition between *in vivo* and *in vitro* experiments. The intrinsic curvature of ER membranes is likely to destabilize the lipid bilayer and so may rely less on the amphipathic tail to facilitate fusion upon binding to the membrane. To test this hypothesis, McNew`s group analyzed the requirement of the tail in *in vitro* fusion using liposomes with altered lipid composition. Phosphatidlyethanolamine (PE) provides curvature and so causes destabilization of the membranes mimicking the properties of lipid bilayer of ER (Churchward et al., 2008). Figure 4-4 shows that as expected, the requirement for the tail for membrane fusion was reduced when proteoliposomes containing PE were used. Altogether the data reveal that requirement of C-terminal tail might be less stringent in ER membranes where lipid bilayer of tubules is much more complex and probably less stable due to the high curvature and presence of integral membrane proteins, than the synthetic liposomes used *in vitro*.

FIGURES

Figure 4-1. The amphipathic character of the C-terminal tail of ATL is conserved across species

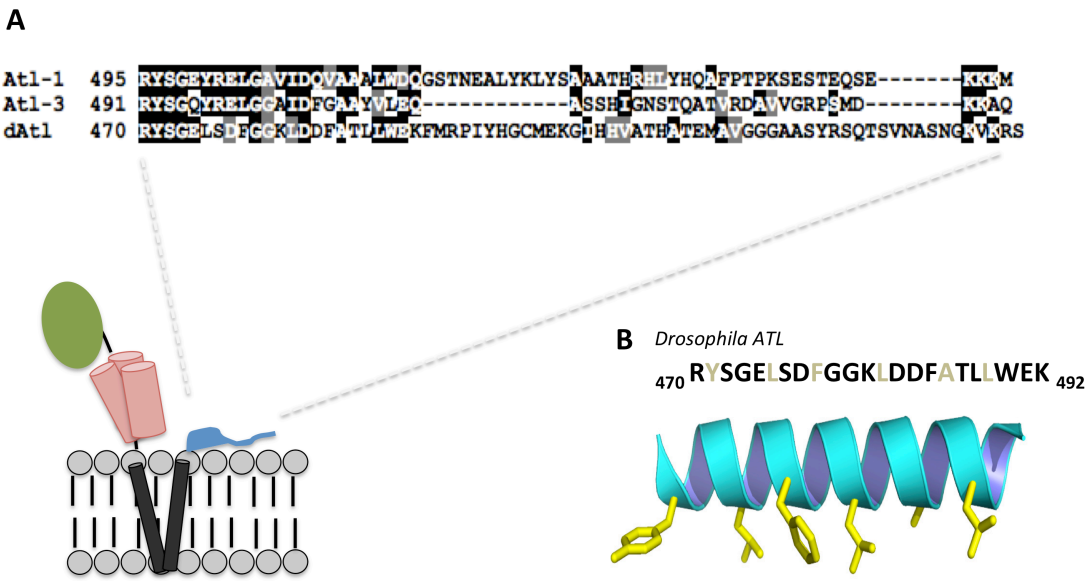

A) Alignment of the C-terminal cytoplasmic tail of human Atlastins and Drosophila Atlastin. Residues at the beginning of the tail fold into an amphipathic helix conserved between humans and drosophila ATL isoforms, **B)** A structural schematic of Atlastin illustrating the C-terminal amphipathic helix shown in a cyan ribbon diagram with the membrane facing hydrophobic side chains, shown as yellow sticks. The amino acid sequence of the Drosophila ATL that fold into the helix, composed of residues 470–492, is shown above the schematic helix. Figure adapted from *Faust et al., 2015* figures 1A and 2A.

Figure 4-2 Drosophila Atlastin can functionally replace human Atlastin in HeLa cells

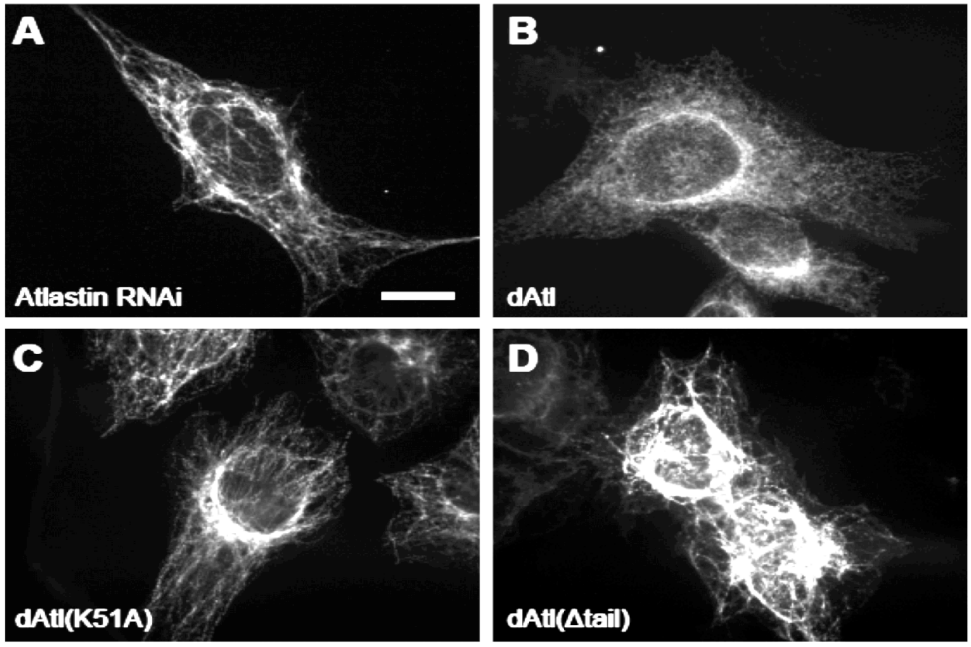

Knockdown replacement assay. 48 h after transfection with a negative control construct (Myc-tagged DP1 (**A**) or the indicated eYFP tagged Drosophila Atl (dAtl) constructs (B-D), cells were transfected with siRNAs targeting ATL-2 and ATL-3. 72 h after knockdown, cells were fixed and stained using an antibody against Myc (**A**) or visualized through eYFP fluorescence (**B**–**D**) and viewed by confocal microscopy. **A**) HeLa cells transfected with DP1-myc and siRNA targeting ATL-2 and ATL-3 show elongated ER tubules and reduced three-way junctions. **B**) Expression of wild-type eYFP-dAtl in these cells restores ER morphology. **C**) A GTP binding mutant dAtl (K51A) does not rescue the abnormal ER morphology of siRNA-treated cells. **D**) A mutant lacking the C-terminal amphipathic tail dAtl (Δtail) also fails to rescue the abnormal ER morphology. Scale bar **,** 10 μm.

Figure 4-3 Charge mutations in the C-terminal tail are more permissive *in vivo*

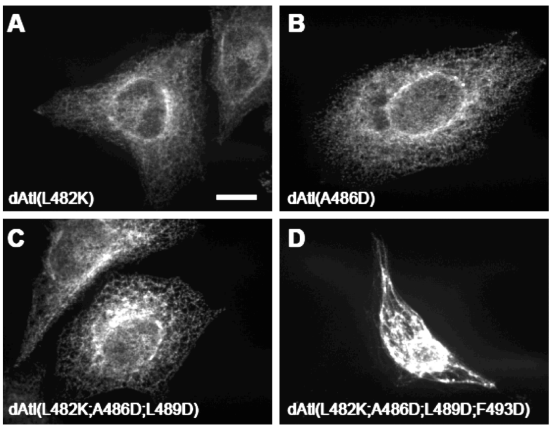

F

	in vitro fusion % of Wt	in vivo rescue % of Atl efficiency
dAtl	100	98.1
K51A	5	~0
Δtail (1-471)	5 (<5*)	20
F478K	66	nd‡
F478K;L482K	16	nd
L482K	21	98
A486D	<5*	97
L489D	<5*	nd
L482K;A486D;L489D	nd	79
L482K;A486D;L489D;F493D	~0	~0

‡ not determined

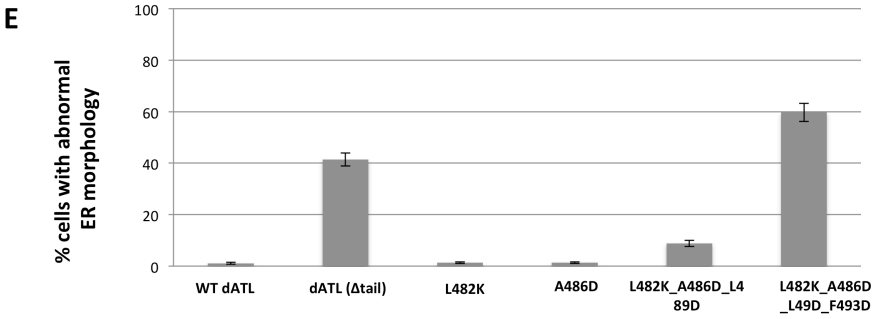

48 h after transfection with the indicated eYFP-Drosophila Atl (dAtl) constructs, cells were transfected with siRNAs targeting ATL-2 and ATL-3. 72 h after knockdown, eYFP fluorescence was viewed by confocal microscopy. **A)** dAtl with a charge mutation in the amphipathic C-terminal tail, dAtl(L482K), is functional in vivo and can rescue the abnormal ER phenotype in cells treated with siRNA targeting ATL-2 and ATL-3. **B)** dAtl with a different charge mutation in the C-terminal tail A486D is also functional in vivo. **C)** dAtl with three charge mutations in the C-terminal tail, L482K_A486D_L489D, is functional in vivo. D) dAtl with four charge mutations in the C-terminal tail, L482K_A486D_L489D_F493D, does not rescue the ER morphology. Scale bar 10 μm. **E)** Quantification of the percentage of cells expressing, distinct eYFP–dAtl constructs (with RNAi) that displayed an abnormal unbranched ER morphology. Values represent the means of three independent experiments (>100 cells each) ± SD. **F)** Summary of the *in vitro* fusion activity of these mutants and their ability to rescue ER morphology in HeLa cells. Figure adapted from *Faust et al; 2015*.

Figure 4-4 The requirements for the C-terminal amphipathic helix is dependent on the lipid composition

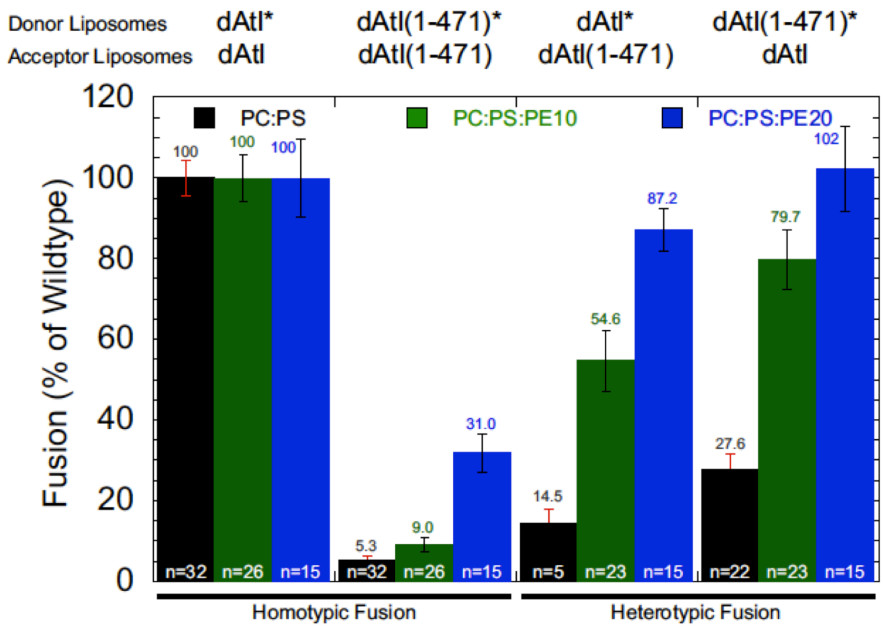

The extent of fusion at 60 min is represented in a histogram as the percentage of the wild type. A) The left half of the graph shows homotypic fusion reactions where the same protein is present in donor and acceptor liposomes. The right half shows heterotypic fusion reactions where mutant dAtl is present in one pool of liposomes, and wild-type dAtl is present in the other pool. Absolute levels of fusion (represented as a percentage of maximum fluorescence) ranged from 8.2–8.9% following background subtraction of 0.9% found in the absence of GTP. The level of background fusion in the absence of GTP did not significantly differ with increased levels of PE. Black, PC:PS (85:15 mol%); green, PC:PS:PE (75:15:10 mol%); blue, PC:PS:PE (65:15:20 mol%). The means +/- S.E are shown with the number of replicates (n) indicated in the histogram. Experiments done by James Mcnew`s group, figure is taken from *Faust et al., 2015.*

Figure 4-5 The C-terminal tail of ATL is functionally conserved across species

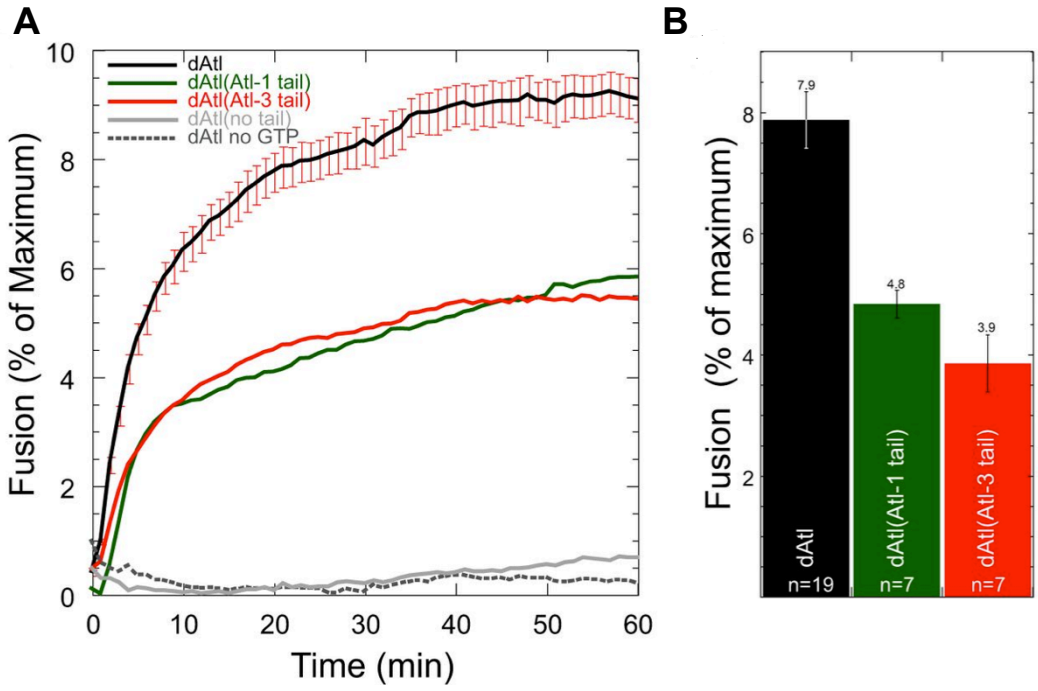

In vitro proteoliposome fusion assay. **A)** Kinetic fusion graph of unlabeled dAtl acceptor proteoliposomes incubated with equimolar amounts of fluorescently labeled dAtl donor proteoliposomes. NBD fluorescence was measured at 1-min intervals, and detergent was added at 60 min to determine maximum fluorescence. In all cases, the same dAtl mutant is reconstituted into both liposome populations. All fusion experiments are **n** = 6. Black, WT GST-dAtl-His8; green, GST-dAtl(Atl1-tail)-His8; red, GST-dAtl(Atl-3-tail)-His8; solid gray, GST-dAtl(1–471)- His8; dashed gray, control reaction in the absence of GTP. **B)** The extent of fusion at 60 min is represented in a histogram as the percentage of fusion. the means +/- S.E are shown. Experiments done by James McNew`s group, figure is taken from *Faust et al., 2015.*

DISCUSSION

Sequence conservation of specific domains of ATL GTPases such as the GTPase head and the middle domain across species highlight their importance in the membrane fusion activity of ATLs. The cytoplasmic tail located at the C-terminus, despite little sequence conservation, has also been shown to be required for fusion. Recent studies pointed out the presence of a stretch of residues predicted to fold into an amphipathic helix at the beginning of the tail and this property is conserved in all ATL isoforms. Demonstrating its importance, a synthetic peptide corresponding to the amphipathic helix was found sufficient when added in trans to rescue the fusion defect of Drosophila ATL construct that lacks the entire tail (Liu et al., 2012).

In this study, James McNew and his group determined that this amphipathic helix can bind directly to membranes and destabilize the lipid bilayer to facilitate fusion. Through mutational analysis and *in vitro* fusion data, they revealed the hydrophobic face of the helix to be required for the membrane binding activity. In support of their *in vitro* data, my analysis showed the importance of the tail in mediating the branched ER network activity of Drosophila ATL, which can functionally replace endogenous ATL-2 and -3 in Hela cells. Surprisingly, this activity *in vivo* was less sensitive to perturbations in the hydrophobic face of the helix compared to the *in vitro* fusion activity, which can be largely inhibited with only single point mutations within the helix. This difference revealed the potential role of the lipid composition on the degree of requirement of the cytoplasmic tail of ATL.

The function of the amphipathic helix was shown further to be transplantable from human ATL isoforms to Drosophila ATL. That is, the entire C-terminal tail of Drosophila ATL could be replaced by the tail of ATL-1 or ATL-3 with only a small reduction in fusion activity (Figure 4-5). This finding suggests the functional conservation of C-terminal tail in human ATL isoforms, and might explain the disease pathogenesis seen with the frameshift mutations that truncate the tail of ATL-1.

REFERENCES

Churchward, M.A., Rogasevskaia, T., Brandman, D.M., Khosravani, H., Nava, P., Atkinson, J. K., Coorssen, J. R. (2008). Specific Lipids Supply Critical Negative Spontaneous Curvature- An Essential Component of Native Ca^{2+} Triggered Membrane Fusion. Biophysical Journal. 94 : 3976- 3986.

Faust, J.E., T. Desai, A. Verma, I. Ulengin, T.L. Sun, T.J. Moss, M.A. Betancourt, H.W. Huang, T. Lee, and J.A. McNew. (2015). The Atlastin C-terminal Tail is an Amphipathic Helix that Perturbs Bilayer Structure during Endoplasmic Reticulum Homotypic Fusion. J Biol Chem. 290(8):4772-83.

Liu, T.Y., Bian, X., Sun, S., Hu, X., Klemm, R. W., Prinz, W.A., Rapoport, T. A., Hu, J. (2012). Lipid interaction of the C terminus and association of the transmembrane segments facilitate atlastin-mediated homotypic endoplasmic reticulum fusion. Proc. Natl. Acad. Sci. USA. 109(32);E2146-54.

Moss, T.J., C. Andreazza, A. Verma, A. Daga , and J.A. McNew. (2011). Membrane fusion by the GTPase atlastin requires a conserved C-terminal cytoplasmic tail and dimerization through the middle domain . Proc. Natl. Acad. Sci. 108 : 11133 – 11138

CHAPTER 5

CONCLUSIONS AND FUTURE DIRECTIONS

My work has surprisingly revealed that certain ATL-1 variants that cause HSP are fully functional in membrane fusion and ER network formation, at least in non-neuronal cells. Whether these variants are also fully functional in neurons, particularly those with the longest axons and that are most affected in HSP patients, remains to be seen. One plausible explanation is that ATL-1 activity in neurons depends on its binding to one or more neuron specific factors. In this case, the R239C and H258R mutations, both surface exposed, would cause HSP as they might impair binding to those factors. To date, several other ER- localized proteins including reticulons, Spastin, REEP1, DP1 and protrudin have been identified to bind to various ATL isoforms (Sanderson et al., 2006; Rismanchi et al., 2008; Hu et al., 2009; Park et al., 2010; Chang et al., 2013). Interactions with reticulons and DP1 seem not to be isoform specific. In contrast, protrudin, an ER protein that influences neurite formation through membrane trafficking, binds preferentially to ATL-3 (Shirane et al., 2006; Chang et al., 2013); and Spastin is reported to specifically interact with ATL-1 (Rismanchi et al., 2008). The functional significance of these interactions is currently unknown, but underline that distinct regulatory elements might to be present to specifically regulate each ATL isoform that is enriched in different tissues in humans. Moreover, several of these interacting partners including Spastin, are also associated with HSP. Therefore it is important that these interactions are further validated and their functional relevance is understood in the context of HSP disease pathogenesis (Fink et al, 2006).

Separately, it is important to understand the functional importance of each region in the atlastin protein. So far the most detailed research has been done on the soluble domain of atlastin, which consists of the GTPase domain and the middle domain. Recent data including my findings in collaboration with James McNew and his group reveal the requirement of the C-terminal tail in membrane fusion and ER network formation. The biochemical assays show an ability of the tail to bind directly to the membrane bilayer to destabilize the bilayer, which in turn facilitates fusion. The function of the C-terminal tail is transplantable from human ATL isoforms to Drosophila ATL, indicating a likelihood that the tail also serves a required function in humans. This would explain the disease

pathogenesis seen with the frameshift mutations that truncate the tail of ATL-1. Interestingly however, the extent to which the lipid destabilizing function of tail is required for ATL function appeared to depend on membrane composition. The requirement was less stringent in membranes with inherently unstable lipid compositions. Whether the ER membranes of neurons differs in composition is not known, but the functional relevance of the ATL-1 tail should be analyzed further in the context of neuronal cells to provide more insight to HSP pathogenesis (Faust et al., 2015).

Similarly, the role of the N-terminal extension present in ATLs across species is yet to be identified. Although my preliminary results show that this extension is unlikely to be required for fusion dependent ER network formation, the particular conservation of this region in ATL-1 across vertebrate species does suggest a critical involvement in neuronal ATL function(s). One possibility is that it is mediating a unique spatial and temporal regulation of fusion dependent ER network formation activity of ATL-1 in neurons by providing a surface for interactions with factors important for regulation of ATL-1 function. Further work is required to determine the presence of such a regulatory binding partner as currently there are no known interactions through this region.

Another area that needs to be investigated in detail is the possibility that ATL-1 carries out neuron specific alternate functions distinct from, or in addition to, its fundamental role in ER network formation. For instance, the localization of ATL-1, in addition to the ER, to the Golgi apparatus (Zhu et al., 2003) and to vesicular structures within neurons suggests roles in vesicle trafficking (Namekawa et al., 2007). Furthermore, ATL-1 is enriched in axonal growth cones and varicosities with suggested roles in axon outgrowth and neurite branching (Zhu et al., 2006). Additionally, ATL-1 has been implicated in bone morphogenetic protein (BMP) signaling. In zebra fish, Danio Rerio, a reduction in BMP receptor endocytosis in addition to severe mobility defects was observed in the larvae depleted of atlastin (Fassier et al., 2010). Further investigation will be necessary to understand the precise role(s) of neuronal ATL-1 as it is possible that the maintenance of the long axons in corticospinal tract involves coordination of these functions. Disease causing mutations might be disrupting one or multiple of these functions. Identifying the pathways that are affected by these mutations would lead to a better understanding of the basis of the disease pathogenesis and might provide tools for treatment.

Finally, it is crucial to understand why the human ATL isoforms including ATL-1, are incapable of mediating fusion between synthetic liposomes. While it is possible that structural elements specific to ATL-1, such as the N-terminal extension, possess a regulatory (perhaps inhibitory) effect on fusion *in vitro;* it is also possible that unlike Drosophila ATL, ATL-1 requires the presence of an interacting partner that helps mediate its fusion activity. Establishing an ATL-1 dependent *in vitro* fusion assay would provide a more direct measurement to understand the true impact of the disease causing mutations.

In sum, a significant gap remains in our understanding of the basis of the HSP pathogenesis. I am confident that a deeper understanding of the role(s) of ATL and its regulations will provide tools for treatment of HSP and possible insights into other neurodegenerative diseases.

REFERENCES

Chang J, Lee S, Blackstone C. (2013). Protrudin binds atlastins and endoplasmic reticulum shaping proteins and regulates network formation. Proc Natl Acad Sci USA.110:14954–14959.

Fassier, C., J.A. Hutt, S. Scholpp, A. Lumsden, B. Giros, F. Nothias, S. Schneider-Maunoury, C. Houart, and J. Hazan. (2010). Zebrafish atlastin controls motility and spinal motor axon architecture via inhibition of the BMP pathway. Nat Neurosci. 13:1380-1387.

Faust, J.E., T. Desai, A. Verma, I. Ulengin, T.L. Sun, T.J. Moss, M.A. Betancourt, H.W. Huang, T. Lee, and J.A. McNew. (2015). The Atlastin C-terminal Tail is an Amphipathic Helix that Perturbs Bilayer Structure during Endoplasmic Reticulum Homotypic Fusion. J Biol Chem. 290(8):4772-83.

Fink, J.K. (2006). Hereditary spastic paraplegia. Curr Neurol Neurosci Rep. 6:65-76.

Hu, J., Shibata, Y., Zhu, P., Voss, Christiane, V., Rismanchi, N., Prinz, W.A., Rapoport, T. A., Blackstone, C. (2009) A Class of Dynamin-like GTPases Involved in the Generation of the Tubular ER Network. Cell 138, 549-561.

Namekawa, M., P. Ribai, I. Nelson, S. Forlani, F. Fellmann, C. Goizet, C. Depienne, G. Stevanin, M. Ruberg, A. Dürr, and A. Brice. 2006. SPG3A is the most frequent cause of hereditary spastic paraplegia with onset before age 10 years. Neurology. 66:112-114.

Park, S.H. and Blackstone, C. (2010). Further Assembly Required: Construction and Dynamics of the Endoplasmic Reticulum Network. EMBO reports. 11, 515-21.

Rismanchi , N. , C. Soderblom , J. Stadler , P.P. Zhu , and C . Blackstone. (2008). Atlastin GTPases are required for Golgi apparatus and ER morphogenesis . Hum. Mol. Genet. 17 : 1591 –1604.

Sanderson CM, Connell J, Edwards TL, Bright NA, Duley S, Thompson A, Luzio P, Reid E. (2006). Spastin and atlastin, two proteins mutated in autosomal dominant hereditary spastic paraplegia, are binding partners. Hum Mol Genet. 15(2): 307-318.

Shirane, M. and Nakayama, K.I. (2006). Protrudin induces neurite formation by directional membrane trafficking. Science. 314: 818-821.

Zhu, P.P., A. Patterson, B. Lavoie, J. Stadler, M. Shoeb, R. Patel, and C. Blackstone. (2003). Cellular localization, oligomerization, and membrane association of the hereditary spastic paraplegia 3A (SPG3A) protein atlastin . J. Biol. Chem. 278 : 49063– 49071

Zhu, P.P., Soderblom, C., Tao-Cheng, J.H., Stadler, J. (2006). SPG3A protein atlastin-1 is enriched in outgrowth cones and promotes axon elongation during neuronal development. Human Molecular Genetics. 15(8) : 1343-1353.